# Isolation and Characterization of DNA Aptamers for Zinc Finger Proteins

Inaugural-Dissertation

to obtain the academic degree

**Doktor rerum naturalium (Dr. rer. nat.)**

submitted to the Department of Biology, Chemistry and Pharmacy

of Freie Universität Berlin

by

**Ying Lin**

from

Dalian, China

January, 2009

Hereby I declare that I have written this thesis by myself, marked the sources of any quotations or content obtained otherwise and mentioned any personal help by name. (Ich erkläre hiermit, das ich die vorliegende Doktorarbeit selbstständig verfasst, die wörtlich oder inhaltlich anderen Quellen entnommenen Stellen als solche kenntlich gemacht und die Inanspruchnahme persönlicher Hilfe namentlich aufgeführt habe.)

Berlin, 2009 Ying Lin

The work for this PhD thesis was performed from November 2004 to August 2008 in the laboratory of Prof. Volker A. Erdmann in the Institute of Chemistry and Biochemistry at the Free University Berlin.

1st reviewer: Prof. Dr. Volker A. Erdmann
2nd reviewer: Prof. Dr. Hans Lehrach

Date of defense: 30. 03.2009

To my parents

# Table of Contents

# 1. Introduction

## 1.1 Zinc Finger Transcription Factors

### 1.1.1 The Zinc Finger Motif

Transcription factors are specialized nuclear proteins with the ability to bind to DNA in order to regulate transcription. Thereby, these proteins contain a DNA binding domain and a domain involved in protein-protein interaction, which allows the transcription factors to stimulate gene expression (Brennan *et al*., 2008). In other functions transcription factors may serve as architectural proteins, which induce chromatin structural rearrangements to facilitate the entry of additional activator or repressor complexes.

The specificity involved in the control of transcription requires that regulatory proteins bind with high affinity to the correct region of DNA. Many DNA-binding proteins contain independently folded domains for the recognition of DNA, and in turn, these domains belong to a large number of structural families. A eukaryotic DNA-binding transcription factor was first identified containing a helix-turn-helix (HTH) motif more than twenty years ago on Cro, CAP, and λ–repressor (Anderson *et al*., 1981; Mckay and Steitz, 1981; Pabo and Lewis, 1982). Other structure domains were identified as the zinc finger (*zf*) motif, the helix-loop-helix motif, leucine zippers, and fork head domains (Brown, 2006). The *zf* motif is, however, the most abundant DNA binding motif in transcription factors (Brennan *et al.,* 2008) and it has recently received much attention because of its multifunctionality.

A *zf* motif was first proposed in 1983 for the protein transcription factor IIIA (TFIIIA; Hanas *et al.,* 1983). Subsequent analysis revealed the presence of small zinc-based domains (termed ‘‘zinc fingers’’) in a wide variety of other proteins involved in gene regulation. Over the past decades, more than 14 classes of such zinc-based domains have been discovered and partly characterized (Berg and Shi, 1996; Matthews and Sunde, 2002). The zinc finger proteins of classical $Cys_2His_2$ and nonclassical $Cys_2Cys_2$ type are broad families of proteins implicated in both transcriptional regulation and RNA processing (Ladomery and Dellaire, 2002).

The most dominant and best studied class of zinc fingers is the classical *zf*, the $Cys_2His_2$ type, which was initially identified in TFIIIA (Fig. 1-1 A). The $Cys_2His_2$ *zf* proteins form the largest family (around 900 members) in more than 2000

hypothetical human genes that encode transcriptional activators (Fig.1-1 B). This class of proteins is also the largest family of activators in *D. melanogaster, C. elegans,* and *S. cerevisiae.* These $Cys_2His_2$ *zf* domains are characterized by tandem arrays of sequences that approximate the consensus template of the general *zf* (Tyr,Phe)-X-Cys-$X_{2-4}$-Cys-$X_3$-Phe-$X_5$-Leu-$X_2$-His-$X_{3-5}$-His, where X represents more variable amino acids. They all have the same structural framework, but achieve specificity through variations in key residues. Each of these *zf* domains consists of two antiparallel ß-strands followed by one α-helix. The three-dimensional structure explains the conserved sequence features: the cysteine and histidine side chains coordinate the zinc and the three other conserved residues (Tyr or Phe, Phe, Leu) pack to form a hydrophobic core adjacent to the metal coordination unit. Structurally, the classical *zf* is little more than a polypeptide loop folded back on itself with the aid of a zinc ion (Klug, 1995).

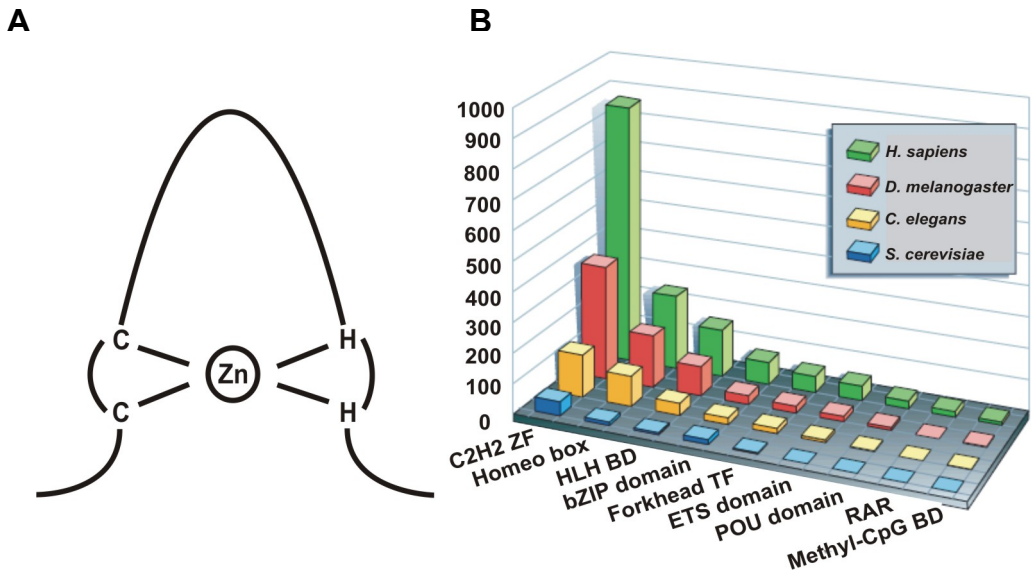


***Fig. 1-1 (A) Schematic presentation of a single $Cys_2His_2$ zinc finger domain.*** *A zinc ion is used in a purely structural role to stabilize a very small functional protein domain or finger.* ***(B) Genome-wide comparisons of transcription activator families in eukaryotes.*** *The relative sizes of transcriptional activator families among Homo sapiens, D. melanogaster, C. elegans, S. cerevisiae are indicated. The transcription factors families shown are the largest of their category out of the 1502 human protein families (adapted from Tupler et al., 2001).*

Krüppel is one of the most predominant families containing $Cys_2His_2$ type *zf*s. The Krüppel is a member of the 'gap' class of segmentation genes of *Drosophila melanogaster*, the mutation of which causes contiguous groups of segments of the fruit fly embryo to fail to develop. Krüppel encodes a protein that contains a DNA-binding motif composed of several 'zinc fingers' of the $Cys_2His_2$ type (Schuh *et al.,* 1986). In mammals, a group of transcription factors were found to exhibit close homology to the *zf* portion of Krüppel. For example, ZFY/ZFX and GLI transcription factors are subfamilies of Krüppel *zf*s (Page *et al.*, 1987; Kinzler *et al.*, 1988).

Another predominant *zf* familiy is the RanBP2 zinc finger of the $Cys_2Cys_2$ type. It contains four cysteines and a conserved tryptophan upstream of the *zf*. Its consensus template can be presented by Trp-X-Cys-$X_{2,4}$-Cys-$X_3$-Asn-$X_6$-Cys-$X_2$-Cys, where X presents more variable amino acids. The RanBP2 *zf* of the $Cys_2Cys_2$ type is found in different proteins that are mainly involved in nuclear transport or localized to the nuclear envelope. Examples of the proteins containing such a domain are TLS (FUS), TAFII68 (RBP56), and EWS (Crozat *et al*. 1993; Bertolotti *et al.* 1996; Ladomery and Dellaire, 2002).

Although *zf*s typically occur in tandem arrays and many transcription factors have three or more *zf*s, each *zf* folds and functions independently as a mini-domain. Many investigations have been carried out concerning the general features of single *zf* architecture. Single *zf*, a peptide containing just 30 amino acids that corresponds to the ''zinc finger'' domain of transcription factor IIIA, can fold in the presence of zinc. The specific binding activity of the *zf* motif to nucleic acids is dependent on the presence of zinc. It is interesting to note that a *zf* motif has a relatively small number of fully conserved residues. The structural stability is mainly provided by the zinc coordination and by the conserved hydrophobic core that flanks the zinc binding site. Metal binding and canonical hydrophobic residues seem to be necessary and sufficient to determine the structure of this class of *zf* peptides (Michael *et al*., 1992).

### 1.1.2 The Nucleic Acid Binding Properties

*Zf* transcription factors are complex proteins, involved in DNA-, RNA- or protein-protein interactions of the transcription. The initial structural information about these interactions came from the crystal structure of the three *zf* domains

from the mouse transcription factor Zif268 bound to a DNA target site (Pavletich and Pabo, 1991). The α-helix of each *zf* in this complex lies in the major groove of the double helix and interacts with the DNA bases through amino acid side chains from the $NH_2$-terminal portion of this helix. Each *zf* domain contacts a contiguous 3-bp subsite, with the majority of the base-specific contacts directed to one DNA strand (Fig. 1-2).

In subsequent studies, several other $Cys_2His_2$ *zf*-DNA structures have been solved, including Tramtrak (Fairall *et al*., 1993), GLI (Pavletich and Pabo, 1993), YY1 (Houbaviy *et al*., 1996), GAGA factor (Omichinski *et al*., 1997) and TFIIIA (Nolte *et al*., 1998). In earlier studies it had been observed that multiple zinc fingers are required for sequence-specific DNA recognition (McColl *et al*., 1999; Wolfe *et al*., 1999; Matthews *et al*., 2002). In the case that only one or two fingers are present, additional secondary structure elements are generally used to facilitate DNA recognition (Wolfe *et al*., 1999). The DNA double helix is essentially regular, despite small, local, sequence-dependent variations, thus the specificity of recognition lies in a particular sequence of the bases. However, to date there are no general rules for *zf*-DNA recognition. The sequences bound by a series of *zf*s turned out not to be completely distinct from each other but instead overlapped: the same DNA triplet can be touched by amino acids from more than one finger (Pearson, 2008).

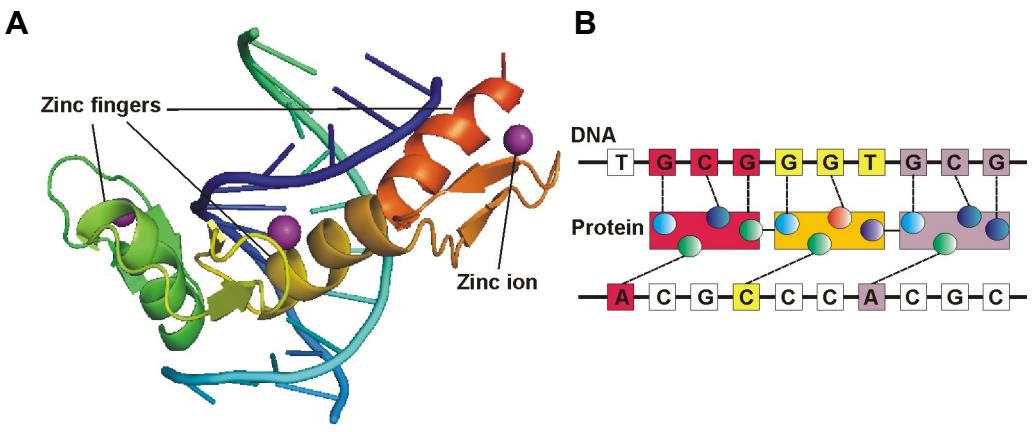


***Fig. 1-2 Zinc finger domains from Zif268 bind to a DNA target site.*** *(A) Three zinc fingers of the protein Zif268 nestle alongside the bases in their stretch of DNA. (B) Amino acids in each finger associate with specific bases in the DNA (adapted from Pearson 2008).*

Today it is commonly known that *zf*s function through interaction with duplex DNAs, but some *zf* proteins may also function through specific interactions with RNAs. TFIIIA was first identified not as a transcription factor but as a protein that binds to 5S RNA in immature *Xenopus oocytes* (Picard and Wegnez, 1979). Subsequent studies found that RNA and DNA binding overlapped. For instance, separable functions of the nine *zf* elements in TFIIIA occurred via fundamentally different molecular mechanisms. TFIIIA binds to RNA on the basis of conserved secondary and/or tertiary structures, independent of the primary sequences (Pieler *et al*., 1984; Pieler *et al*., 1986; Theunissen *et al*., 1992). Clemens *et al.* (1993) have also reported that different sets of zinc fingers were found to be responsible for high affinity interactions with RNA and DNA. Additionally, *zf* proteins require also specific amino acids in α-helices for high affinity RNA binding.

Over the past two decades, a number of $Cys_2His_2$ *zf* proteins from mammalians were found to be involved in RNA binding, *e.g*. p43 (Joho *et al.,* 1990), *Xenopus* XFG 5-1 (Koster *et al*., 1991), *Xenopus* Xfin (Andreazzoli *et al.,* 1993), Wilms tumor suppressor gene WT1 (Caricasole *et al.,* 1996), the human and mouse $MOK_2$ proteins (Arranz *et al*., 1997), h*ZF*P100 (Dominski *et al.,* 2002), Wig-1 (Mendez-Vidal *et al.,* 2002), and JAZ (Chen *et al.,* 2004). However, it has been an enigma how *zf* proteins bind to RNAs exactly. This has been resolved by the crystal structure of a three-zinc finger complex with 61 bases of RNA, derived from the central regions of the complete nine-finger TFIIIA-5SRNA complex (Lu *et al*., 2003)**.** The structure reveals two modes of *zf* binding: first, the *zf*s interact with the backbone of a double helix; and second, the *zf*s specifically recognize individual bases positioned for access in otherwise intricately folded "loop'' regions of the RNA. Both of the two *zf* binding modes to RNA differ from that in common use for DNA. RNA molecules form complex structures comprising internal 'loops' and double helices, which are sometimes closed by hairpin loops. The *zf* domain seems to be able to recognize all of these different elements, either sequence-dependent or structure-directed.

In summary, zinc finger domains, although small, appear to be quite versatile. The $Cys_2His_2$ *zf* scaffold can be used for base-specific recognition of the DNA major groove, backbone recognition of the RNA major groove, and almost customized RNA base and loop recognition (Hall, 2005).

### 1.1.3 Disease-Associated Zinc Fingers

Dysregulated or mutated transcription factors lead to the breakdown or abnormal control of the transcriptional machinery. Many transcription factors are multifunctional proteins and are implicated in human diseases including cancer, inflammatory diseases and heart diseases. For instance, transcription factors were shown to be key determinants in the orchestration of myeloid identity and differentiation fates. They show cell-lineage-restricted and stage-restricted expression patterns, indicating the requirement for tight regulation of their activities (Rosenbauer and Tenen, 2007). Therefore, transcription factors would potentially make good targets, *e.g.* for cancer diagnosis and even treatment of cancer (Brennan *et al.*, 2008). A predominant feature of many disease-associated transcription factors is the zinc finger. In particular, the *zf* transcription factors of the $Cys_2His_2$ type are the most predominant class, which are largely involved in development and disease, especially cancer.

The ZFY gene was first discovered in 1987 in the human Y chromosome, which encodes a *zf* protein ZFY (Page *et al.*, 1987). All members of the ZFY gene family (ZFY and *ZF*X in human) encode highly homologous proteins with the same overall structure. All of them have thirteen *zf*s of the Krüppel $Cys_2His_2$ type, encoded by a single exon (Koopman *et al.*, 1991). The ZFY gene family was suggested to have a fundamental cellular role in spermatogenesis (Koopman *et al.*, 1991). Recent studies show that murine ZFX functions as a shared transcriptional regulator of embryonic and hematopoietic stem cells, suggesting a common genetic basis of self-renewal in embryonic and adult stem cells. The identification of ZFY should also facilitate the molecular dissection of self-renewal mechanisms in tumor-initiating cancer stem cells (Galan-Caridad *et al*., 2007).

The GLI gene was originally identified to be amplified in glioblastoma (Kinzler *et al.*, 1988), encoding a *zf* protein containing five repeats of the $Cys_2His_2$-type *zf* motif. GLI was later found to be amplified in other tumors as well. It functions primarily as an oncogene if tumors arise, due to its overexpression, and therefore it is considered as a promising therapeutic target for tumor treatments (Berg, 1990; Matise and Joyner, 1999; Ladomery and Dellaire, 2002). Moreover, *zf* transcription factors of the GLI family play critical roles in the mediation and interpretation of Hedghog signals, which are associated with a surprising number of human diseases (Altaba *et al.*, 1999; Kasper *et al.*, 2006).

Matrin-3 was cloned and sequenced first from a rat insuloma cDNA library (Belgrader *et al.*, 1991), encoding a *zf* protein containing one classical $Cys_2His_2$-type *zf* (Matsushima *et al.*, 1997). It is a highly conserved nuclear matrix protein that has a positively charged N-terminal region and a negatively charged C-terminal domain. Matrin-3 belongs to the nuclear phosphoproteins of HeLa cells (Beausoleil *et al*., 2004). The bipartite nuclear localization signal of matrin-3 was characterized and found to be essential for its nuclear localization and also cell proliferation (Hisada-Ishii *et al.*, 2007). In addition, the functions of matrin-3 could be regulated by both $Ca^{2+}$-dependent interaction with calmodulin and caspase-mediated cleavage (Valencia *et al.,* 2007). In clinical studies, Matrin-3 showed significantly decreased levels of expression in fetal Down's syndrome brain (Bernert *et al.* 2002) and Alzheimer disease (Berntenis *et al*., 2007).

WT1 was first described in 1990 as a tumor suppressor gene associated with Wilms tumour (nephroblastoma) and encodes a typical transcription factor with four *zf*s of the Krüppel $Cys_2His_2$ type (Call, *et al*., 1990; Gessler *et al.,* 1990). It is involved in the development of several organ systems, and is both a tumor suppressor and oncogene (Ladomery and Dellaire, 2002; Morrison *et al.,* 2008).

In addition, several other disease-associated zinc finger transcription factors of the $Cys_2His_2$ type are described in the literature (Engelkamp and Heyningen, 1996; Ladomery and Dellaire, 2002; Rosenbauer and Tenen, 2007; Hanna *et al*., 2007; Brennan, *et al*., 2008, Wernig *et al*., 2008). Besides the common *zf*s of the $Cys_2His_2$ type, many disease-associated *zf* proteins contain $Cys_2Cys_2$ fingers. For instance, TAFII68 (also known as RBP56) and TLS (also known as FUS) belong to the TET family (TLS/FUS, EWS, TAFII68), which has $Cys_2Cys_2$ *zf* of the RanBP2 family. TLS was cloned from a breakpoint associated with myxoid liposarcoma (Crozat *et al*., 1993); TAFII68 is a TBP-associated factor encoded by TAF15 (TATA-binding protein, basal transcription). TAFII68 shares extensive 74% sequence similarity with TLS and both of them may both be present in TFIID complexes (Bertolotti *et al.*, 1996). Wild-type TLS and TAFII68 can function as classical transcription factors in addition to their better-known functions in splicing and mRNA transport. They have been found in a variety of cancer-associated fusion genes, leading to form aberrant transcription factors. The formation of these fusion genes is thought to be one of the primary causes of cancer (Law *et al.*, 2006).

Today's clinical practice has already been modified by the significant progress made in identifying transcription factors as the predominant components in myeloid differentiation and cancer. Research is on the way for the discovery of molecules that specifically alter the functions of transcription factors, so that new ways may be found to treat cancer (Rosenbauer and Tenen, 2007). Moreover, *zf* transcription factors dosage is critical at certain times in development (Engelkamp and Heyningen, 1996). Employing target-specific diagnostic tests would make early detection approaches feasible (Vogelstein and Kinzler, 2002). Early detections are perhaps the most promising and feasible means to reduce cancer deaths in a foreseeable future.

## 1.2 *In vitro* Selection

### 1.2.1 Systematic Evolution of Ligands by Exponential Enrichment

Over the past two decades, oligonucleotides have emerged as a viable alternative to virus-mediated gene complementation, which has proven to be effective in the treatment of genetic diseases in clinical trials. Since the discovery in the early 1980s that RNA was not simply a passive carrier of genetic information but could participate directly in catalysis in living cells, the understanding of oligonucleotide structure and function has been in constant flux (Stark *et al.,* 1978; Kruger *et al.,* 1982). Some RNA molecules exhibit a function without being translated into proteins, such as tRNAs, rRNAs, ribozymes, high-affinity RNAs and small nuclear RNAs from splicesomes. The diagnostic and therapeutic potential of oligonucleotides has been explored using antisense oligonucleotides, ribozymes, decoy oligonucleotides, aptamers and, more recently, small-interfering RNAs (siRNAs) (Doudna and Cech, 2002; Hannnon, 2002: McManus and sharp, 2002; Barciszewski and Erdmann, 2003; Erdmann *et al.,* 2006 and 2008; Kurreck, 2008).

In 1989, Oliphant and his coworkers selected binding sites of the GCN4 protein from a dsDNA pool with 23 nucleotides of random sequence. A year later, Tuerk and Gold (1990) selected RNA ligands to bacteriophage T4 DNA polymerase. The protocol for such *in vitro* selection experiments was introduced and called '*Systematic Evolution of Ligands by EXponential Enrichment' (SELEX*). At the same time RNA ligands were isolated to bind a variety of organic dyes

(Ellington and Szostak, 1990) and individually characterized RNA-molecules with high affinities for selected targets were termed ‘aptamers’ (from the Latin ‘aptus’ meaning ‘fitting’ and the Greek work ‘meros’ meaning ‘particle’).

The process of *in vitro* selection requires different methods of molecular biology, which are used to select those molecules from a combinatorial library that have a desired biological function. To apply genetic selections directly to populations of molecules, genotype and phenotype must be linked. In fact, oligonucleotides combine phenotype and genotype within one molecule. This means that every individual oligonucleotide not only forms a distinct three-dimensional structure that is able to interact specifically with a potential target by shape complementarity, but at the same time contains the necessary information for its own propagation (Gold *et al.,* 1995).

High affinity molecules can be isolated from a library of completely random sequences that were generated by chemical synthesis. The initial library of oligonucleotides typically consists of a large number ($10^{15}$ to $10^{16}$) of random sequences. In principle, larger libraries of up to $10^{20}$ oligonucleotides are technically feasible (Gold et al., 1995), but are rarely used in practice. Alternatively, a library based on a given secondary structure can be generated by mutagenesis. In most cases, the selection starts with a library of sequences that are completely random except for the flanking constant regions. This allows for a maximally unbiased sampling of the sequence space. Since the large initial pool of oligonucleotides typically saturates the relevant sequence space, the strongest binders already exist in the starting pool (Djordjevic, 2007).

A typical process of *SELEX* of ssDNA aptamers is outlined in Figure 1-3. A DNA library is chemically synthesized with a region of random sequence flanked on each end by constant sequences. This DNA is amplified by a few cycles of the polymerase chain reaction (PCR). Subsequently ssDNA is obtained either by separation of unequal-length strands or digestion of one strand by an exonuclease. The ssDNA molecules are then partitioned based on whether they bind to the chosen target compound, *e.g*. by passing them through a target affinity column. The bound ssDNAs are eluted, amplified by PCR, and then the entire cycle is repeated. The ratio of target binding increases with successive rounds of selection. After several rounds, the pool becomes potentially dominated by the initially rare molecules that can bind to the target. The double-stranded DNA

(dsDNA) that is generated in the last selection round is cloned and sequenced after sufficient enrichment. Consensus primary and secondary structure motifs are then analyzed on the basis of the alignment of cloned sequences. Subsequently, the aptamers are characterized with respect to the minimal sequence length that is indispensable for interacting and binding the target.

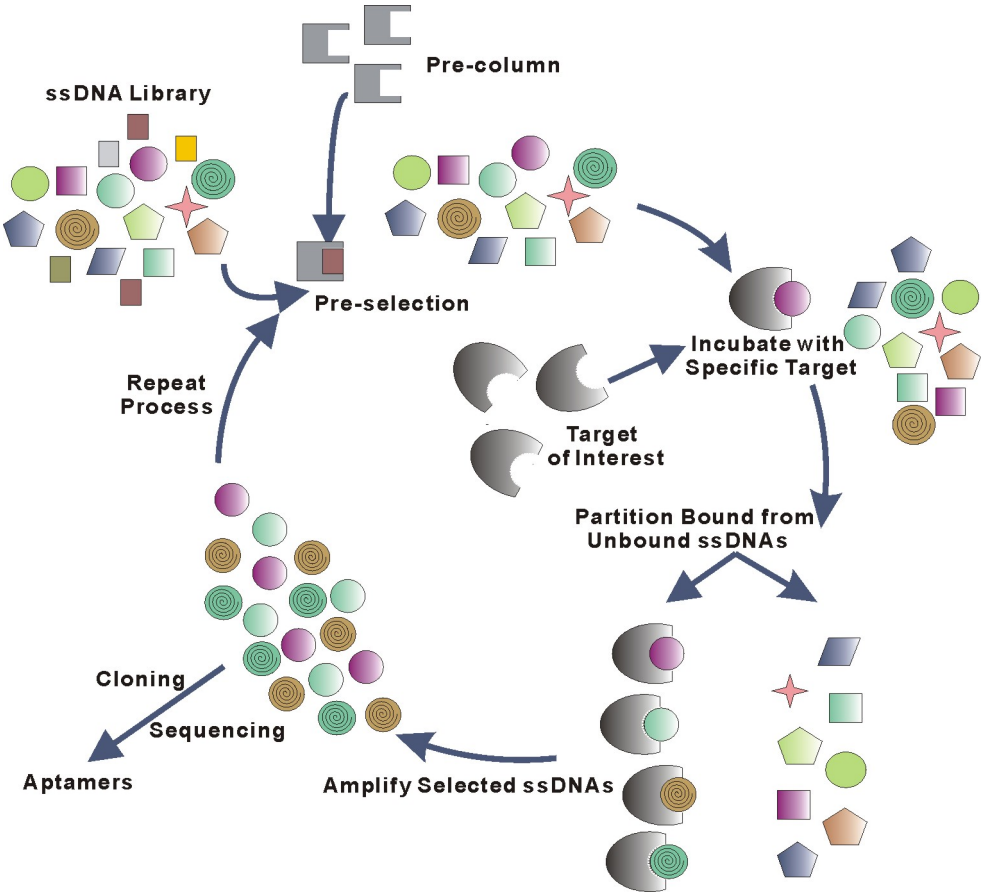


***Fig. 1-3 In vitro selection cycle (adapted from White et al., 2000).***

Both RNAs and ssDNAs can be designed by *in vitro* selection. RNAs have riboses containing 2'-hydroxyl groups, which are absent in ssDNAs, and can fold into more stable complex tertiary structures than ssDNAs. However, ligand-binding ssDNAs may be sometimes more suitable than RNAs as potential pharmacological reagents, because of their greater chemical stability and lower production costs (Ellington and Szostak, 1992).

### 1.2.2 Stability of Aptamers

Aptamer biostability and bioavailability are very important for later diagnostic and therapeutic applications. However, the omnipresence of degrading enzymatic activities by nucleases accounts for rapid decomposition of oligonucleotides, especially in biological systems. Considerable improvements have been made over the past few years to the biostability of nucleic acid aptamers (Bunka and Stockly, 2006; Stoltenburg *et al*., 2007).

Chemically modified oligonucleotide libraries compatible with polymerases were used to increase the nuclease resistance. Typical modifications concern the 2'-position of the sugar in RNA libraries. Frequently, the ribose 2'-OH group of pyrimidine nucleotides is replaced with a 2'-$NH_2$ or 2'-F group. Modifications of the phosphate backbone of nucleic acids were also applied to *in vitro* selections of aptamers. A common modification is the replacement of the non-binding oxygen in the phosphodiester linkage by sulfur (Jhaveri *et al*., 1998; Andreola *et al*., 2000; King *et al*, 2002).

After a successful selection, further chemical modifications can be introduced in order to enhance biostability of the aptamers. For instance, a substitution of the 2'-OH groups of ribose to 2'-F, 2'-$NH_2$ or 2'-O-methyl groups increases the nuclease resistance of RNA (Green *et al*., 1995; Ruckman *et al*., 1998; Rhodes *et al*., 2000). The modification can also be made by a 3'-end capping with streptavidin-biotin, inverted thymidine (3'-idT that creates a 3'-3' linkage) or several 5'-caps (amine, phosphate, polyethylene-glycol, cholesterol, fatty acids, proteins, *etc*.), to protect from exonuclease degradation (Dougan *et al*., 2000; Marro *et al*., 2005). In addition, locked nucleid acids (LNAs) (Petersen and Wengel, 2003) are good candidates to stabilize aptamers. In LNA nucleotides, the sugar is made bicyclic by covalently bridging the 2'-oxygen and the 4'-carbon with a methylene (Darfeuille *et al*., 2004; Schmidt *et al*., 2004). This modification was successfully introduced after a selection to improve the properties of aptamers.

Another elegant possibility to achieve biostability is the use of mirror-image oligonucleotides (Klussmann *et al*., 1996; Nolte *et al*., 1996). They are not susceptible to nucleases since nature did not evolve any respective enzymatic degrading activities. By mirror-image *in vitro* selection, unmodified DNA or RNA aptamers were isolated against the non-natural enantiomeric configuration of the target. After the *SELEX* experiment, the best candidates of aptamers are finally

synthesized using L-phosphoramidite building blocks in order to generate L-RNA- or L-DNA-oligonucleotides. By rules of symmetry, these L-oligocucleotides bind to the target in its natural configuration. Originally, biostable mirror-image aptamers were selected against the nucleoside adenosine (Klussmann *et al*., 1996) and the amino acid arginine (Nolte *et al*., 1996), and the term ‘‘Spiegelmer’’ (Spiegel is the German word for mirror) was coined to differentiate a ‘‘mirror-image aptamer’’ from a ‘‘normal aptamer’’. For all mirror-image *in vitro* selections, the mirror image of a given target molecule needs to be synthetically available. Therefore, peptides as well as small protein targets are synthesized by solid-phase peptide synthesis with unnatural building blocks. However, for larger protein targets, protein domains have to be identified that can be accessed by chemical synthesis.

### 1.2.3 Aptamers against Peptides and Proteins

Aptamers can be developed for molecules connected with nucleic acids, but also for molecules not associated with nucleic acids by nature. Single-stranded oligonucleotides can be selected to bind with high affinity to diverse targets such as organic dyes, amino acids, antibiotics, peptides, proteins, or vitamins. But so far most of the aptamers were selected for proteins or for peptides as special epitopes of a protein of interest. The reason for this is that proteins carry out a particularly wider range of structural and catalytic roles in biology and are extensively used in diagnostic, therapeutic and industrial applications. Great interest has also been generated in the development of methods for *in vitro* selection and directed evolution of proteins (Roberts and Szostak, 1997; Keefe and Szostak, 2001; Lamla and Erdmann, 2003).

Aptamers bind to their targets by a combination of complementarities in shape, stacking interactions between aromatic compounds and the nucleobases of the aptamers, electrostatic interactions between charged groups or hydrogen bondings (Patel, 1997; Patel *et al.,* 1997; Hermann and Patel, 2000). Numerous selections to a broad spectrum of proteins have now been reported, and it appears that it is possible to find high-affinity nucleic acid aptamers for most proteins (Gold *et al.,* 1995, Wilson and Szostak, 1999; Klussmann, 2006; Djordjevic, 2007; Stoltenburg *et al.,* 2007; Erdmann, 2008). Examples of peptide and protein targets are summarized in Table 1-1.

***Table 1-1 Examples of peptide and protein targets for in vitro selection***

| *Target* | *Aptamer* | $K_D$ | *References* |
|---|---|---|---|
| ***Peptides and Proteins:*** | | | |
| T4 DNA polymerase | RNA | 5-30 nM | Tuerk and Gold, 1990 |
| α-Thrombin | DNA | 200 nM | Bock *et al*., 1992 |
| | RNA | <1-4 nM | White *et al*., 2001 |
| HIV-1 RT | RNA | ~5 nM | Tuerk *et al*. 1992 |
| | DNA | ~1 nM | Schneider *et al*., 1995 |
| | DNA | 180-500 pM | Mosing *et al*., 2005 |
| Bacteriophage R17 Coat Protein | RNA | 5.4 nM | Schneider *et al*., 1992 |
| Rho (E. Coli) | RNA | 1 nM | Schneider *et al*., 1993 |
| VEGF | RNA | 0.1-2 nM | Jellinek *et al*., 1994 |
| | RNA | 50-130 pM | Ruckman *et al*., 1998 |
| | DNA | 130-500 nM | Ikebukuro *et al*., 2007 |
| HIV-1 integrase | RNA | 10-800 nM | Allen *et al*., 1995 |
| Substance P | RNA | 190 nM | Nieuwlandt *et al*., 1995 |
| | L-RNA | 40 nM | Eulberg *et al*., 2005 |
| Basic fibroblastic growth factor | RNA | 350 pM | Jellinek *et al*., 1995 |
| Immunglobulin E | RNA | 30-35 nM | Wiegand *et al*., 1996 |
| | DNA | 10 nM | Wiegand *et al*., 1996 |
| | DNA | 23-39 nM | Mendonsa and Bowser, 2004 |
| HIV-Rev | RNA | 19-36 nM | Xu and Ellington, 1996 |
| PDGF | DNA | 100 pM | Green *et al*., 1996 |
| L-Selectin | DNA | 1.8-5.5 nM | Hicke *et al*., 1996 |
| Taq DNA polymerase | DNA | 0.04-9 nM | Dang and Jayasena, 1996 |
| Interferon-γ | RNA | 2.7 nM | Kubik *et al*., 1997 |
| Vasopressin | L-DNA | 1.2 µM | Williams *et al*., 1997 |
| P-Selectin | RNA | 19-39 pM | Jenison *et al*. 1998 |
| C5 protein | RNA | 2-5 nM | Biesecker *et al*., 1999 |
| Factor VIIa | RNA | 11 nM | Rusconi *et al*., 2000 |
| ppERK2/ERK2 | RNA | 4.7-50 nM | Seiwert *et al*., 2000 |
| Oncostatin M | RNA | 7 nM | Rhodes *et al*., 2000 |
| HIV-1 Tat | RNA | 120 pM | Yamamoto *et al*., 2000 |
| MCP-1 (mouse) | RNA | 180-370 pM | Rhodes *et al*., 2001 |
| Microcystin | DNA | 1 mM | Nakamura *et al*., 2001 |
| Streptavidin | RNA | 70-200 nM | Srisawat and Engelke, 2001 |
| | RNA | 7 nM | Tahiri-Alaoui *et al*., 2002 |
| | DNA | 57-85 nM | Stoltenburg *et al*., 2005 |

***Tabel 1-1 (continued)***

| ***Taget*** | ***Aptamer*** | ***$K_D$*** | ***References*** |
|---|---|---|---|
| Prion protein ($PrP^C$) | RNA | 0.1-1.7 nM | Proske *et al*., 2002 |
| GnRH | L-RNA | 190 nM | Leva *et al*., 2002 |
| | L-DNA | 45 nM | Wlotzka *et al*., 2002 |
| Amyloid peptide βA4(1-40) | RNA | 29-48 nM | Ylera *et al*., 2002 |
| Neurotensin receptor NTS-1 (rat) | RNA | 370 pM | Daniels *et al*., 2002 |
| Factor IXa | RNA | 650 pM | Rusconi *et al*., 2002 |
| Angiopoietin-2 | RNA | 2.2 nM | White *et al*., 2003 |
| RNase H1 | DNA | 10-80 nM | Pileur *et al*., 2003 |
| Bovine thrombin | RNA | 164-240 nM | Liu *et al*., 2003 |
| $PrP^{sc}$ fibrils | RNA | 23.4 nM | Rhie *et al*., 2003 |
| Neuropeptide calcitonin gene-related peptide 1 | RNA | 2.5 nM | Vater *et al*., 2003 |
| Colicin E3 | RNA | 2-14 nM | Hirao *et al*., 2004 |
| Ghrelin | RNA | 35 nM | Helmling *et al*., 2004 |
| Neuropeptide nociceptin/orphanin FQ | RNA | 300 nM | Faulhammer *et al*., 2004 |
| HGF | DNA | 19-25 nM | Saito and Tomida, 2005 |
| Hepatitis C virus NS3 helicase | DNA | 140 nM | Zhan *et al*., 2005 |
| Hepatitis C virus RdRp | DNA | 1.3-23.5 nM | Jones *et al*., 2006 |
| Protein kinase C delta | DNA | 122 nM | Mallikaratchy *et al*., 2006 |
| Tumor marker MUC1 | DNA | 0.1-34 nM | Ferreira *et al*., 2006 |
| ***Transcription factors:*** | | | |
| E2F | RNA | 4 nM | Ishizaki *et al*., 1996 |
| | RNA | 100 pM | Giangrande *et al*., 2007 |
| NF-κB | RNA | 1.34 nM | Lebruska *et al*., 1999 |
| | RNA | 10-40 nM | Wurster and Maher *et al*., 2008 |
| TTF1 | DNA | 3.3-67 nM | Murphy *et al*., 2003 |
| TBP (yeast) | RNA | 3-10 nM | Fan *et al*., 2004 |
| HSF | RNA | 20-40 nM | Zhao *et al*., 2006 |
| TFIIB | RNA | 1 nM | Sevilimedu *et al.,* 2008 |
| ***Zinc finger peptides or proteins:*** | | | |
| WT1 | RNA | 700 nM | Bardeesy and Pelletier, 1998 |
| | RNA | 13.8-87.4 nM | Zhai *et al*., 2001 |
| HIV-1 nucleocapsid protein | RNA | 0.84-1.4 nM | Kim *et al*., 2002<br>Kim and Jeong, 2003<br>Jeong *et al*., 2008 |
| TFIIB | RNA | 1 nM | Sevilimedu *et al.,* 2008 |

Since small peptides are less complex targets than proteins and can also be synthesized chemically, aptamers were selected successfully against some peptides. A small peptide like substance P has been used as a target for selection (Nieuwlandt *et al*., 1995). Xu and Ellington (1996) have selected aptamers against a peptide fragment of the Rev protein of human immunodeficiency virus type 1 (HIV-1). Amyloid peptide β A4 (1-40), which is involved in the pathology of Alzheimer's disease by deposition in the brain, has been studied as a target to select high-affinity RNA aptamers (Ylera *et al.,* 2002). In addition, biostable L-RNA spiegelmers were designed for several peptide targets: GnRH, neuropeptide CGRP1, neuropeptide N/OFQ, Ghrelin, and substance P (Wlotzka *et al*., 2002; Vater *et al*., 2003; Faulhammer *et al*., 2004; Helmling *et al*., 2004; Eulberg *et al*., 2005).

As mentioned above, most of the aptamers were selected for proteins. However, only a few of them have been generated against transcription factors that recognize specific DNA sequences. RNA ligands were isolated that bind to the E2F family of proteins and these RNAs succesfully blocked E2F binding to its DNA binding site (Ishizaki *et al*., 1996; Giangrande *et al*., 2007). Other well known examples are RNA aptamers specific for either the p50 and p65 subunit of the classical NF-κB heterodimer (Lebruska and Maher, 1999; Wurster and Maher, 2008). In addition, DNA aptamers were selected to recognize specifically the thyroid transcription factor 1 (TTF1) (Murphy *et al*., 2003). Fan and colleagues (2004) generated RNA aptamers against the yeast transcription factor TATA-binding protein (TBP), which inhibit transcription in crude cell extracts. Furthermore, RNA aptamers were selected against the heat shock factor (HSF) transcription activator (Zhao *et al.,* 2006). It seems that the selection of aptamers against different transcription factors is just at the beginning.

Although $Cys_2His_2$-type *zf* proteins form the most abundant family in transcription factors and are potential biomarkers in cancer and other diseases, few selections have been used to identify aptamers that bind to these *zf* proteins. Three selections of RNA aptamers have previously been performed, which are capable of binding to *zf* proteins: WT1 (Bardeesy and Pelletier, 1998; Zhai *et al*., 2001), HIV-1 nucleocapsid protein (Kim *et al*., 2002; Kim and Jeong, 2003; Jeong *et al*., 2008), and TFIIB (Sevilimedu *et al.,* 2008). However, among these *zf* proteins, only the WT1 transcription factor contains four contiguous classical *zf*s of

the $Cys_2His_2$-type. Aptamer selection against a single *zf* motif has so far not been demonstrated yet.

The single *zf* motif is, however, an attractive and challenging target for selection. Many selection results provide support for the concept that DNA-binding domains in transcription factors tend to be included in the preferred (RNA) aptamer binding site, when transcription factors are the target of (RNA) aptamer selection (Lebruska and Maher, 1999; Cassiday and Maher, 2002; Huang *et al*., 2003; Zhao *et al*., 2006). Since *zf* transcription factors are very complex targets for developing molecular ligands, *zf* domains containing normally multiple zinc fingers would be the best choice as the preferred target. On the other side, as mentioned previously a single $Cys_2His_2$ *zf* peptide already forms a stable tetrahedral structure with the help of metal ion-coordination and the *zf* motif is highly conserved in many *zf* proteins. Friesen and Darby (2001) reported that a single $Cys_2His_2$ *zf* can be sufficient to confer RNA binding. Therefore, specific aptamers for recognition of *zf* transcription factors seem feasible to be constructed for a single *zf* motif. These aptamers will help to study the interaction of a single *zf* motif to nucleic acids and will have further value to identify natural binding sequences for that specific motif. Once aptamers are selected against a single peptide with a well-ordered *zf* structure, there is a fair chance that the *zf* structure could be recognized by aptamers in proteins containing related *zf*s. Such *zf*-binding ligands will be very useful for diagnostic and even therapeutic applications in related diseases, especially cancer.

### 1.2.4 Applications

Aptamers have high affinities comparable to those observed for monoclonal antibodies, but inherit many advantages over antibodies. For instance, aptamers have high reproducibility in their production and seem not to be immunogenic. They can distinguish between chiral molecules and recognize a distinct epitope of a target molecule (Jenison *et al.,* 1994; Michaud *et al.,* 2003). In addition, *SELEX* of aptamers is the selection of ligands beyond natural systems by use of chemically produced oligonucleotide libraries. The properties of aptamers can be changed and further modified on demand. Selection conditions can be manipulated to obtain aptamers with properties desirable for *in vitro* diagnostics. Toxins as well as molecules that do not elicit good immune responses can be used

to generate high-affinity aptamers. Moreover, little or no batch-to-batch variation is expected in aptamer production. They can maintain structure and function by being denatured and regenerated carefully, which can be a problem with antibodies (Mukhopadhyay, 2005). They are also stable to long-term storage and can be transported at ambient temperature (Jayasena, 1999; Stoltenburg *et al.,* 2007). Therefore, aptamers have important research, diagnostic and therapeutic applications.

For research applications, *in vitro* selection is widely used to recognize RNA motifs to which a given protein binds strongly (Djordjevic, 2007). Catalytic nucleic acid aptamers can also be identified by *SELEX*. Aptamers are often able to interfere with a biological function of the target molecule and can be widely used in medical and pharmaceutical research.

Aptamers can also be used in diagnostic applications, as an alternative to antibodies, and also in analytical chemistry, with applications that range from separation techniques (affinity chromatography, affinity capillary electrophoresis, capillary electrochromatography, and flow cytometry) to biosensors (Kleinjung *et al*., 1998; Erdmann *et al*., 2006; Stoltenburg *et al*., 2007; Djordjevic, 2007). Most diagnostic applications of aptamers rely on ligand-induced conformational changes, so called ‘aptamer beacons’. Aptamer-based microarrays are now being developed (Collett *et al*, 2005; Yamanomo-Fujita and Kumar, 2005; Cho *et al*., 2006). An interesting development in the diagnostic application of aptamers was recently reported in a simple assay based on ligand interactions with aptamers bound to the surface of gold nanoparticles (Liu and Lu, 2006). The broad market of immunological diagnostics in the medical area will create an increasing competition between antibody- and aptamer-based test kits. The enzyme linked oligonucleotide assay (ELONA), based on ELISA technology, is one example for using aptamers instead of antibodies (Drolet *et al.,* 1996). It is therefore highly likely that aptamers will be used in standardized diagnostic test kits in the near future (Stoltenburg *et al*., 2007).

For therapeutic applications, several aptamers, which are known to inhibit various target proteins, are currently tested in pre-clinical and clinical trials. As far as these targets mediate the control of the expression of a gene, the cognate aptamers constitute specific artificial modulators of biological processes, mimicking the behavior of decoy or antisense sequences. As specific binders, aptamers are

potential inhibitors of protein function. Aptamers, selected *in vitro* against a purified peptide or protein, retain their binding efficacy on endogenous targets and may modulate their biological functions. The first approved aptamer with therapeutic function is an anti-human vascular endothelial grow factor (VEGF) aptamer (Tucker *et al.,* 1999). The PEGylated form of this aptamer was called Pegaptanib and is used as the medicinal active component of the newly developed drug for the treatment of wet age related macular degeneration. The pharmaceutical product Macugen® (pegaptanib sodium injection) from Pfizer Inc./OSI Pharmaceuticals was approved in December 2004 for USA and in January 2006 for Europe (Maberley, 2005; Chapman and Beckey, 2006).

Despite these very encouraging achievements, research on aptamers is still at the beginning. One disadvantage is the unavailability of a standardized protocol for aptamer development, which is applicable without specific modifications for different targets (Stoltenburg *et al.,* 2007). Efficiency of aptamers in diagnostic and therapeutic applications should be enhanced by chemical modifications that provide resistance of oligonucleotides against enzymatic degradation in body fluids. To obtain highly stable molecules, mirror-image *in vitro* selection was developed. This procedure leads to Spiegelmers, which have all of the diversity characteristics of aptamers, but possess a structure with unsurpassed stability that prevents enzymatic degradation. Due to their highly nuclease-resistant properties, Spiegelmers have a promising future in aptamer-based applications.

# 2 Task

The central task of this thesis is the isolation and characterization of DNA aptamers for zinc finger (*zf*) proteins. The $Cys_2His_2$ *zf* class of DNA binding proteins is the most abundant class of transcription factors and largely involved in development and diseases, including cancer. Therefore, *zf* proteins are potential biomarkers for distinguishing different types of cells, such as normal vs. tumor cells, or even different types of stem cells. *Zf* transcription factors, however, are very complex targets for developing molecular ligands. Since a single *zf* peptide already forms a stable tetrahedral structure by metal ion-coordination, it seems feasible to construct specific molecular ligands for *zf* peptides in order to recognize transcription factors. However, very few *zf* proteins have been applied for aptamer selection. So far, aptamer selection against a single *zf* motif has not been demonstrated yet.

With the help of *in vitro* selection (*SELEX*), DNA aptamers will be isolated against two *zf* peptide targets of choice in two separated processes. Both of the targets, ZFY and GLI, belong to the Krüppel $Cys_2His_2$ –type *zf* protein family and their correct tetrahedral folding in solution will be confirmed by experimental data. The selection protocol will be established and optimized. After the repeated cycles for enrichment, DNA molecules will be sequenced and characterized. The binding constants will be determined, the effect of metal binding will be investigated and the possible binding motif will be studied. In addition, the results from two selections will be compared.

Once aptamers are raised against a *zf* structure, there is a fair chance that the *zf* structure will be recognized within the context of the whole protein with even related *zf*s. Therefore aptamers with higher affinities to *zf* peptides will be tested whether they bind to the whole protein or even a protein with related $Cys_2His_2$ *zf*. Moreover, a more complex mixture of proteins will be accounted for later possible employment of isolated aptamers, such as in diagnosis. However, no assay has been described yet for aptamer affinity capture of zinc finger proteins or transcription factors directly from cell extract or nuclear extract. In this work aptamer affinity capture assays will be established from a complex mixture of proteins in the cell extract or nuclear extract. The isolated proteins will be identified and analyzed.

# 3 Methods

## 3.1 Molecular Biological Methods

### 3.1.1 DNA Amplification

Different PCR set-ups in different *SELEX* processes were applied for diverse amplification purposes. A thermostable DNA polymerase from the *Thermus aquaticus*, GenTherm$^{TM}$ DNA polymerase (Rapidozym), was used for DNA extension. For preparative PCR, the PCR product was purified by denaturing polyacrylamide gel electrophoresis, unless a different protocol is given.

**Normal PCR:** After each round of selection, the eluted single-stranded (ss)DNAs were amplified for the next round. In addition, the clones and aptamers were also amplified by PCR for different binding tests and characterization. Radioactive [α-$^{32}$P]-dCTPs (Amersham) were used in addition to the dNTPs in the PCR reaction for the radioactive labeling of oligonucleotides. In Tables 3-1 and 3-2, the protocol of PCR reaction and the temperature program are listed. For the experiments described below these protocols were applied, unless other descriptions are given.

***Table 3-1 Protocol of a 100 µl normal PCR***

| Components | Amounts (µl) | End Concentration |
|---|---|---|
| DNA template | | 1-10 pmol |
| 100 µM Forward primer | 3 | 3 µM |
| 100 µM Reverse primer | 3 | 3 µM |
| 50 mM $MgCl_2$ | 4 | 2 mM |
| dNTPs (25 mM) | 0.8 | 0.2 mM |
| 10x PCR reaction buffer | 10 | 1x |
| GenTherm$^{TM}$ polymerase | 1 | 5 U/100µl |
| add dd $H_2O$ to 100 µl | | |

***Table 3-2 PCR program***

| Temperature (ºC) | Time (min) | Cycles |
|---|---|---|
| 95 | 3-5 | |
| 95 | 1 | |
| 62 | 0.5 | 19 x |
| 74 | 0.5 | |
| 74 | 4 | |
| 4 | End | |

**Preparative PCR for First Round:** The reaction condition and temperature program for the preparative PCR for the first round are shown in Tables 3-3 and 3-4. The concentrated primers and prolonged extension times were employed to ensure that each DNA template was amplified.

***Tabel 3-3 Protocol for a 100 µl preparative PCR***

| Components | Amounts (µl) | End concentration |
|---|---|---|
| DNA template | | 20 pmol |
| 100 µM Forward primer | 5 | 5 µM |
| 100 µM Reverse primer | 5 | 5 µM |
| 25 mM $MgCl_2$ | 8 | 2 mM |
| dNTPs (25 mM) | 1 | 0.25 mM |
| 10x PCR reaction buffer | 10 | 1x |
| GenTherm™ polymerase | 1 | 5 U/100µl |
| add dd $H_2O$ to 100 µl | | |

***Table 3-4 PCR program***

| Temperature (ºC) | Time (min) | Cycles |
|---|---|---|
| 95 | 5 | |
| 95 | 1.5 | |
| 62 | 1.5 | 15 x |
| 74 | 10 | |
| 4 | End | |

**PCR for Amplification of Cloned Sequences:** The supernatant (2 µl) of the boiled cells from each clone was used as a template for a 25 µl PCR reaction. The DNA library served as a positive control and a sample without DNA template was included as a negative control. The forward and reverse primers of the original DNA library were used to amplify the designed DNA fragment. Afterwards the PCR products were analyzed on a 2% agarose gel. The clones, of which the PCR products displayed a correct band of the length of the inserted DNA fragment, were then further prepared for sequencing.

**PCR for Sequencing:** For sequencing of the positive clones, a pUC/M13 primer was used for PCR as a forward or a reverse primer. The supernatant (2 µl) of the boiled cells from each positive clone was added to a 25 µl PCR reaction. The PCR products were purified by Nucleospin® Extract II (MACHEREY-NAGEL) according to the manufacturer's protocol.

**PCR with Unequal-Length Primers for the Production of ssDNAs:** During the selection cycles ssDNAs were obtained by PCR with unequal-length primers (Figure 3-1; Williams and Bartel, 1995). Two strands of doube-stranded (ds)DNA with different length have different separation behaviors in a denaturing PAGE; therefore, they were readily separated by PAGE.

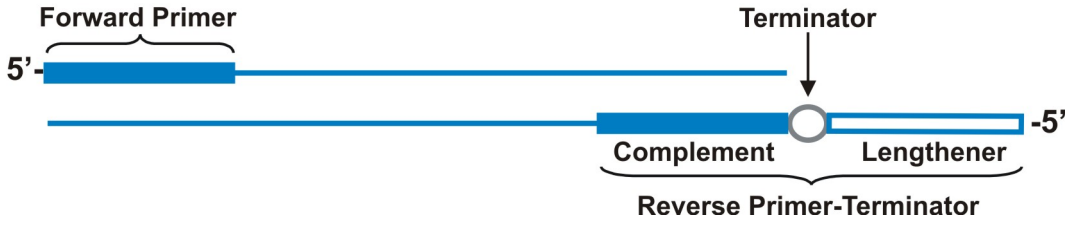


***Figure 3-1 The principle of PCR with unequal-length primers.*** *The reverse primer-terminator has a complement segment (reverse primer), terminator (HEGL), and a lengthener segment (poly-dA$_{20}$).*

### 3.1.2 Digestion of Phosphorylated Strands of dsDNA

The selective digestion of phosphorylated strands was utilized to obtain ssDNA molecules for binding tests and aptamer characterization. With a phosphorylated reverse primer, dsDNA with a phosphorylated strand was prepared by PCR. Lambda exonuclease (Fermentas) was used to selectively digest the phosphorylated strand. The reaction mixture (Tab. 3-5) was incubated at 37ºC for 10 to 30 min. The reaction was stopped by heating at 80ºC for 10 min. The ssDNA product was purified by gel electrophoresis or by YM-spin columns (Millipore, see manufacturer's protocol).

***Table 3-5 Protocol for digestion by Lambda exonuclease***

| Components | Volumes | End Concentration |
|---|---|---|
| 10x Digestion buffer | 5 µl | 1 x |
| dsDNA | | 40 ng/µl |
| Lambda exonuclease (10U/µl) | 1 µl | 0.2 U/µl |
| | add dd$H_2O$ to 50 µl | |

### 3.1.3 Gel Electrophoresis

#### 3.1.3.1 Denaturing Polyacrylamide Gel Electrophoresis (PAGE)

Denaturing PAGE was used for the analysis or purification of PCR or enzyme digestion products. For DNA or RNA molecules of 20-90 nucleotides in length, 10% gels were prepared (Tab. 3-6). TBE buffer (1x) was used as running buffer. The DNA and RNA samples were prepared in 10 µl of (1x) loading buffer for urea PAGE and heated to 95°C for 3 min. A voltage of 500-600 V (25-30 mA) was applied to the gel for 3-5 h. Following the separation, the gel was stained, the bands visualized, and a digital record of the gel made. For the preparative purification of DNA, the bands were excised from the gel and the DNA was extracted from the gel pieces.

***Table 3-6 Protocol for 10% Denaturing Polyacryamide Gel (8.3 M Urea)***

| Components | 10% |
|---|---|
| 30% Acrylamide/Bisacrylamide (37.5:1) | 33.3 ml |
| Urea | 49.85 g |
| 10x TBE buffer | 10 ml |
| 10% (w/v) APS | 0.8 ml |
| TEMED | 80 µl |
| | add $ddH_2O$ till 100 ml |

#### 3.1.3.2 Agarose Gel

The analysis of PCR products, the purification of plasmids and PCR products for ligation occurred on agarose gels. Agarose gels (2%) were used for DNA fragments of about 90-200 nt. Agarose powder (1 g) was mixed with 50 ml TAE buffer to prepare the gel solution. Samples were mixed with loading buffer for the agarose gel and a current of 110 V was applied.

#### 3.1.3.3 Denaturing SDS-PAGE

The running gel and the stacking gel solution were prepared as shown in Table 3-7. The protein samples were mixed with an appropriate volume of 1x loading buffer for SDS gel and heated to 95ºC for 3 min to denature the proteins. The gel was run under 20 mA and 60 V in a SDS gel electrophoresis buffer. After the dye front had moved into the running gel, the voltage was increased to 100-120 V. Finally, the

protein gel was stained by Coomassie Roti® Blue. The sensitivity of the method was below 30 ng of protein.

***Table 3-7 Protocol for preparing gels for SDS-PAGE***

| Gel components | Stacking gel 5% | Running gel 8% | Running gel 15% |
|---|---|---|---|
| Water | 1.7 ml | 3.45 ml | 1.75 ml |
| 1 M Tris-HCl, pH 6.8 | 0.315 ml | - | - |
| 1.5 M Tris-HCl, pH 8.8 | - | 1.9 ml | 1.9 ml |
| 10% (w/v) SDS | 0.025 ml | 0.075 ml | 0.075 ml |
| 30%/0.8% (w/v) Acrylamide/Bisacrylamide | 0.415 ml | 2 ml | 3.75 ml |
| 10% (w/v) APS | 0.05 ml | 0.075 ml | 0.075 ml |
| TEMED | 0.0025 ml | 0.0045 ml | 0.0075 |
| | 2.5 ml | 7.5 ml | 7.5 ml |

### 3.1.4 Detection of Nucleic Acids on Gel

#### 3.1.4.1 Ethidium Bromide Staining

Agarose or polyacrylamide gels were stained by soaking in a solution of EtBr (1 µg/ml in 1x TBE buffer) for 15 min and washed then with water for 2 min. To visualize DNA, the gel was placed on an ultraviolet transilluminator at 306 nm. The document and analysis of the gel image was achieved by a program of *Quantity one* from BioRad.

#### 3.1.4.2 UV Shadowing

UV shadowing was applied for the preparative purification of nucleic acids. The technique used shortwave UV light (254 nm) and a fluor-coated (60 F254) TLC plate. The polyacryamide gel was covered with plastic film after electrophoresis. The gel was then put on top of the fluor-coated TLC plate in a dark room. The nucleic acid bands, which were separated on the gel, were visualized by shining a UV-light source at 254 nm on the surface of the gel. The positions of the bands of desired nucleic acids were marked and the gel pieces were cut. This step was performed as quickly as possible to avoid the possible damage of nucleic acids under UV light. The detection limit of UV shadowing was approximately 0.3 µg nucleic acids.

#### 3.1.4.3 Autoradiography

Polyacylamide gels with [$^{32}$P]-labeled oligonucleotides were covered by a plastic film and marked by three phosphorescent markers. A sheet of X-ray film was placed on the gel and put in an X-ray film cassette in the darkroom. The gel and film were taped securely in place and imaged for a certain exposition time according to the strength of radioactivity (from 10 min to 24 h). However, for a longer exposition time, the gel has to be stored at -70ºC to prevent diffusion of nucleic acids. After the exposition time X-ray films were developed and fixed. For a preparative gel, the bands of nucleic acids were excised by the help of phosphorescent markers and the nucleic acids were eluted from gel sclices.

#### 3.1.4.4 Measurement of Radioactivity

Quantitative measurement of $^{32}$P-labeled nucleic acids was accomplished by Cherenkov-counting. The $^{32}$P-labeled samples were placed in glass scintillation vials, which were loaded in the scintillation counter (LS 6000 SC, Beckman) with a special program for $^{32}$P Cherenkov-counting. This program displays values in cpm (counts per minute). This value reflects the number of atoms that are detected by counter as decayed. However, only part of dpm (disintegrations per minute) can be measured as decayed under consideration of count efficiency rate.

cpm =count efficiency rate x dpm

Since the count efficiency rate is the same for all samples measured, values in cpm were used for calculation.

### 3.1.5 Gel Elution of Nucleic Acids

#### 3.1.5.1 Gel Elution of Nucleic Acids from Agarose Gel

The amplified dsDNAs from PCR products of enriched pools after *SELEX* experiments were resolved by an agarose gel. The bands were detected under UV light and removed from the gel. NucleoSpin® Extract II from MACHEREY-NAGEL was applied to elute the nucleic acids from the gel slices.

#### 3.1.5.2 Gel Elution of Nucleic Acids from Denaturing Polyacrylamide Gel

The bands of desired oligonucleotides were detected by autoradiography or UV shadowing. The bands were cut out by using a sharp razor blade and placed on a

glass plate. The gel slice was chopped into fine pieces and transferred to small tubes. Approximately 2 volumes of water were added to each tube and the whole mixture was shaken overnight at RT. The sample was then centrifuged at 12000 x g for 5 min. The supernatant was recovered. One additional volume of water was added to each pellet and shaken again for 2 h. The supernatants were combined after centrifugation. Alternatively, the sample was dried under vacuum to a proper volume and given to a gel filtration column to remove urea and salts. Finally the DNA was precipitated with ethanol.

### 3.1.6 Purification of Nucleic Acids

#### 3.1.6.1 Phenol-Chloroform Extraction

The phenol-chloroform extraction was carried out for the removal of proteins from the nucleic acids sample. Phase partitioning of nucleic acids is pH-dependent. The ready-to-use phenol:chloroform:isoamyl alcohol mixture (25:24:1) from Roth for DNA isolation is buffered to pH 8.0 and for RNA isolation pH 4.5. The nucleic acid solutions were mixed with an equal volume of the mixture. The whole sample was vortexed for one minute and then spun for another two minutes at 13000 x g. After carefully removing the aqueous layer to a new tube, the phenol layer was extracted again with an equal volume of water. The combined aqueous layers were mixed again with an equal amount of chloroform:isoamylacolhol (24:1). The whole mixture was vortexed for one minute and centrifuged once again. Traces of phenol remained in the organic solvent. The aqueous phase was precipitated with ethanol or concentrated by YM-spin filtration, so that traces of chloroform were also removed.

#### 3.1.6.2 Silica-Based Resin Purification

StrataClean$^{TM}$ resin (Stratagene) was used as an alternative and phenol-free technique for DNA purification to remove proteins. The protocol was performed according to the manufacturer's instruction.

#### 3.1.6.3 Gel Filtration

Nucleic acids were purified by gel filtration from other small molecular components. Standard gel filtration columns with Sephadex G-25 and G-50 material

from Amersham (NAP™ 5, 10, 25 or NICK™ column) were used. The protocol was performed according to the manufacturer's instruction.

#### 3.1.6.4 Ethanol Precipitation

Precipitation with ethanol was used to concentrate and purify nucleic acids. Ethanol (2.5 volumes) and NaOAc (3 M, pH 5.2, 0.1 volumes) were added to the solution of nucleic acids. Glycogen (1 µl of 20 mg/ml) was given into each 400 µl nucleic acid solution, to achieve a better yield for very small amounts of nucleic acids. The whole sample was mixed and stored for 2 h at -20ºC or overnight to let DNA precipitate. The solution was then centrifuged at 13000 x g for 30 min at 4ºC. The supernatant was discarded and the pellet was washed again with 70% ethanol. The mixture was centrifuged at 13000 x g for 20-30 min at 4ºC. The supernatant was discarded. The pellet was air-dried for 20 min, then dried under vacuum for another 2 min, and finally dissolved in a suitable volume of water or buffer.

### 3.1.7 Concentration Determination of Nucleic Acid Solutions

DNA or RNA samples were measured with a UV spectrophotometer (Shimadzu) from 220 nm to 320 nm of UV light. DNA with a slight impurity has an $A_{260}/A_{280}$ between 1.5 and 2.0. The concentration and quality of a sample were calculated by the absorption at 260 nm with the values listed as following (Sambrook and Russell, 2001):

| | |
|---|---|
| dsDNA | 1 $OD_{260\ nm}$ = 50 µg/ml |
| ssDNA | 1 $OD_{260\ nm}$ = 33 µg/ml |
| RNA | 1 $OD_{260\ nm}$ = 40 µg/ml |

### 3.1.8 Ligation

The PCR products of the enriched pools were inserted into pGEM®-T easy vector (Promega) by a ligation procedure. The T-vector cloning method was used, which is based on that *Taq* polymerase can add a single non template-directed deoxyadenosine residue to the 3' end of duplex PCR products (Clark, 1988). Such PCR products can be easily cloned into a vector with a 3' terminal thymidine to both ends. The reaction was carried out overnight at 4ºC (Tab. 3-8).

***Table 3-8 Protocol for DNA ligation***

| Components | Volumes | End Con. |
|---|---|---|
| pGEM®-T easy vector (50 ng/µl) | 1 µl | 50 ng |
| Insert DNA | | 15 – 25 ng |
| 10x T4 DNA ligase buffer | 1 µl | 1x |
| T4 DNA ligase (6 Weiss U/µl) | 1 µl | 0.6 Weiss U/µl |
| | | add $ddH_2O$ to 10 µl |

### 3.1.9 Transformation of Competent Cells

Following ligation the T-vector with the insert of interest was transformed into the *E. Coli* JM109 competent cells (Promega), in order to isolate and analyze the individual variants. For each transformation, the cells (50 µl) were mixed with 2 µl ligation mixture. The mixture was placed for 30 min on ice, heat shocked for 45 sec at 42ºC in a water bath and finally placed for another 2 min on ice. SOC medium (950 µl) was added to the sample and the mixture was incubated for 90 min at 37ºC with shaking at 150 rpm. The transformation mixture (200 µl) was plated onto a LB-agar plate. The plate was incubated overnight at 37ºC in an incubator.

### 3.1.10 Selection of Positive Clones

The anaylsis of the resultant colonies, to confirm whether cloning was successful, was accomplished by means of PCR. Single clones were amplified on LB agar plates and scratched from the plate. The cells from each clone were dissolved in 20 µl water and heated to 95ºC for 5 min. With this procedure, the cells were ruptured. The whole cell suspension was centrifuged in the end at 14000 x g for another 2 min. The supernatant contained the isolated plasmids, which were used as templates for PCR reaction to identify the successful inserts (see 3.1.1).

### 3.1.11 5'-labeling of Polyoligonucleotides

Polyoligonucleotides can be phosphorylated at the 5'-hydroxyl terminus with T4 polynucleotide kinase. The kinase catalyzes the transfer and exchange of γ-phosphate of ATP to the 5'-OH of polyoligonuleotides. As template served 5'-dephosphorylated ssDNA. The protocol is described in Table 3-9. The mixture was incubated for 30 min at 37ºC. Subsequently 1 µl of 0.5 M EDTA (pH 8.0) was added, and finally the mixture was heated for 10 min at 80ºC to stop the reaction.

***Table 3-9 Protocol for 5'-labeling***

| Components | Volumes | End Concentrations |
|---|---|---|
| 10x T4 polynucleotide kinase buffer | 2 µl | 1 x |
| ssDNA | | 1-20 pmol |
| T4 polynucleotide kinase (10 U/µl) | 1 µl | 0.5 U/µl |
| γ- 32P ATP (10 µCi/µl) | 0.5-1 µl | 5-10 µCi |
| | add $ddH_2O$ to 20 µl | |

## 3.2 Preparation of Peptide and Protein Targets

### 3.2.1 Peptide Synthesis

ZFY peptides were synthesized by Biosyntan and GLI peptides by Genosphere. The sequences of the synthesized peptides are shown in Table 3-10, which include an additional biotin at the N-terminus to enable the immobilization on Neutravidin agarose gels or Streptavidin magnetic beads. The ZFY peptide contains an amide group at the C-terminus.

***Table 3-10 The sequences of target peptides.***

| Peptide | Sequence |
|---|---|
| ZFY (30 a.a.) | Btn-Ahx-KTYQ**C**QY**C**EKRFADSSNLKT**H**IKTK**H**SKEK-Amide |
| GLI (29 a.a.) | Btn-Ahx-KPYV**C**KLPG**C**TKRYTDPSSLRK**H**VKTV**H**G |

*Btn = biotin; Ahx = 6-aminohexanoic acid.*

### 3.2.2 Peptide Reduction

Due to their cysteines, ZFY and GLI peptides are stable in solution under acidic conditions only. At higher pH, the peptides would be oxidized by atmospheric oxygen to form the dimer via disulfide bonds ($R\text{-}SH + R\text{-}SH \xrightarrow{\text{Oxidation}} R\text{-}S\text{-}S\text{-}R + 2H$). Tris(2-carboxyethyl)phosphine (TCEP) was used to reduce disulfide bonds in the oxidized peptides (Elise *et al.,* 1999; Fig. 3-2). Ten-fold molar excess of TCEP was added to the peptide solution and incubated for 1 h at 22 ºC (John *et al.,* 1991).

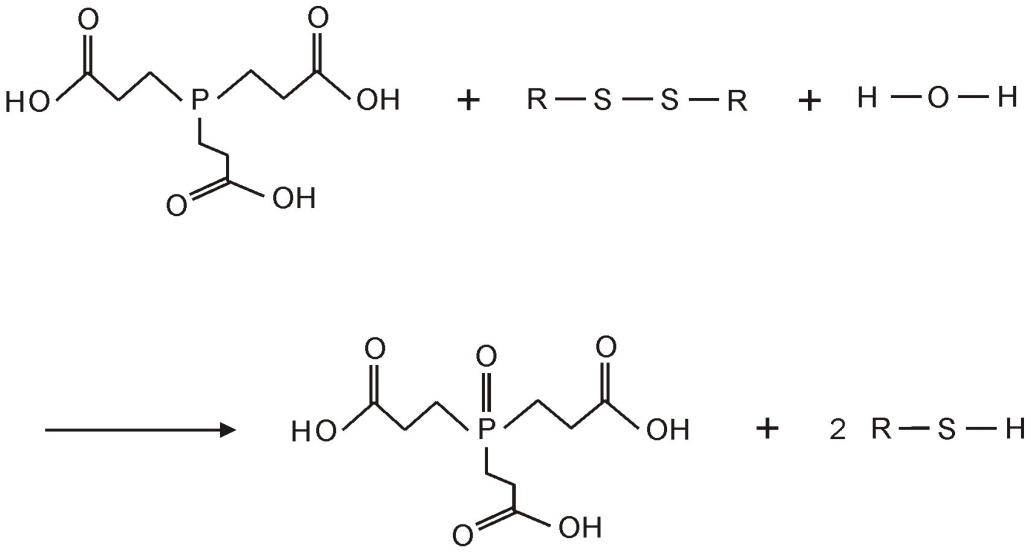


***Figure 3-2 Reduction of disulfides by TCEP.***

### 3.2.3 Analysis and Purification by HPLC

A reversed stationary phase, Luna C8 (10 µm) was applied on a HPLC-instrument (Thermo Separation Products) for analysis and purification of the peptides. The peptides (10 µl 1 mM) were injected into the HPLC and a gradient elution by 0-70% ACN in water was run over 30 min with a flow rate of 1 ml/min. The buffer was degassed before use. The eluted samples were determined by a diode-array detector (DAD) at 220 nm. The peaks were collected after the HPLC column. The sample of the reduced form was then injected directly again and that of oxidized form was divided into two parts: one of them was reduced with TCEP before injection and the second part was injected directly without reduction. For preparative HPLC, the synthetic peptides were reduced completely by TCEP and the peak of the reduced form with a retention time of 14.3 min was collected in a 1 ml reaction tube. The eluted samples in the solvent of acetonitrile/water/TFA were lyophilized in a SpeedVac concentrator (SC110AR, Savant) and weighed. To prevent reoxidation, the lyophilized samples were filled with argon and stored at -70ºC until further use. The HPLC experiments were performed in the work group of Prof. Dr. B. Koksch (FU, Berlin).

### 3.2.4 Concentration Determination of Protein Solutions

#### 3.2.4.1 UV Absorption

The protein solutions were measured in a UV spectrometer from a wavelength of 200 nm to 320 nm. The extinction coefficient of a given protein can be found in databases (e.g. Expasy). The extinction coefficients and molecular weights of ZFY and GLI peptides are listed in Table 3-11.

***Table 3-11 Extinction coefficients and molecular weights***.

| Peptides | $\varepsilon_{280}$ (cysteins) [$M^{-1}cm^{-1}$] | $\varepsilon_{280}$ (half cystines) [$M^{-1}cm^{-1}$] | M [g/mol]* |
|---|---|---|---|
| ZFY | 2560 | 2680 | 3631,1 |
| GLI | 2560 | 2680 | 3299,9 |

**molecular weight is calculated on the basis of the weights of the amino acids, but not other building blocks.*

#### 3.2.4.2 Bradford

Protein concentrations were also measured by the Bradford assay (Bradford, 1976). The concentration of protein can be calculated with BSA standard. For the standard curve, BSA was dissolved in 800 µl water and 200 µl Bradford reagents to have a concentration of 2 µg/ml to 25 µg/ml. The reaction mixtures were incubated for 10 min at RT and then measured at 595 nm in a spectrometer. To determine the concentration of protein samples, 50 µl were added to 750 µl water and 200 µl Bradford reagents. The concentration of protein samples was calculated by standard curve.

### 3.2.5 Preparation of $Zn^{2+}$-Coordinated Peptides

Lyophilized reduced peptides (1.2 mg ZFY and 2.1 mg GLI) were resuspended in degassed water to give a concentration of 1 mM. The peptide solutions were filled with argon, sealed and stored at -70ºC until use. The concentrations of the peptide solutions were confirmed by UV absorption.

Prior to use, the $Zn^{2+}$-coordinated ZFY or GLI peptides were prepared in 20 mM HEPES buffer to a concentration of 0.16 mM containing 0.4 mM $Zn^{2+}$ and 1.6 mM TCEP, pH = 7.5. The reaction tube was sealed and the mixture was incubated at 22ºC for 1 h. Thereby, a ten-fold molar excess of TCEP was used to reduce peptides

(see 3.2.2). A 2.5-fold molar excess of $Zn^{2+}$ ions were applied to ensure the formation of correct zinc finger structures (Kochoyan *et al.,* 1991a; Weiss *et al.,* 1990a). In addition, the zinc finger peptides have an optimal pH for metal coordination between 6.5-7.5 (Weiss and Keutmann, 1990b). However, the solubility of $Zn^{2+}$ ions is limited in a pH 7.5 buffer up to a concentration of 0.45 mM (calculated by equilibrium relation between $Zn^{2+}$ and $OH^-$). At higher concentrations $Zn^{2+}$ ions tend to precipitate out of solution.

### 3.2.6 Preparation of Nuclear and Cellular Proteins (Native)

To prepare nuclear extracts, HeLa cells (8 x $10^7$) were collected, which were cultured at 37ºC in M1 medium. The medium was aspirated off and the cells were washed in PBS. The cells were incubated with trypsin shortly at 37ºC and transferred into a Falcon tube. The suspension was centrifuged at 700 x g for 3 min, the pellet was washed twice in 10 ml iced PBS and resuspended in 1 ml iced PBS. This suspension was transferred into a 1.5 ml reaction tube. After centrifugation at 700 x g for 5 min at 4ºC, the cell pellet was resuspended in 500 µl of buffer A with fresh protease inhibitors (Wadman *et al.,* 1997) and incubated on ice for 15 min. NP-40 was added to a final concentration of 0.5% and this cell suspension was vortexed for 10 sec. The nuclei were precipitated by centrifugation at 6500 x g for 20 sec at 4 ºC, and resuspended in 100 µ buffer C with protease inhibitors. The nuclei suspension was incubated for 5 min on ice under continuous shearing by a syringe. The sample was centrifuged at 12500 x g for 10 min at 4ºC. Aliquots of the nuclear extract were frozen immediately under liquid nitrogen and stored at -80ºC till use. To prepare cellular extracts, the cell pellet collected was resuspended directly in 100 µl buffer C with fresh protease inhibitors. The cell suspension was passed repeatedly through a syringe needle for 10 min on ice and then centrifuged at 13000 x g at 4ºC. The resultant supernatant contained total cellular protein. To avoid oxidation of zinc finger proteins, TCEP (final conc. 0.5 mM) was added just before use into all buffers. Extracts were analyzed by SDS-PAGE and the protein concentrations of the extracts were determined by the Bradford assay.

### 3.2.7 Preparation of Cellular Proteins (Non-Native)

To detect small amounts of cellular proteins by western blotting, an extraction of non-native cellular proteins was done using SDS lysis buffer. Each 7 - 8 x $10^4$

HeLa cells were washed in PBS, added directly with 30 µl SDS lysis buffer containing DTT, and gently scraped down. The cell suspension was removed into a 1.5 ml reaction tube, heated to 95ºC for 5 min, quickly frozen in liquid nitrogen and then stored at -20ºC till use.

## *3.3* Systematic Evolution of Ligands by Exponential Enrichement

### 3.3.1 Immobilization of Biotinylated Zinc Finger Targets

#### 3.3.1.1 Neutravidin Agarose Column

Neutravidin (NA) agarose gels (Pierce) were used to immobilize biotinylated peptides during early cycles of selection (round 1-8), since abundant amounts of peptide target were applied. Neutravidin agarose gels (100 µl) were filled in spin columns (MoBiTec) with a small filter (10 µm pore size) and equilibrated with five column volumes of *SELEX* buffer (500 µl). The biotinylated peptide solution (34 µM) in 100 µl *SELEX* buffer was added and allowed to enter the gel bed. The bottom and top caps were replaced and incubated with slight rotation for 30 min at 4ºC. The gels were washed with three column volumes of *SELEX* buffer. To confirm binding of the peptide target to the column material the eluted fractions were analyzed via HPLC. In addition, to mimic the selection process 486 µl *SELEX* buffer (without DNA sample) were incubated with the gel-bound peptide with slight rotation for 1 h at 4ºC. The gels were washed again with three column volumes of *SELEX* buffer. Finally the eluted fractions after the mimic selection were also analyzed via HPLC, to ensure that the peptide target is still attached to the column material.

#### 3.3.1.2 Streptavidin Magnetic Beads

To immobilize biotinylated peptides, Streptavidin (SA) magnetic beads (Dynal) were applied during later cycles of selection (round 9-15) and also for binding tests of individual clones. Thereby, the bead concentration was kept at 10-50 mg/ml. The binding capacity of the beads to the biotinylated peptides was also addressed via HPLC. The beads (30 µl) were shaken gently, separated by a magnet separator for 2 min, washed twice with 150 µl *SELEX* buffer, then incubated with zinc finger peptides (45 pmol) for 40 min, and finally washed twice with 150 µl *SELEX* buffer. The eluted

fractions were collected for the measurement by HPLC to confirm the binding of the peptide target to the beads. The *SELEX* buffer (180 µl) was added to the beads containing target peptides (final conc. 0.25 µM). The mixture without DNA was incubated for 1 h at 4°C. Afterwards the beads were washed twice and the eluted solutions were also analyzed via HPLC.

### 3.3.2 Process of *in vitro* Selection

The chemically synthesized template-DNA (IBA GmbH) was amplified by preparative PCR with unequal length primers, in the presence of [α-$^{32}$P] dCTPs (3000 Ci/mmol, Amersham). The ssDNA was gel purified on a 10% denaturing polyacrylamide gel. A ratio of DNA to target 2:1 was used in the early two rounds. Later rounds would utilize lower target quantities to increase the stringency of *SELEX* at a time when the highest affinity ligands were numerically sufficient to survive a competitive binding situation. Therefore, a ratio of DNA to target of 4:1 was used in the later rounds (3$^{rd}$-15$^{th}$).

*1$^{st}$ Round:*

The DNA samples (20 µM) were heated to 95°C for 5 min, cooled to RT for 2 h and to 4°C.for 1 h. At the same time, fresh Neutravidin agarose gels (100 µl each) were filled in a spin column and equilibrated with five column volumes of *SELEX* buffer A. The equilibrated gels were resuspended in 85 µl *SELEX* buffer A, and 15.2 µl of 0.16 mM biotinylated peptides were added and mixed with slight rotation for 30 min at 4°C. The peptide-bound gels were then washed with three column volumes of *SELEX* buffer A. The radioactively labeled ssDNA library (243 µl 20 µM) was added to 243 µl of (2x) *SELEX* buffer A. The gel-bound peptides (2.43 nmol) were then added to this mixture and incubated with end-over-end rotation for 1 h at 4°C. The gels were washed with ten column volumes of *SELEX* buffer A. The bound ssDNA molecules were eluted three times with 200 µl of 8 M urea for 15 min at 90°C, precipitated by ethanol, and amplified by PCR. PCR products with unequal-length strands were separated by PAGE and ssDNA of 90 nucleotides was isolated for the next round.

*2$^{nd}$ -8$^{th}$ Rounds*:

Pre-selection against the partitioning matrix or alternate partitioning protocols can be important (Gold *et al.,* 1995). The pre-selection can exclude the DNA

molecules that bind to the matrix in an unspecific manner. In this work, no pre-selection was done in the first round for a lower stringency at the beginning, but started from the second cycle (Tab. 3-12). The DNA pool (5 µM) in *SELEX* buffer A was added to 50 µl gels and incubated with rotation in the absence of the peptides for 1 h at 4ºC. The eluted solution from the pre-selection was then added to the gel-bound peptides (200 pmol) in a 200 µl *SELEX* buffer A. The mixture was incubated with rotation for 1 h at 4°C. The gels were washed with ten column volumes of *SELEX* buffer A. The bound ssDNA molecules were eluted twice with 200 µl of 8 M urea. The amount of DNA varied due to the individual yields in different selection rounds (Table. 3-13).

The Neutravidin agarose gels were used in an excess to ensure that the immobilization of peptide was complete. The eluted target-bound DNAs were amplified by PCR, purified by PAGE and then the cycle was repeated.

*9-11$^{th}$ Rounds:*

Although pre-selection was performed, the amount of unspecific binders to gels increased during the early selection rounds. The Neutravidin agarose gels were, thus, replaced by Streptavidin (SA) magnetic beads (Dynal) starting from round 8 (Tab. 3-12). The DNA sample was denatured as in the first round. The magnetic beads (30 µl) were shaken gently and separated by the magnet separator for 2 min. The beads were then washed twice with 150 µl *SELEX* buffer A and mixed with DNA sample (final conc. of 5 µM). This mixture was incubated for 1 h at 4ºC. The tubes were applied to a magnet separator and the supernatant was removed. The peptides (40 pmol) were added to 30 µl fresh beads, incubated for 40 min and the beads were then washed twice with 150 µl *SELEX* buffer A. The supernatant from the pre-selection was added to the bead-bound peptides (final conc. of DNA 1 µM; of peptide 0.25 µM). The mixture was incubated for 1 h at 4ºC. The beads were then washed twice with 150 µl *SELEX* buffer A. Finally, the bound ssDNA molecules were eluted twice with 200 µl of 8 M Urea with vigorous shaking for 15 min at 90ºC.

*12-14$^{th}$ Rounds:*

A higher concentration of potassium ions was utilized in *SELEX* buffer starting from round 12, in order to decrease the unspecific binders due to ionic exchange (Tab. 3-12). The concentration of potassium ions was increased from 70 mM to

150 mM (*SELEX* buffer A to B). After 14 rounds, the enriched ssDNA pool was cloned and sequenced.

***Table 3-12 Overviews of four phases with increasing stringency in selection***

| Rounds | Pre-selection | Resin | Conc. ($K^+$) in Buffer |
|---|---|---|---|
| 1st round | No | NA agarose gel | 70 mM |
| 2nd-7th rounds | Yes | NA agarose gel | 70 mM |
| 8-11th rounds | Yes | SA magnetic bead | 70 mM |
| 12-14th rounds | Yes | SA magnetic bead | 150 mM |

***Table 3-13 Overview of the amount of ssDNA and zf peptide used in each round***

| Round | DNA (μM) pre-selection | DNA (μM) main-selection | Resin (μl) | ZFY or GLI (μM) | Molar Ratio DNA : Peptide |
|---|---|---|---|---|---|
| **1** | - | 10 | 100 | 5 | 2:1 |
| **2** | 5 | 4 | 50 | 2 | 2:1 |
| **3** | 5 | 4 | 50 | 1 | 4:1 |
| **4** | 5 | 4 | 50 | 1 | 4:1 |
| **5** | 5 | 4 | 50 | 1 | 4:1 |
| **6** | 5 | 4 | 50 | 1 | 4:1 |
| **7** | 5 | 4 | 50 | 1 | 4:1 |
| **8** | 5 | 1 | 30 | 0.25 | 4:1 |
| **9** | 5 | 1 | 30 | 0.25 | 4:1 |
| **10** | 5 | 1 | 30 | 0.25 | 4:1 |
| **11** | 5 | 1 | 30 | 0.25 | 4:1 |
| **12** | 5 | 1 | 30 | 0.25 | 4:1 |
| **13** | 5 | 1 | 30 | 0.25 | 4:1 |
| **14** | 5 | 1 | 30 | 0.25 | 4:1 |

## 3.4 Biochemical and Biophysical Methods

### 3.4.1 Circular Dichroism (CD)

CD spectra of 0.16 mM peptides in the presence or absence of 0.4 mM $ZnCl_2$ were measured in degassed water containing 1.6 mM TCEP, pH 7.0 adjusted by

NaOH, at 4ºC on a JASCO J-600 spectropolarimeter. Five sets of spectra were recorded from 250 to 200 nm at 0.2 nm resolution in a 0.1 cm quartz cell, and the spectra from the five scans were accumulated. Raw data were adjusted by smoothing and subtraction of blank spectra. CD values were expressed as the mean residue molar ellipticity, and the secondary structure contents were estimated by the PEPFIT program (Reed and Reed, 1997).

### 3.4.2 MALDI-TOF-MS

Matrix assisted laser desorption/ionization-time of flight-mass spectrometry (MALDI-TOF-MS) was applied to analyze peptide targets and to identify gel-resolved proteins by peptide mass fingerprinting.

Peptides ZFY and GLI (each 2 µl of 1 mM in 20 mM Tris-HCl) were diluted 100-fold with 40% ACN/TFA and then mixed with an equal amount of matrix CCA (α-cyano-4-hydoxy-cinnamic acid). The samples were then spotted on a MALDI target plate and measured on a Bruker Ultraflex II TOF/TOF instrument (Bruker Daltonics) in reflector mode. Peptides were measured before and after reduction by ten-fold molar excess of TCEP.

After affinity capture assays of nuclear or cellular proteins from HeLa cells using aptamers, MALDI-TOF-MS was applied for protein identification by peptide mass fingerprintings. The gel slices of the protein spots of interest were incubated with 20 µl acetonitrile/100 mM $NH_4HCO_3$ (1:1) for 15 min at RT. The supernatant was discarded and another 20 µl acetonitrile was added to the gel slices. The mixture was incubated at RT until the gel slices turned milk-white. Then the gel slices were lyophilized and mixed with 20 µl of 100 mM DTT in 100 mM $NH_4HCO_3$ for 30 min at 56°C, to reduce disulfide bonds. The treatment by acetonitrile was repeated afterwards to remove the traces of DTT. The gel slices were incubated with 20 µl of 55 mM Iodacetamide in 100 mM $NH_4HCO_3$ for 20 min at RT in the dark, washed with 20 µl of 100 mM $NH_4HCO_3$ for 15 min at RT, then treated by acetonitrile again as described above, and finally lyophilized. A 12.5 ng/µl trypsin solution ($V = V_{gel\ absorption}$ + 3 ul) was added to the lyophilized gel slices, incubated on ice for 30 min and then overnight at 37°C. The tubes were then centrifuged briefly and left at 37°C for at least 30 min. Afterwards the tubes were centrifuged briefly and the supernatant (1 µl) was taken for the measurement. The data obtained from MALDI-TOF-MS were used for peptide mass fingerprinting (PMF). The fragment ion spectra of individual protein

spot were taken to search protein databases using the *Mascot* search program (Blackstock and Weir, 1999; Yates, 2000). With the *Mascot* program the experimental mass values were compared against calculated peptide mass databases. The protein score, which is -10*Log(P) where P is the probability that the observed match is a random event, for each entry was calculated. In general, positive identifications were made on the basis of a *Mascot* score $\geq$ 74 ($p < 0.05$) for a single peptide, or a score $\geq$ 40 for each of two or more peptides.

### 3.4.3 Magnetic Bead Binding Assays

Streptavidin magnetic beads were also used to confirm the enrichment of ssDNA pool and the binding of individual clones to target peptides. The binding reactions were performed in a total of 50 µl in binding buffer. Radioactively labeled ssDNA (10 µM) was measured by scintillation counting, and heated to 95ºC for 10 min, cooled slowly for 30 min to room temperature, and then for 1 h to 4ºC. DNA was brought into contact with biotinylated target peptide with a molar ratio of 1:1 (0.25 µM each). Incubation was for 1 h at 4ºC. The original ssDNA library served as a control. The sample was then added to Streptavidin magnetic beads (1.25 pmol biotinylated target per µl beads) and incubation was continued for further 30 min at room temperature. Finally, the beads were washed with 200 µl binding buffer and the radioactivity of peptide-DNA complexes retained on the beads was measured by scintillation counting. DNA bound (%) was calculated by the ratio of radioactivity retained on the beads and 100% input DNA. Each data was the mean of at least double independent determinations.

### 3.4.4 Binding Constants

The affinity of an aptamer to its target can be described by the dissociation constant (binding constant) of complex formation. The equilibrium state of molecular binding, i.e. the balance between the binding and dissociation processes after infinite reaction time, may be formalized as the unbound compounds (reactants, *A* and *B*) transforming into a complex (product, *C*):

$$A + B \rightleftharpoons C$$

The rate of complex formation is described by $k_{on}$, and that of complex dissociation by $k_{off}$. The association constant and the dissociation constant are described as,

$$K_{ass} = \frac{k_{on}}{k_{off}} = \frac{[C]}{[A] \times [B]}$$

$$K_{diss} = \frac{k_{off}}{k_{on}} = \frac{[A] \times [B]}{[C]}$$

where brackets signify equilibrium molar concentrations. The unit of the association constant is l/mol. The affinity between *A* and *B* is proportional to the value of the association constant. However, the reverse directionality is used for the dissociation constant, because the resulting formalism is a reaction of first order and thus its dimension is always in mol/l. The value of the dissociation constant is therefore anti-proportional to the affinity between *A* and *B*.

### 3.4.4.1 Surface Plasmon Resonance

Aptamer-peptide interactions were studied by surface plasmon resonance (SPR). The principle is illustrated briefly by Figure 3-3 A. The SPR angle depends on the refractive index of the material close to the non-illuminated side of the gold surface on a sensor chip, where the binding reaction takes place. Such a change will result in a shift of the SPR angle from angle 1 to angle 2, which is recorded by the detector and displayed in the form of a sensorgram. A sensorgram is a graphic representation of the signal generated during a binding cycle (Fig. 3-3 B; derived from Katsamba, *et al.,* 2002).

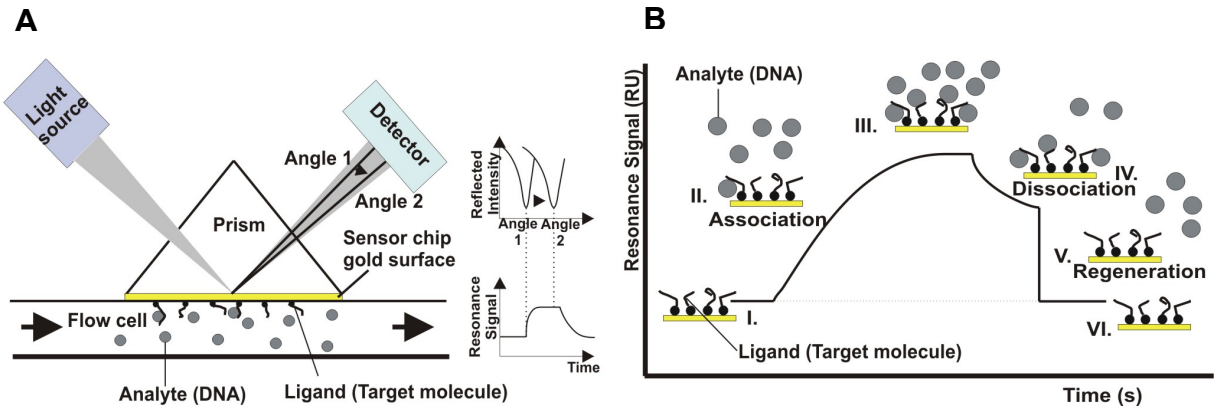


***Figure 3-3 (A) The principle of surface plasmon resonance. (B) Graphic representation of a sensorgram****. I: baseline; II: association; III: equilibrium state; IV: dissociation; V: regeneration (adapted from Katsamba et al., 2002)*

Binding experiments were performed on a BIACORE X instrument (Biacore AB) at 20ºC. Biotinylated zinc finger peptides were immobilized on Streptavidin-coated sensor chips (Biacore AB). The sensor chip was activated shortly by 10 µl of 1 M NaCl/50 mM NaOH (10 µl/min). Biotinylated ZFY or GLI peptides (1050 RU) were then directly immobilized, by repeated 20 µl injection of 20 nM peptide solutions (5 µl/min). After denaturing as described in 3.4.3, the ssDNA was serially diluted to a concentration of 40 nM to 600 nM in running buffer, which was freshly prepared just before use by the addition of TCEP, filtered, and degassed. After each injection of 80 µl at 5 µl/min, bound ssDNA was allowed to dissociate freely for 3 min. Disruption of any complex that remained bound after dissociation was achieved using a 30-µl injection of 0.5 M NaCl and 0.1 mM HCl at 30 µl/min serially. A random DNA pool was included as a negative control. The evaluation of sensorgrams, determination of binding model and binding constants were achieved by BIAevaluation Software Version 3.1 (Biacore AB). Non-random noise was removed by subtracting a buffer injection from each curve. The affinity, as described by the $K_D$, was determined by a global fit, assuming Langmuir (1:1) binding. The maxima RU-values near equilibrium were plotted against the concentrations applied accordingly. Each data point was the mean of two independent determinations.

#### 3.4.4.2 Nitrocellulose Filter Binding Assays

To characterize the aptamer-protein interaction, the association of proteins to aptamers and the binding constants were determined by nitrocellulose filter binding assays. Figure 3-4 illustrates briefly the principle of the binding assays. This method is rapid, reproducible and can be used to extract accurate equilibrium constants (Stockley, 2001).

Binding affinity of aptamer and protein complexes was measured using a nitrocellulose filter binding assay. Filters (Millipore type HAWP, 0.45 µm pore size, 25 mm diameter, 180 µm thickness) were soaked in 0.5 M KOH at RT for 20 min, washed extensively with distilled water, then incubated for 45 min in the binding buffer at RT and finally stored in the binding buffer at 4ºC till use (McEntee *et al.*, 1980). Peptide (ZFY and GLI) or protein targets (ZNF593) were serially diluted into 10 µl binding buffer to give final concentrations ranging from 0.1 µM to 5 µM. Because binding between proteins and nitrocellulose filters requires their hydrophobic interactions, some proteins, notably those of small molecular weight,

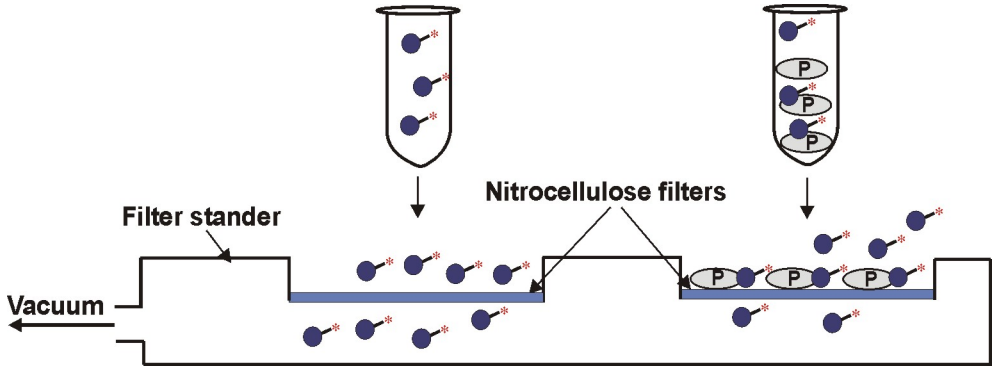


***Figure 3-4 Brief schematic representation of nitrocellulose filter binding assays.*** *Proteins (P) bind to nitrocellulose filters (right well), although free radioactively labeled nucleic acids (blue cycles with yellow asterisk) pass freely through filters (left well). If DNA binds to protein, it will result in retention of a fraction of the protein-DNA complex. The amount of radioactively labeled DNA retained on filters can be determined by scintillation counting*.

bind with reduced affinity (Oehler *et al.*, 1999). The peptide targets labeled with biotin at N-terminus have a molecular weight of less than 4 kDa. To increase the binding affinity between peptide targets and nitrocellulose filters, the biotinylated peptides were incubated with 1 mg/ml Streptavidin solution in a molar ratio of 1:1 for 30 min on ice. Thereby, the biotins in the peptides bound tightly to Streptavidin to form stable complexes. Assays were started by the addition of 10 µl of radioactivelylabeled ssDNA (final concentration <1 nM) containing 0.05 mg/ml tRNA and 0.6 mM TCEP. The tubes were spun briefly (5 s) to mix the samples and then placed on ice. Prior to filtering, the radioactivity of 100% input ssDNA was determined by scintillation counting. After a 30-min interval on ice to allow equilibrium to be established, samples (20 µl each) were removed from each tube, and filtered on a pre-treated filter. Filters were then washed three times with 1 ml binding buffer. The amount of labeled DNA retained on the filters was determined by scintillation counting. Assays were performed in duplicate. DNA retention on filters was plotted as a function of target concentration, and a background retention determined by filtration in the absence of peptide or protein target was subtracted from each point. The binding constants were calculated by the program *SigmaPlot* (version 9.0).

### 3.4.5 Affinity Capture Assays of Aptamer-Bound Proteins

#### 3.4.5.1 Immobilization of Biotinylated ssDNA

The affinity capture assay took advantage of a high binding affinity between Neutravidin-conjugated agarose gels and biotinylated ssDNA, which allows for pulling down DNA-bound proteins by centrifugation. At first the 5'-biotinylated ssDNA was attached to Neutravidin agarose gels (Pierce). According to the manufacturer's specifications, binding of biotin is on the order of $\geq$20 µg/ml of gels. To confirm the binding of biotinylated 90-nt ssDNA to the gels, the eluted fractions in the immobilization steps were analyzed. The Neutravidin agarose gels (120 µl) were washed twice with 500 µl binding buffer. Biotinylated ssDNA library (80 pmol) was denatured and incubated in 300 µl binding buffer containing the Neutravidin agarose gels for 1 h at 4ºC. After centrifugation at 2500 x g for 1 min, the gels were washed twice with 500 µl binding buffer. The supernatants were adjusted by a Speed Vac to a suitable volume for gel analysis. Finally the samples were analyzed on a 10% denaturing polyacrylamide gel.

#### 3.4.5.2 Affinity Capture Assays from Nuclear Extracts

Aptamer immobilized to agarose gels was utilized for native zinc finger protein capture assays. A direct affinity capture assay (method No. 1) from nuclear extracts of HeLa cells was used in the initial experiment. Nuclear extracts from HeLa cells were prepared as described under 3.2.6. Neutravidin agarose gels (75 µl each) were washed twice with 1 ml binding buffer. The supernatants were removed after centrifugation at 2500 x g for 1 min. Biotinylated aptamer (50 pmol) was heated to 95°C for 5 min, cooled to room temperature for 2 h and stored at 4°C for 1 h. This material was added to 500 µg nuclear extract and 75 µl gels, and binding buffer was added to give a final volume of 250 µl. The mixture was incubated at 4ºC with gentle rotation for 1 h. The sample was then centrifuged at 3000 x g for 1 min. The supernatant was removed for gel analysis. In order to determine the level of non-specific binding to the matrix, the capture assay was performed with a biotinylated oligonucleotide (20 nt) bound, instead of aptamer. After incubation, the gel pellet was washed four times with 500 µl iced PBS. Finally, the gels containing aptamer-bound nuclear proteins were resuspended in 20 µl SDS loading buffer, and heated to 95ºC for 5 min. Eluted proteins (10 µl) were then analyzed by SDS-PAGE on an 8% gel

and stained with Coomassie blue. Several major bands were excised from the SDS gel and the proteins were identified accordingly by MALDI-TOF-MS.

A competitive binding experiment (method No. 2) was applied in the later development of the assay. Neutravidin agarose gels (450 µl each) were washed three times with 1 ml binding buffer. The supernatants were discarded after centrifugation at 2500 x g for 1 min. Biotinylated aptamer or random ssDNA pool (300 pmol each) were denatured as described in 3.4.3 and incubated with 450 µl gels in 1 ml binding buffer containing 0.125 µg/µl poly(dI-dC) and 0.6 µg/µl BSA for 1 h at 4ºC (final conc. of DNA 300 nM). The mixture was centrifuged at 2500 x g for 1 min, the supernatants were removed, and the gels were washed twice with 1 ml binding buffer. Nuclear extracts (500 µg) were preincubated with gel-bound random ssDNA pool in 1 ml binding buffer containing 0.125 µg/µl poly(dI-dC) and 0.6 µg/µl BSA for 30 min at 4ºC. The supernatant was then added to gel-bound aptamer. The sample was mixed with gentle rotation for 30 min at 4ºC. Both of the tubes, where the pre-incubation and main-incubation were performed, were centrifuged at 2500 x g for 1 min. The supernatants were removed and the gels were washed four times with 1 ml binding buffer. Finally the aptamer-bound nuclear proteins were eluted using i) 450 µl of 1.9 mM biotin solution; ii) 450 µl SDS loading buffer; iii) 400 µl of 5 M urea. For each elution step the mixture was heated to 95ºC for 5 min. The supernatant was removed after centrifugation for gel analysis. To confirm the elution of the aptamer from the gels, the supernatants (15, 15, and 13 µl from the first, second, and third elution) were loaded onto a 10% denaturing urea PAGE gel. Each residual eluted sample was adjusted by a Speed Vac to a volume of 10 µl. The aptamer-bound proteins were analyzed by SDS-PAGE on an 8% gel. Proteins of interest were identified as described above.

#### 3.4.5.3 Affinity Capture Assays from Cell Extracts

Affinity capture assays were also tried for total cell extract. The Neutravidin agarose gels (150 µl each) were washed twice with 500 µl binding buffer. The supernatants were discarded after centrifugation at 2500 x g for 1 min. Biotinylated aptamer or random ssDNA pool (100 pmol each) was denatured as described under 3.4.3 and incubated with 150 µl Neutravidin agarose gels in 300 µl binding buffer containing 0.1 µg/µl poly(dI-dC), 0.05 µg/µl random ssDNA pool and 0.6 µg/µl BSA for 1 h at 4ºC (final conc. of DNA 330 nM). Total cell extracts (1 mg) were then

preincubated with gel-bound random ssDNA in 300 µl binding buffer containing 0.1 µg/µl poly(dI-dC), 0.05 µg/µl random ssDNA pool and 0.6 µg/µl BSA for 30 min at 4ºC. The following steps were performed as described previously for the affinity capture assays (method No. 2) of nuclear extracts. Finally the supernatants were removed and the gels containing aptamer-bound cellular proteins were washed four times with 500 µl binding buffer. These proteins were then eluted using i) 40 µl of 1.9 mM biotin solution; ii) 40 µl SDS loading buffer; iii) 40 µl of 5 M urea, and resolved on an 8% SDS-PAGE gel. Several major bands were excised from the gel and the proteins were identified by MALDI-TOF-MS.

### 3.4.6 Western Blotting

Western blotting was applied to identify ZFX protein in the extracts of HeLa cells. Protein samples were prepared as described in 3.2.6 and 3.2.7. They were then separated from one another on a SDS gel. Proteins were transferred from the gel onto a membrane, Hybond P® PVDF (polyvinylidene fluoride), in an electrical field at 70 mA for 1 h 10 min. The transfer was done in semi-dry conditions. To confirm the successful transfer of the proteins, the membrane was incubated with Ponceau red (0.2% Ponceau S and 3% acetic acid) for 5 min, washed in water for 1 min and evaluated visually. The membrane with the transferred proteins was washed shortly in TBS buffer, incubated with 10-20 ml blocking buffer for 1 h, and then washed three times shortly in TTBS buffer. The primary antibodies (1:10.000 - 1:15.000 in TTBS buffer), anti-ZFX serum, were added to the membrane overnight at 4ºC. To remove residual primary antibody, the membrane was washed three times shortly in TTBS buffer, then in TTBS for 15 min and finally three times for 5 min respectively. It was then incubated with the secondary antibodies, goat anti rabbit-horseradish peroxidase (HRP)-conjugate (1:5000 – 1:10.000 dilutions from a 10 µg/ml solution). Again, the membrane was washed in TTBS three times shortly, three times for 10 min and then in TBS for 10 min. Enhanced chemiluminescence kit, SuperSignal®-kit (Pierce), was finally used for visualization of the immune complexes.

# 4 Results

Many transcription factors contain $Cys_2His_2$-type zinc fingers (*zf*), which are largely involved in development and diseases, especially cancer. Some selection results provide support for the concept that DNA-binding domains in transcription factors tend to be included in the preferred aptamer binding site, when transcription factors are the target of aptamer selection (Lebruska and Maher, 1999; Cassiday and Maher, 2001; Huang *et al*., 2003; Zhao *et al*., 2006). Since z*f* transcription factors are very complex targets for developing molecular ligands, DNA binding domain (*zf* domain) would be the best choice as the preferred target. On the other side, a single *zf* peptide can already fold into a stable tetrahedral metal-coordinated structure with the help of $Zn^{2+}$ ions and *the zf* motif is highly conserved in many *zf* proteins. Therefore, specific aptamers for recognition of *zf* transcription factors seem feasible to be constructed for a single *zf* motif. In this work DNA aptamers were first isolated in two independent selections to recognize two peptides (ZFY and GLI) each containing the single classical $Cys_2His_2$ *zf* domain. Later, aptamers against the peptides were studied for binding to a related *zf* protein, and finally for affinity capture assays of *zf* proteins from HeLa cell extracts.

## 4.1 Design, Characterization and Preparation of Target Peptides

### 4.1.1 Design of Target Peptides

First of all, a stable and homologous *zf* target is important for a successful selection. One of the target peptides (Fig. 4-1), ZFY, is derived from the sixth finger (residue 161-191) of *zf* domain of the human ZFY transcription factor, which plays an important role in the regulation of embryonic and hematopoietic stem cells (Galan-Caridad *et al*., 2007). There is experimental evidence that this ZFY peptide correctly forms a *zf* structure with $Zn^{2+}$ ions in solution (Kochoyan *et al*., 1991b). In addition, the ZFY peptide contains a C-terminal lysine in place of methionine in the native sequence to enhance the solubility of the peptide and to avoid methionine oxidation. Its second residue of proline in the native sequence is replaced by threonine to enhance stability under acidic conditions and to be more characteristic among the related *zf* sequences.

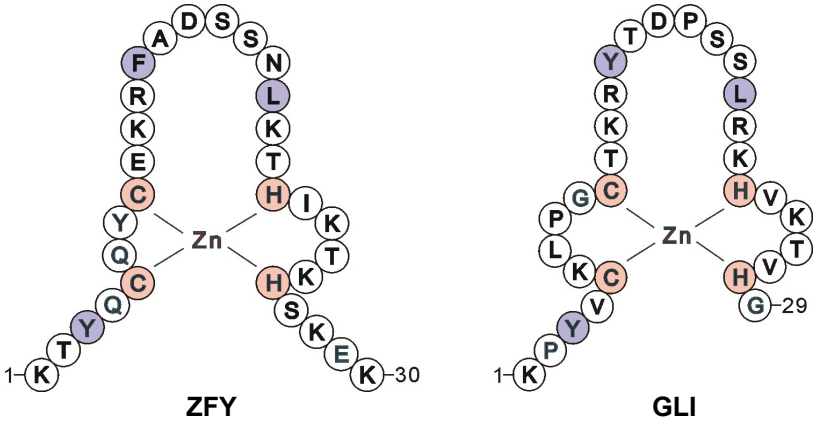


***Figure 4-1 Models of target peptides used in SELEX experiments (SELEX against ZFY and SELEX against GLI).*** *Conserved positions, where the metal-coordinated residues and the three hydrophobic residues are located, are labeled in colors. The peptides were synthesized chemically with an additional biotin at the N-terminus to enable the immobilization for SELEX experiment.*

The other target peptide (Fig. 4-1), GLI, is derived from the fifth finger (residue 360-388) in the *zf* domain of the human GLI transcription factor, a glioblastoma oncogene protein. GLI plays a critical role in the mediation and interpretation of Hedghog signals, which are associated with a surprisingly high number of human diseases (Altaba *et al.*, 1999; Kasper *et al.*, 2006). The crystal structure of a complex has been determined containing the five *zf*s from the human GLI and a high-affinity DNA binding site (Pavletich and Pabo, 1991). Superimposing fingers shows that their tertiary structures are very similar. However, only fingers four and five of GLI make extensive base contacts in a conserved nine base-pair region. The contacts made by finger five are spread over a 4-bp region (GACC) of the GLI binding site.

### 4.1.2 Analysis of ZFY and GLI Peptides by HPLC

Since both peptides (ZFY and GLI) contained two cysteines each, they could form intra- and inter-chain disulfide bonds. The oxidation of the peptides by disulfide bonds prevents the formation of $Zn^{2+}$ complex (Larabee et al., 2005). Therefore, to ensure the reduced form for later metal coordination, the peptides were analyzed, reduced, and then purified by HPLC.

HPLC chromatograms for ZFY are shown in Figure 4-2. The peak of the oxidized form was observed at a retention time (RT) of 14.0 min. It was eluted from the column earlier than the reduced form, which has a retention time at 14.3 min. It

indicates that part of peptides contains probably an internal disulfide bond that could be prohibitive for the formation of a tetrahedral *zf* structure. Therefore, the peptides ZFY and GLI were reduced immediately before complex formation with $Zn^{2+}$ ions.

The reducing reagent, Tris(2-carboxyethyl)phosphine (TCEP) was utilized to reduce cystine to cysteine. The integrity and efficiency of reduction by TCEP was addressed by analytical HPLC. A partly oxidized sample of the ZFY peptide has two peaks of oxidized and reduced forms, which were collected after the column with retention times of 14.0 min and 14.3 min, respectively (Fig. 4-2 B). The sample of the reduced form, which was injected directly (Fig. 4-2 D), shows only a reduced peak (RT = 14.3 min). The sample of the oxidized form, which was injected directly without reduction, shows only an oxidized peak with a retention time of 14.0 min (Fig. 4-2 A); whereas in the case that the sample of the oxidized form was reduced with TCEP before injection, the peak shifted mostly to the position with a retention time of 14.3 min (Fig. 4-2 C).

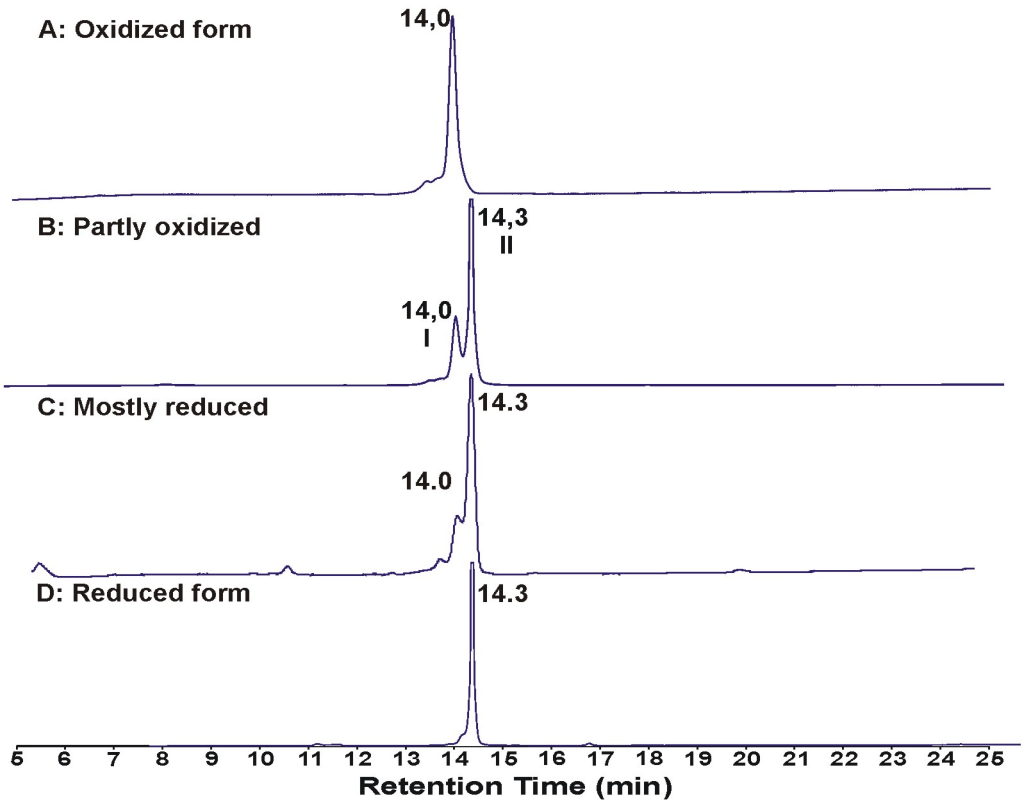


***Figure 4-2 Demonstration by HPLC for reduction of the ZFY peptides using TCEP.*** *By reverse phase $C_8$ HPLC with a gradient of 0-70% ACN in water at 1 ml/min, the oxidized and reduced forms of the ZFY peptides have peaks at 14.0 min and 14.3 min, respectively.*

The chromatographic results demonstrate that the *zf* peptides were reduced successfully by TCEP. It was found that incubation at 22ºC for 1 h with a ten-fold molar excess of TCEP gave more than 90% reduction of the disulfide.Mass Control and Integrity of Reduction by MS

### 4.1.3 Mass Control and Integrity of Reduction by MS

The integrity of the targets was further confirmed by MALDI-TOF MS before starting the selection. The peptides ZFY and GLI were analyzed before and after reduction. As exhibited in Figure 4-3 A, the spectrum of the reduced, metal-free ZFY allows for the experimental monoisotopic mass of 3967.99 Da to be assigned to the reduced ZFY in agreement with the theoretical value of 3967.96 Da. Figure 4-3 B depicts the mass spectrum of GLI. It shows that the experimentally determined mass of 3637.87 Da corresponds to the calculated monoisotopic average mass of 3636.92 Da.

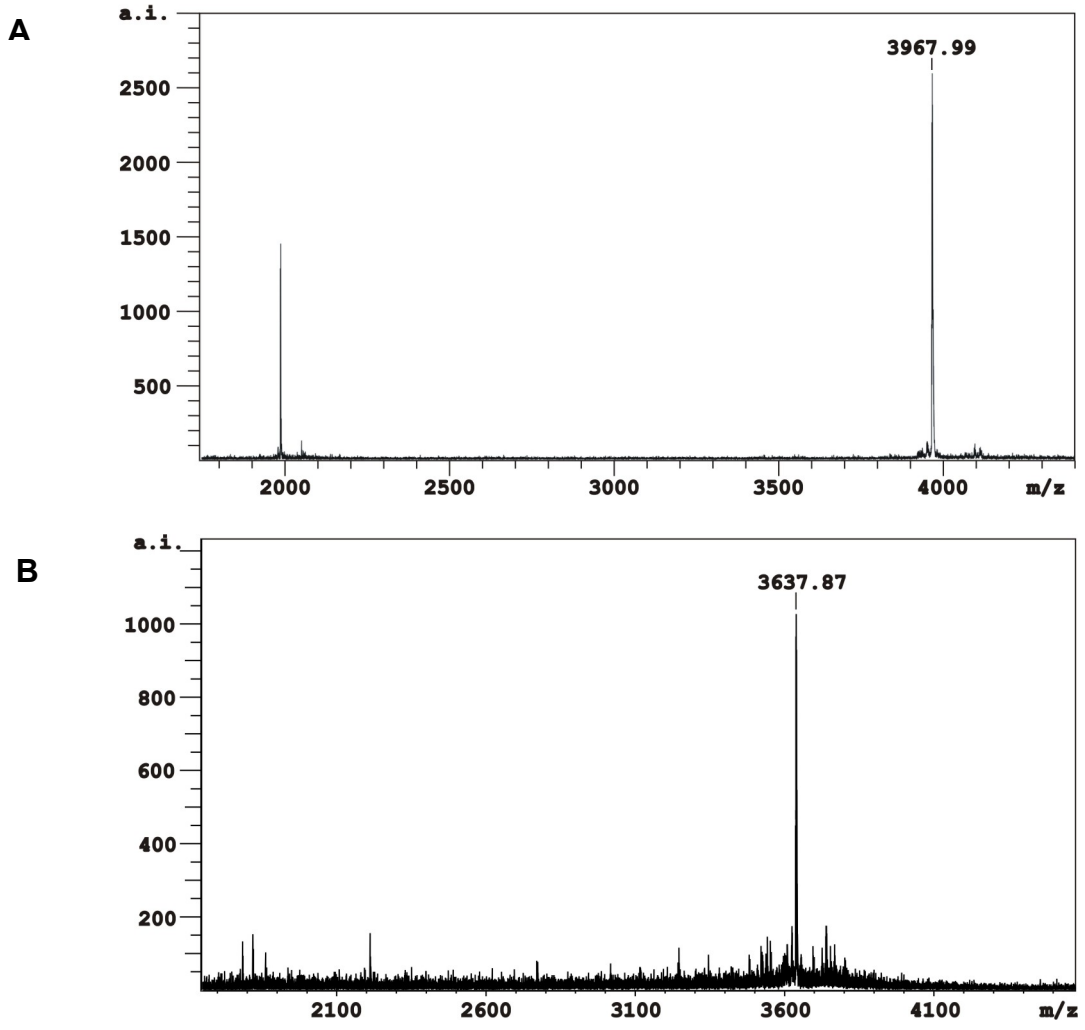


***Figure 4-3 MALDI mass spectra of ZFY (A) and GLI (B).***

The natural isotopic cluster spectra produced by the ZFY peptide allow for a more accurate analysis of cys redox activities. The monoisotopic mass is defined as the first peak within the peptide isotope cluster that consists of a combination of the lowest mass isotopes in the molecular formula (primarily $^{12}C$). This measurement is more precise than the average molecular mass and allows for single Dalton mass changes to be discerned (Larabee *et al.,* 2005). Small mass changes could be monitored, e.g., disulfide bond formation where a mass shift corresponds to the loss of two protons per disulfide bond. Since the ZFY peptide was partly oxidized before TCEP reduction, the isotopic mass cluster for the oxidized ZFY peptide is observed in Figure 4-4 A. The cluster of peaks shifts to the left (lower mass), which indicates the loss of 2 Da and the formation of a single disulfide bond. After TCEP reduction, a pattern of isotope peaks (Fig. 4-4 B) is revealed for cys thiol-reduced ZFY by resolving the natural isotope cluster. The monoisotopic peak (3965.96 Da) of the oxidized peptide could not be observed. These spectrometric results confirm again the successful reduction of the ZFY peptide.

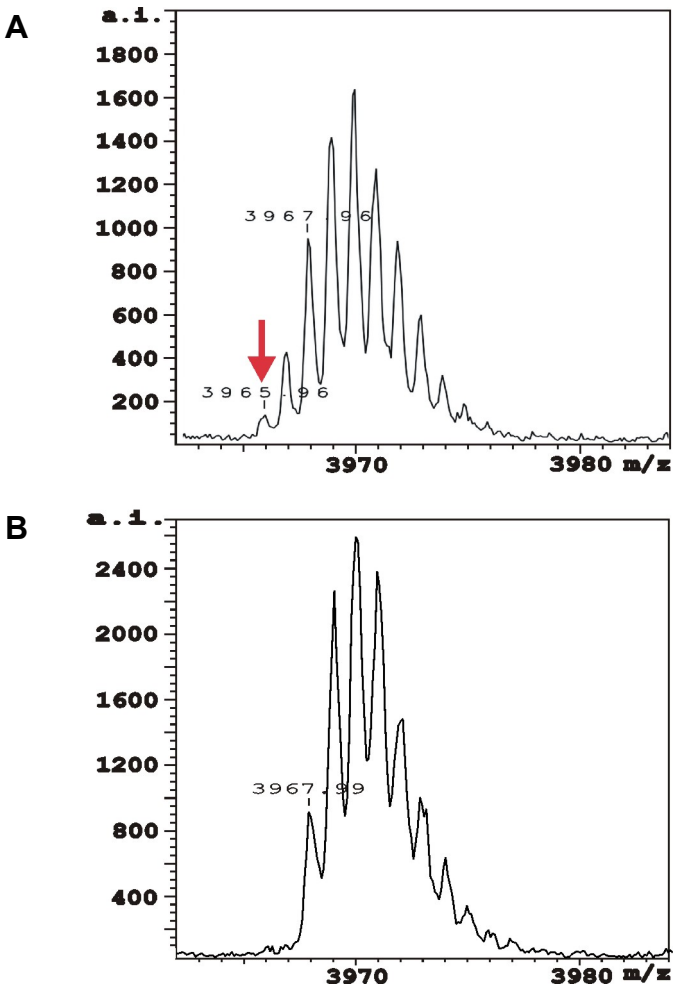


***Figure 4-4 Resolution of the natural isotope clusters of the partly oxidized (A) and the reduced ZFY (B) peptide.*** *In the spectrum of the partly oxidized ZFY peptide (A), the monoisotopic mass of the oxidized peptide (marked by a red arrow) with probably an internal disulfide bond gives a mass of 2-Da less than that of the reduced peptide (B).*

The integrity of GLI reduction has also been analyzed by natural isotope cluster spectra. The observation agrees with the results obtained for the ZFY peptide as described above. The isotopic mass cluster for the oxidized GLI peptide is shown in Figure 4-5 A. After reduction, a pattern of isotope peaks is revealed in Figure 4-5 B for cys thiol reduced GLI. These results demonstrate that the GLI peptide was also reduced successfully.

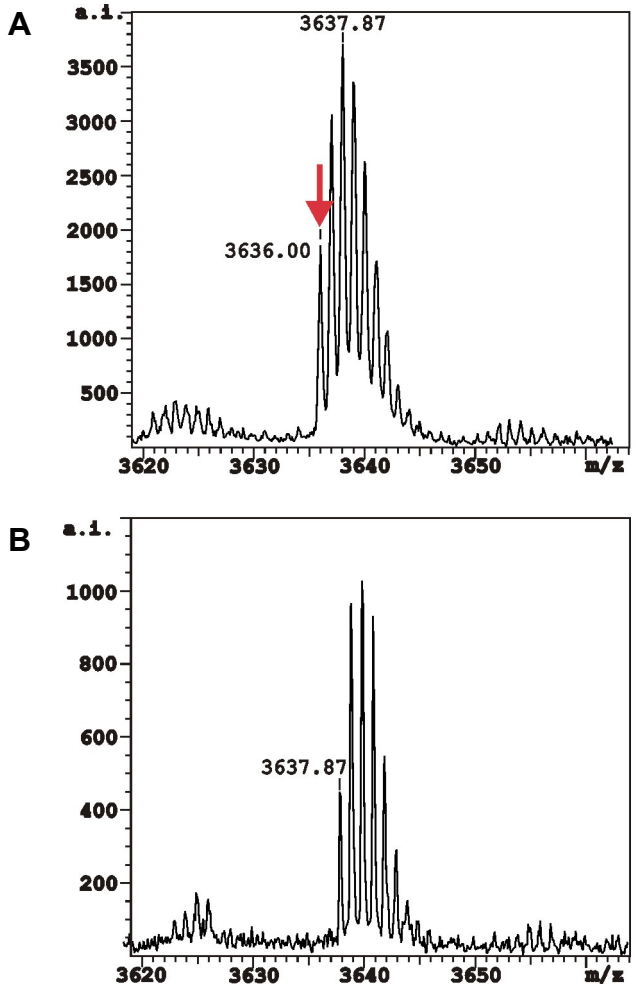


***Figure 4-5 Resolution of the natural isotope clusters of the partly oxidized (A) and the reduced GLI (B) peptide.*** *In the spectrum of the partly oxidized GLI peptide (A), the monoisotopic mass of reduced peptide is observed at 3637.87 Da and the monoistopic mass of the oxidized peptide with probably an internal disulfide bond gives a mass of 2-Da less (3636.00 Da; marked by a red arrow). In the spectrum of the reduced peptide (B), only the monoiostopic mass of the reduced GLI peptide is determined at 3637.87 Da.*

### 4.1.4 Determination of Tetrahedral Metal Coordination by Circular Dichroism

The proper conformation of target peptides is an important point for a successful enrichment in a *SELEX* experiment. To confirm the tetrahedral metal coordination with $Zn^{2+}$ ions, circular dichroism (CD) spectroscopy was used to monitor the peptide folding. The CD spectra give valuable information about the secondary structures of peptides and proteins. Characteristic differences can be observed in the model spectra of an α-helix, a β-sheet or a random coil (Fig. 4-6). The different percentages of conformations, of which the secondary structure is

composed, can be estimated by fitting the spectra of these model peptides to the experimental spectrum.

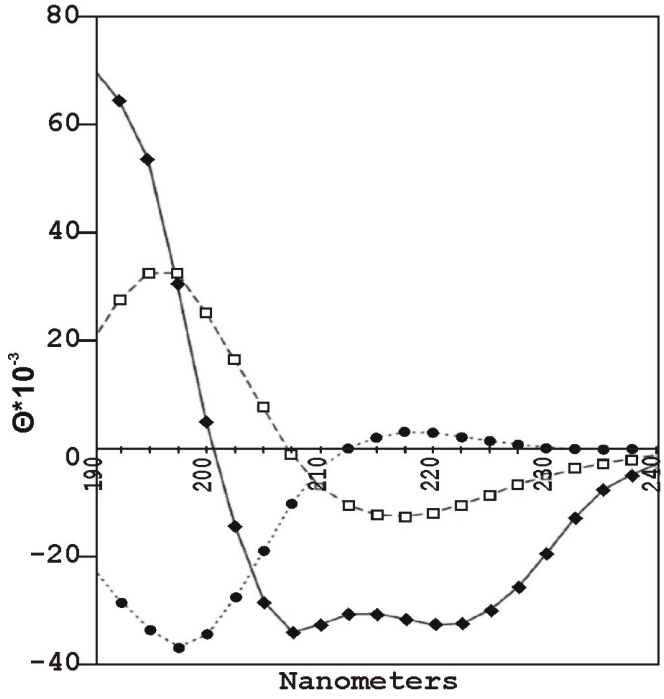


***Figure 4-6***
***Graphical representation of model spectra****. For the α-helix (filled rhomboids), two minimums around 208 nm and 220 nm as well as a maximum around 190 nm can be observed. For the β-sheet (empty squares), a minimum around 218 nm appears and a maximum around 200 nm can be observed. For the random coil (filled cycles), there is a minimum around 200 nm (adapted from Reed and Reed, 1997).*

$Zn^{2+}$-denpendent folding transitions in ZFY and GLI peptides were observed by CD. The peptides were dissolved in water to a final concentration of 0.16 mM in the presence or absence of $Zn^{2+}$ ions at pH 7.0. $Zn^{2+}$ ions were added as a 2.5-fold molar excess to peptides. To avoid oxidation of peptides, TCEP (10-fold molar excess) was used in solution. The spectra were accumulated by five scans and corrected by blank spectra. The spectrum of the metal-free ZFY peptides (Fig. 4-7 A) has a minimum near 200 nm. Upon adding $Zn^{2+}$ ions, a significant change could be observed. The minimum shifted to 208 nm and 220 nm. In addition, there was also significant reduction in the negative molar ellipticity near 200 nm.

As expected, the CD spectrum of the metal-free GLI peptides is similar with that of the metal-free ZFY peptides (Fig. 4-7 B). Upon adding $Zn^{2+}$ ions, there is a significant change at 200 nm, but only a slight difference at 220 nm. This spectrum is characterized as a relatively weak CD band. However, there are significant reductions in the negative molar ellipticity near 200 nm and 205 nm.

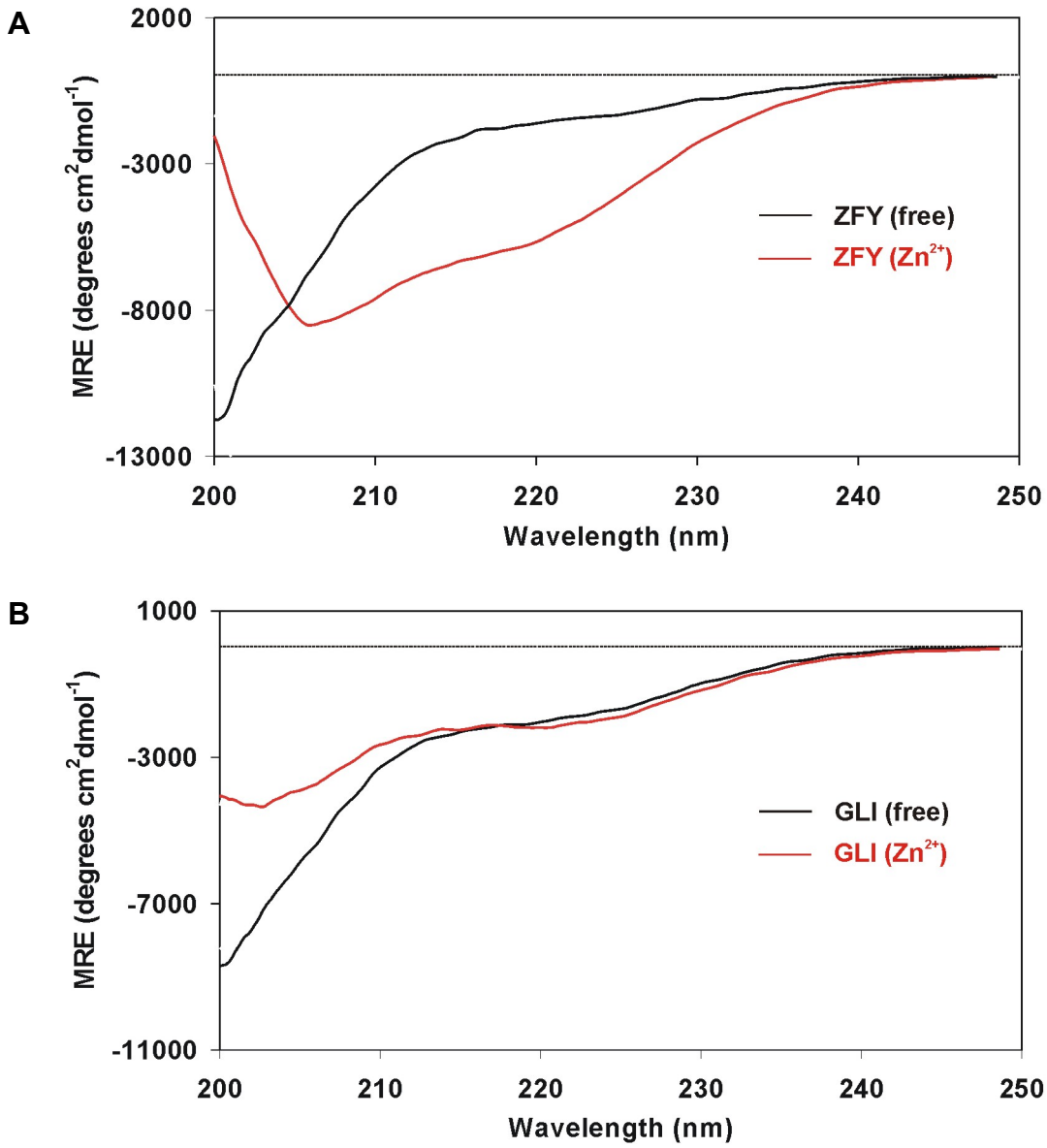


***Figure 4-7 (A) CD spectra of $Zn^{2+}$-coordinated (red) and metal-free (black) ZFY peptides. (B) CD spectra of $Zn^{2+}$-coordinated (red) and metal-free (black) GLI peptides.*** *MRE is the mean residue ellipticity.*

To calculate the percentages of α-helix, β-sheet and random coil, the CD spectra were deconvoluted using the *PEPFIT* algorithm program (Reed and Reed, 1997; Tab. 4-1). The secondary structure contents estimated for the metal-free ZFY peptides showed a high content of random-coil (66%) and no α-helix. Upon adding $Zn^{2+}$ ions, the fraction of the α-helix increased from 0% to 14% and the fraction of the random coil decreased from 66% to 44%. The trend of these $Zn^{2+}$-denpendent folding transitions is less pronounced for GLI peptides, but could still be observed.

***Table 4-1 Contents of secondary structure elements estimated with the PEPFIT.***

| Figure 4-7 | Peptide/Conditions | % α-helix | % β-sheet | % random |
|---|---|---|---|---|
| A (black) | ZFY (free) | 0 | 34 | 66 |
| A (red) | ZFY ($Zn^{2+}$) | 14 | 42 | 44 |
| B (black) | GLI (free) | 0 | 38 | 62 |
| B (red) | GLI ($Zn^{2+}$) | 9 | 33 | 55 |

## 4.2 Design of a ssDNA Library

In this work, aptamers with high affinity to *zf* peptides were selected from an oligonulceotide library by *in vitro* selection. An ssDNA library was designed according to the scheme outlined in Figure 4-8 and chemically synthesized by IBA GmbH (Göttingen). The template molecule contained a region (50 nt) with randomly incorporated sequences. The random region was framed by two constant DNA regions each with 20 nt that served as annealing sites for forward and reverse primers.

Theoretically, the random region (50 nt) could account for $4^{50}$ = 1.3 x $10^{30}$ different sequences. However, a library with a complexity of 1.48 x $10^{15}$ different sequences (2.43 nmol) was applied to be amplified by PCR with an amplification efficiency of 11-fold in 15 cycles. Since only ssDNA instead of dsDNA can fold a variety of complex tertiary structures, which could interact with target molecules, two primers with unequal lengths were used to produce a dsDNA library with two strands of different lengths (Williams and Bartel, 1995). These two strands were separated by denaturing PAGE (see example in Figure 4-9) and ssDNA molecules (90 nt) were purified from the gel.

Copies for each sequence and sufficient target were used in early rounds of selection to ensure the capture of the highest affinity ligands, when lower affinity ligands were present in a far more abundant manner (Gold *et al*., 1995). DNA templates (4.86 nmol; 2 copies of each sequence; 1.48 x $10^{15}$ different sequences) were applied to start the first round of selection. Theoretically, this diversity of the DNA pool is sufficient for the selection of high affinity ligands (Gold *et al*., 1995)


***Figure 4-8 Design of the DNA library.*** *In the first PCR cycle the reverse primer-terminator (41 nt) hybridized to the DNA template molecule. The DNA polymerase prolonged the reverse primer-terminator in the 3'-direction. In the following cycle the forward primer (20 nt) attached to the newly synthesized DNA strand, which was generated in the first cycle. Again, the complementary strand was synthesized in the 3'-direction. Both of these DNA strands were amplified in the following PCR cycles.*

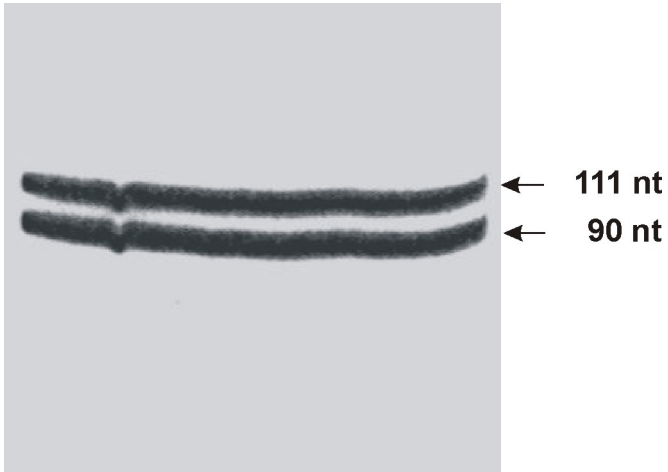


***Figure 4-9***
***Separation of two strands with unequal lengths.*** *The two strands of dsDNA with different lengths were separated by denaturing PAGE on a 10 % gel. The upper one corresponds to 111 nt with reverse primer-terminator (41 nt), while the lower one refers to 90 nt with normal primers (20 nt).*

## 4.3 Optimization of *In vitro* Selections against Peptides

Two *SELEX* experiments were performed against two *zf* peptides respectively. The selection conditions were optimized experimentally. To avoid reoxidation of the peptide targets, the reduced and purified *zf* peptides were dissolved in degassed water, sealed with argon and stored at -70ºC. Just before use, the $Zn^{2+}$-coordinated peptides (160 µM) were prepared freshly.

### 4.3.1 Immobilization of Biotinylated Peptides

For capture of complexes of biotinylated *zf* peptide target and DNA, Neutravidin agrose gels (Pierce) and Streptavidin magnetic beads (Dynal) were applied in the selection rounds. The biotinylated *zf* peptides were immobilized on a solid support containing Neutravidin, or Streptavidin, by utilizing the strong non-covalent interaction between biotin and Neutravidin (or Streptavidin).

In the early selection cycles, Neutravidin agarose gel was used to immobilize biotinylated target, since substantial amounts of target could be loaded on this resin. To confirm the efficient binding of the peptides to the gels, a selection process was performed in which the DNA molecules were absent. The eluted fractions were analyzed by HPLC in comparison with the standard solutions of the peptides. The peptides were detected neither in the eluted solutions directly after immobilization, nor after 1 h incubation (data not shown). The chromatographic results demonstrate that the immobilization of both peptide targets was successful to Neutravidin agarose gels. The binding capacity was estimated to be at least 30 pmol of biotinylated ZFY or GLI per µl gel.

Although pre-selection was performed starting from round two, the background during the partitioning step still led to the isolation of some matrix-binders. Therefore, it was necessary to change the matrix from Neutravidin agarose gel to Streptavidin magnetic bead from round eight, so as to reduce matrix-binders. Moreover, magnetic beads require only small amounts of target and enable a very simple handling. It was suitable for the later rounds where lower amounts of peptide targets were utilized. Binding of the biotinylated peptides to the beads was also confirmed by analytical HPLC (data not shown). The binding capacity of the Streptavidin beads was estimated to be at least 1.5 pmol of biotinylated ZFY or GLI per µl beads.

### 4.3.2 Monovalent Salt Dependence of ssDNA Binding to *zf* Peptides

Peptides bind to oligonucleotides non-specifically due to ion exchange between the positively charged amino acids and the negatively charged phosphate backbone. Monovalent ions can, however, influence this ion exchange by competing with the positively charged peptides to bind to DNA. The effects of monovalent salt concentration on the efficiency of the binding of *zf* peptides to ssDNAs were evaluated by varying the $K^+$ concentration in the buffer from 70 to 150 mM. The binding assay was performed with a 1:1 ratio of ssDNAs and peptides (each 1 µM), using Streptavidin magnetic beads to capture the peptide•ssDNA complexes. As presented in Figure 4-10, the data demonstrate that the concentration of monovalent ions has a significant influence on peptide-ssDNA interaction. By increasing the concentration of $K^+$ ions, the non-specific binding between peptides and ssDNAs was decreasing. This effect was utilized to increase the stringency during the selection process. In the early rounds ($1^{st}$-$11^{th}$) the concentration of $K^+$ ions was 70 mM in the *SELEX* buffer A and it was then increased to 150 mM in the later rounds (12-$14^{th}$). This increase of stringency during the *SELEX* process is supposed to enhance the likelihood of successful selections (Stoltenburg *et al.*, 2007).

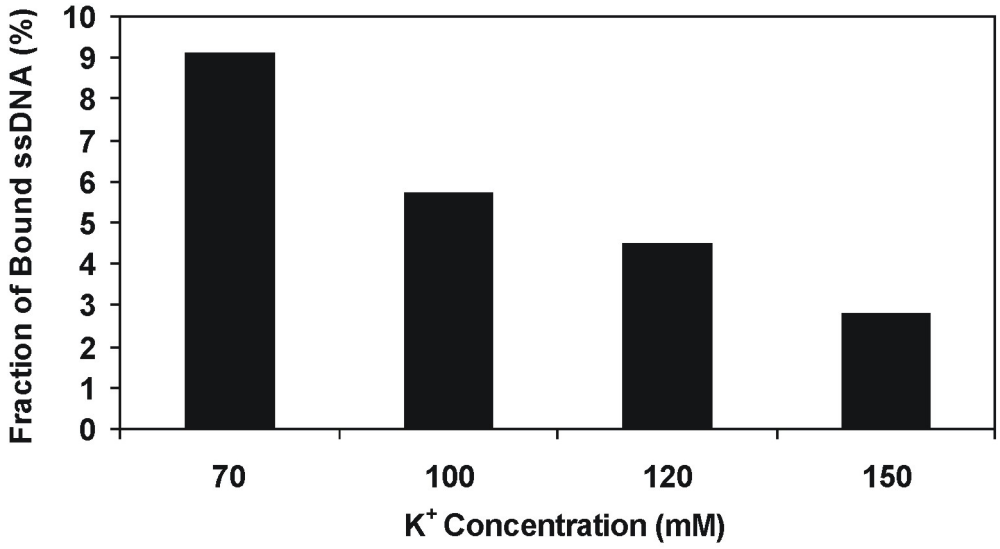


***Figure 4-10 Effect of monovalent salt concentration on the binding of ZFY zf to random ssDNAs.*** *The potassium ion concentration was varied as indicated.*

## 4.4 Aptamers against Peptide GLI

### 4.4.1 Selection of GLI-Bound Sequences

*In vitro* selection was used at first for the isolation of DNA aptamers binding to the GLI peptide. The peptide was analyzed and characterized as discussed under 4.1. The ssDNA pool was designed and prepared as described under 4.2. During the selection process the stringency was increased as described under 3.3.2 and DNA binding was enriched using fourteen rounds of selection. Magnetic bead binding assays were performed comparing the DNA pools before round one and after round fourteen. The DNA pools were incubated with the GLI peptide in a 1:1 molar ratio of DNA and target (0.25 µM for each). A peptide containing 23-residue, which is derived from the sequence (residue 136-158) of prion protein in golden hamster, was used as a control for demonstrating the GLI-specific binding of the enriched DNA pool. In addition, BSA and the matrix served also as negative controls. The binding results revealed a clear enrichment for specific GLI-bound DNA sequences (Fig. 4-11).

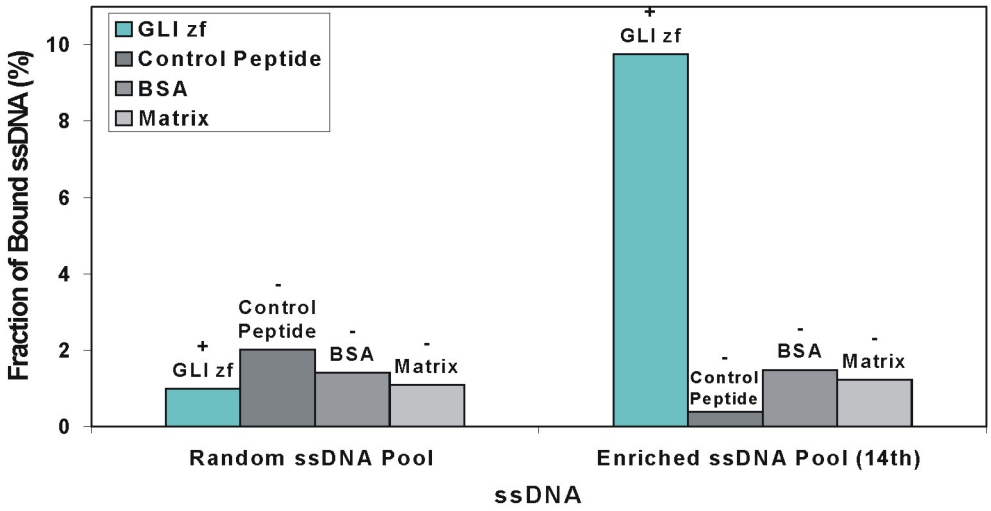


***Figure 4-11 Selection of GLI ssDNA aptamers from a random ssDNA pool.*** *The random ssDNA pool before round one and the GLI-bound sequences enriched after round fourteen were compared for binding in the magnetic bead binding assays as described under 3.4.3. The fractions of bound ssDNA (%) in the random pool (left) and enriched pool (right) to the GLI peptides (+) are indicated by green columns. As controls, the fractions of bound ssDNA (-) to the 23 amino-acids peptide, BSA and the matrix are indicated by grey columns.*

### 4.4.2 Primary Structures

Sequencing of twenty-three clones from the eluted fraction of bound ssDNAs after round fourteen revealed seventeen different sequences. Three sequences were found third times and one sequence occurred twice: II(R16)=II(B18)=II(R12); II(B23)=II(R13)=II(B09); II(R03)=II(R07). Besides the normal length of 50 bases, clone II(R21) was isolated with a random region of 49 bases. This change can be attributed to erroneous DNA replication. The primary structures in the random region were compared by *BioEdit* and aligned by *ClustalW* (Thompson *et al*., 1994).

Conserved sequences can be very helpful to provide information about the nucleotides that are important for target binding. They can also help to predict secondary and tertiary structures. Therefore, all sequences in random region were analyzed based on the program *ClustalW*, which improves the sensitivity of progressive multiple sequence alignment through sequence weighting, position specific gap penalties and weight matrix choice. Sequence analysis of seventeen different clones revealed that they can be classified into five subgroups, based on nucleotide conservation at specific residues (Tab. 4-3).

Interestingly, a highly conserved motif occurs in all sequences, a 5-nt sequence (5'-GGACA-3'). In addition, the sequences in groups 1, 2 and 3 contain a further conserved motif, a 5-nt sequence (5'-TGAGC-3'). In groups 1, 4 and 5 another conserved motif was found, a 6-nt sequence (5'-CCTTTA-3'). The occurring frequencies of these conserved motifs are shown in Table 4-2.

***Table 4-2 The occurring frequencies of the conserved motifs***

| Motif No. | Conserved Motif | Different Groups | Nr.of Sequences | Sequence (%) |
|---|---|---|---|---|
| CM-1 | GGACA | 5 | 23 | 100 |
| CM-2 | TGAGC | 3 | 17 | 74 |
| CM-3 | CCTTTA | 3 | 13 | 57 |

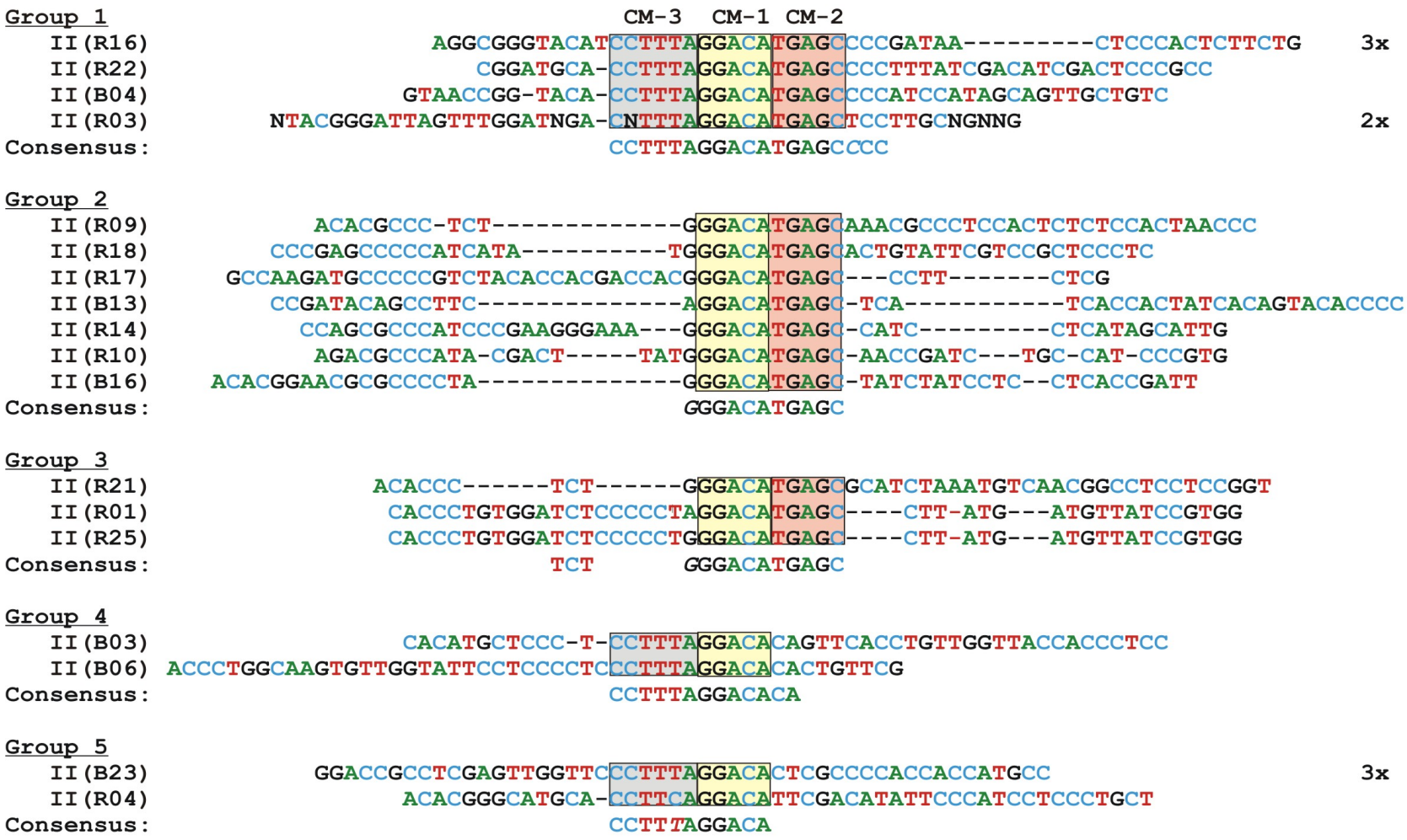


***Table 4-3 Comparison of sequences of GLI-bound ssDNAs based on the nucleotides in random region.*** *The highly conserved motifs (CM-1 CM-2 and CM-3) are marked in squares. The gaps shown here are indicated by hyphens. Consensus sequences are shown below each group, in which italic letters stand for the conserved nucleotide positions with mutations. The number of identical clones is indicated on the right side of the sequences, unless only once.*

### 4.4.3 Binding Affinities of Single Clones

Eight individual clones were analyzed for binding to GLI by the magnetic bead binding assays. Each clone was incubated with 250 nM peptides. As a control, the ssDNA pool with random sequences of the first round displayed only a very weak affinity to the peptides, which excluded the possibility of unspecific binding by ion exchanges between aptamers and peptides. The binding results revealed specific GLI-binding of all clones, with different affinities (Fig. 4-12).

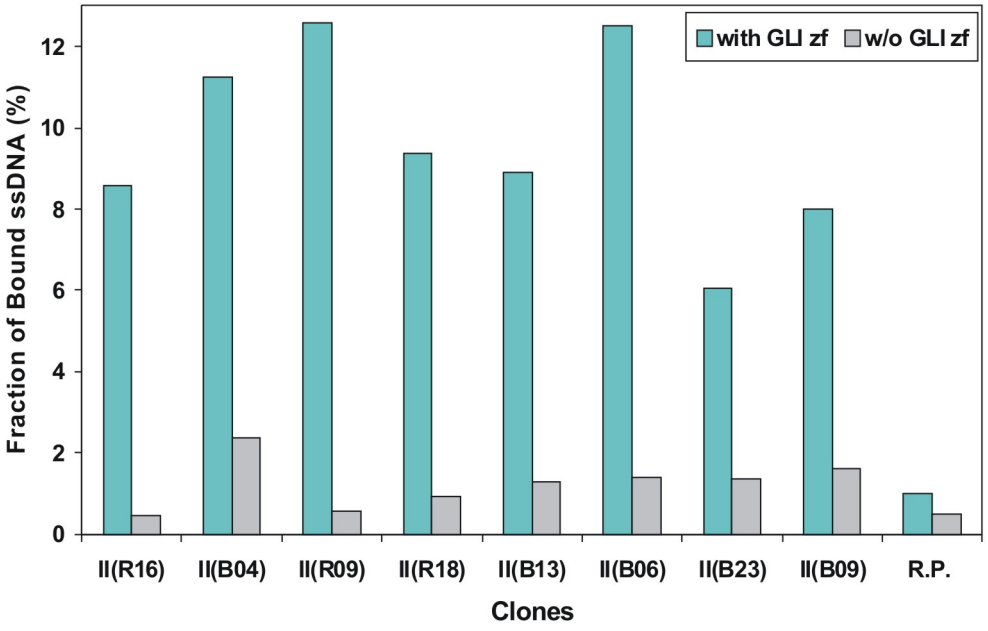


***Figure 4-12 Magnetic bead screens of the clones obtained after round fourteen of SELEX against GLI.*** *The fractions of bound ssDNA in presence of GLI are indicated by green columns, whereas those against the matrix are shown by grey columns. The ssDNA source is indicated below the column. The random ssDNA pool (R.P.) was used as control.*

### 4.4.4 Secondary Structures

The secondary structures of these GLI-bound ssDNA ligands were predicted by computer analysis using the program *mfold* version 3.2, based on the *Zuker* DNA folding algorithm (Zuker, 2003; SantaLucia, 1998). This program of *Zuker* calculates the potential secondary structures of single-stranded nucleic acids by an energy minimizing method considering stems, loops and bulges. The 90-nt sequence with primer regions was analyzed for secondary structure prediction, because primer regions might also contribute to the interaction.

Computer analyses assess stable secondary structures for these ssDNAs. The structures of the clones in each group are quite similar. In addition, there are

several similarities in the structures of the clones among the groups. In the group 1, the two guanines of the conserved motif CM-1, form a small hairpin with the conserved motif CM-3. GG and CC pair in the stem of the hairpin. TTT are located in the loop. In addition, the conserved motif CM-2 is part of another hairpin. The nucleotides (G)AG form the stem with (C)TC in the 3'-downstream. Between these two hairpins, the conserved nucleotides ACAT(G) from the motifs CM-1 and CM-2 are located in single strand (Fig. 4-13). In the groups 2 and 3, the conserved motifs CM-1 and CM-2 fold into similar secondary structures with the according regions in group 1 (Fig. 4-14 and 4-15 A). In the groups 4 and 5, the conserved nucleotides of the motifs CM-1 and CM-3 are involved in the predicted secondary structures very similarly with those in group 1 (Fig. 4-15 B and C).

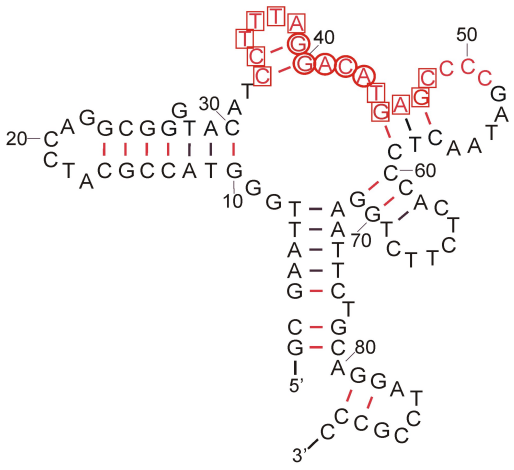

II(R16), dG = -20,17 kcal/mol

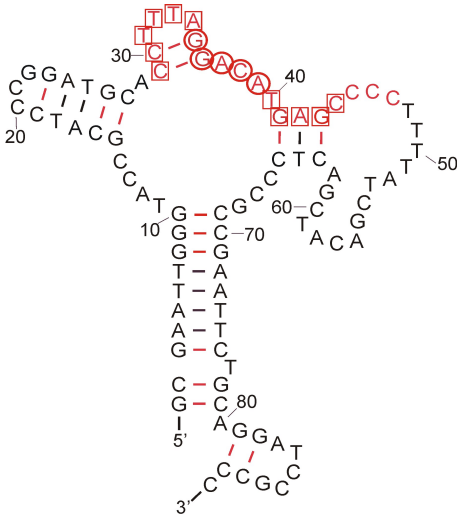

II(R22), dG = -21.22 kcal/mol

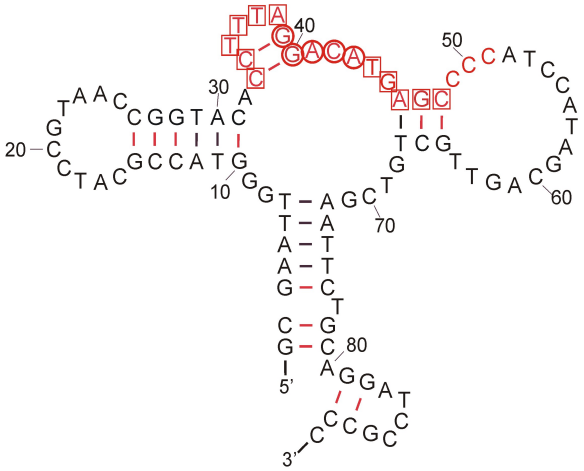

II(B04), dG = -18.81 kcal/mol

***Figure 4-13 The secondary structures of clones in group 1 as predicted by the Zuker mfold program.*** *The conserved nucleotides in this group are indicated in red, those of which in the conserved motif CM-1 are marked by cycles; in the conserved motifs CM-2 and CM-3 by squares. Positions 1-20 and 71-90 contain primer regions. Strong base pairs (G-C) are marked by red hyphens and weak base pairs (A-T or wobble base pairs) are indicated by black hyphens.*

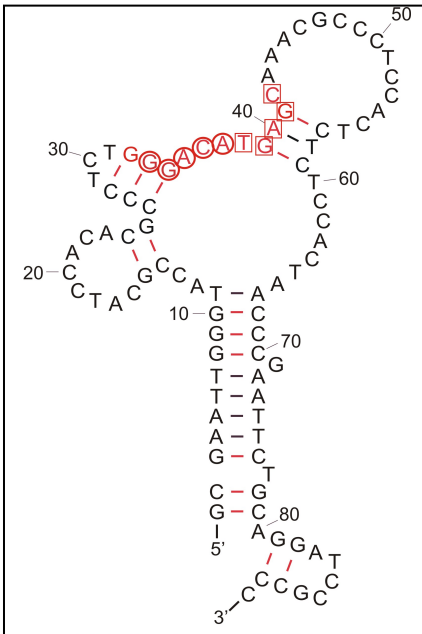

II(R09), dG = -15.77 kcal/mol

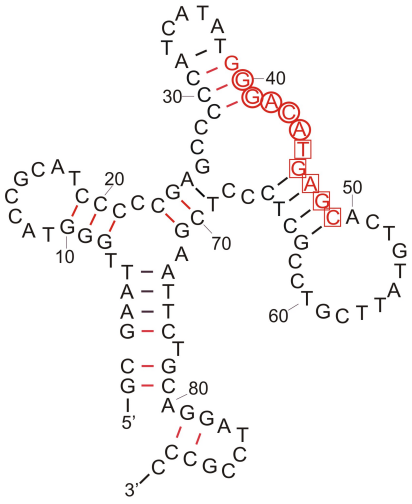

II(R18), dG = -22.53 kcal/mol

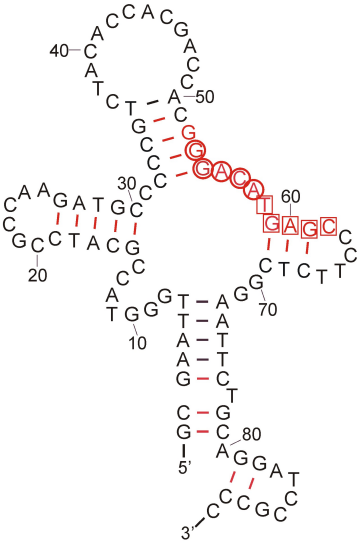

II(R17), dG = -22.87 kcal/mol

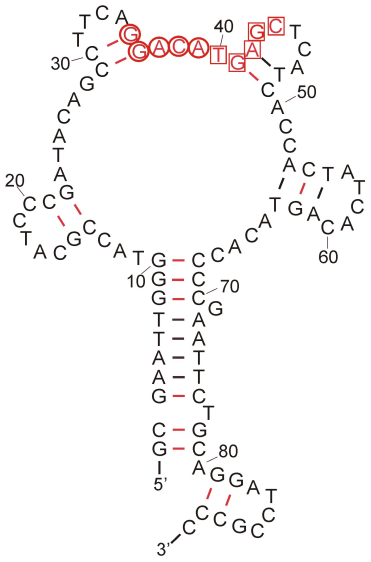

II(B13), dG = -16.67 kcal/mol

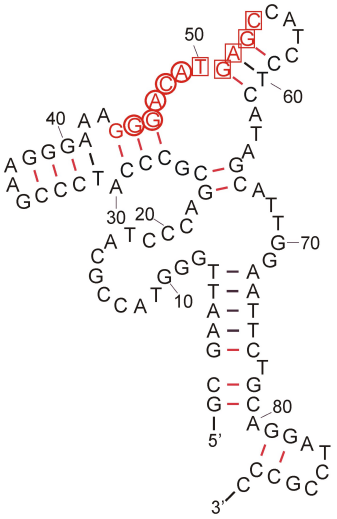

II(R14), dG = -23.57 kcal/mol

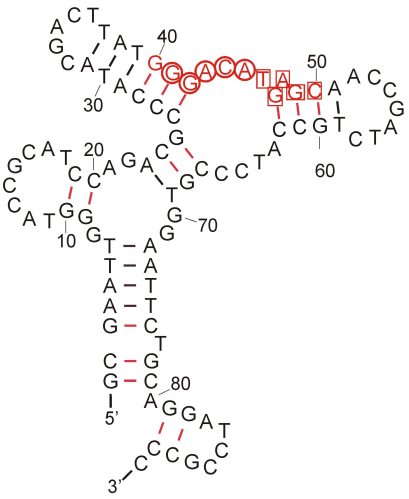

II(R10), dG = -18.98 kcal/mol

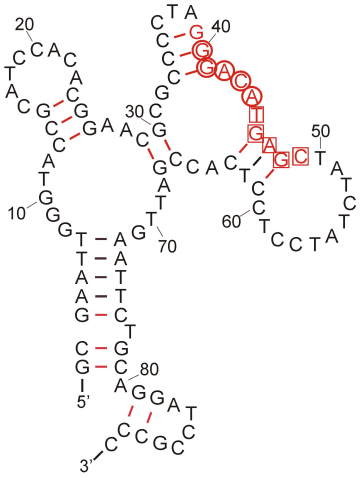

II(B16), dG = -17.39 kcal/mol

***Fig. 4-14***

***The secondary structures of clones in group 2 as predicted by the Zuker mfold program.*** *The conserved nucleotides in this group are indicated in red, those of which in the conserved motif CM-1 are marked by cycles; in the conserved motif CM-2 by squares.*

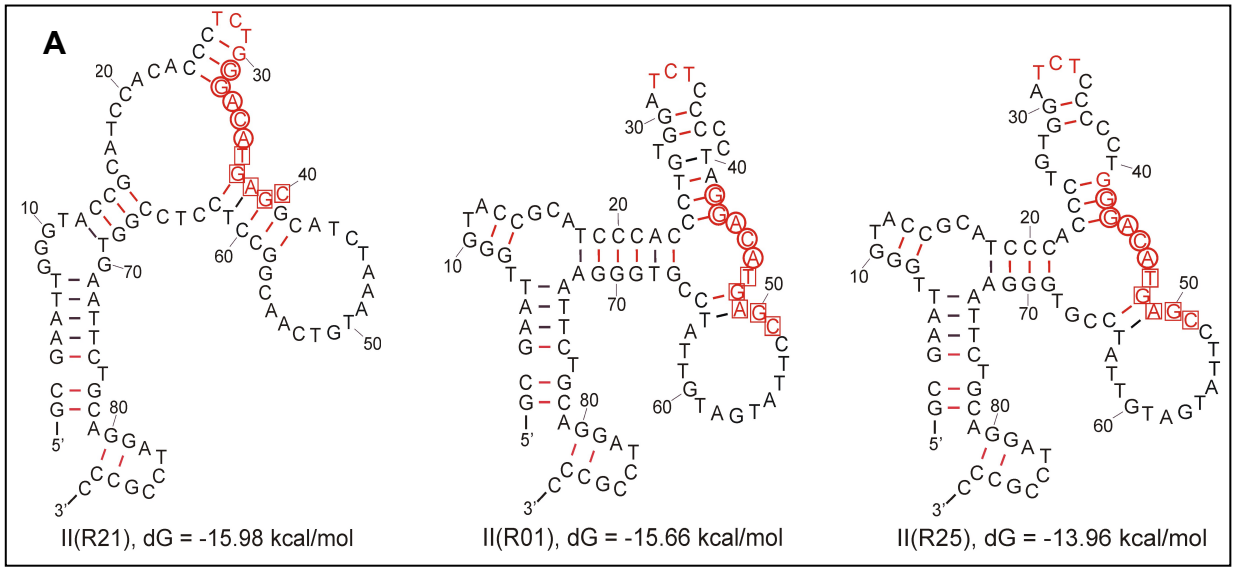


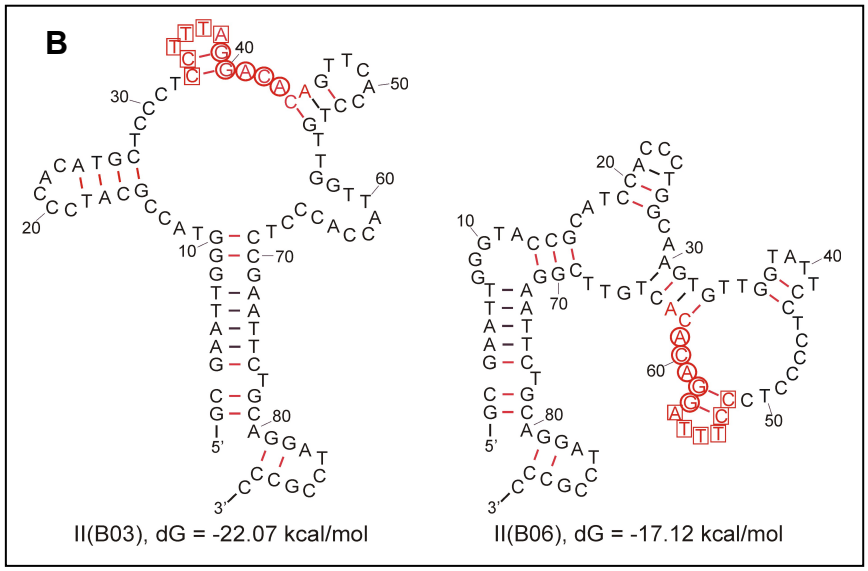


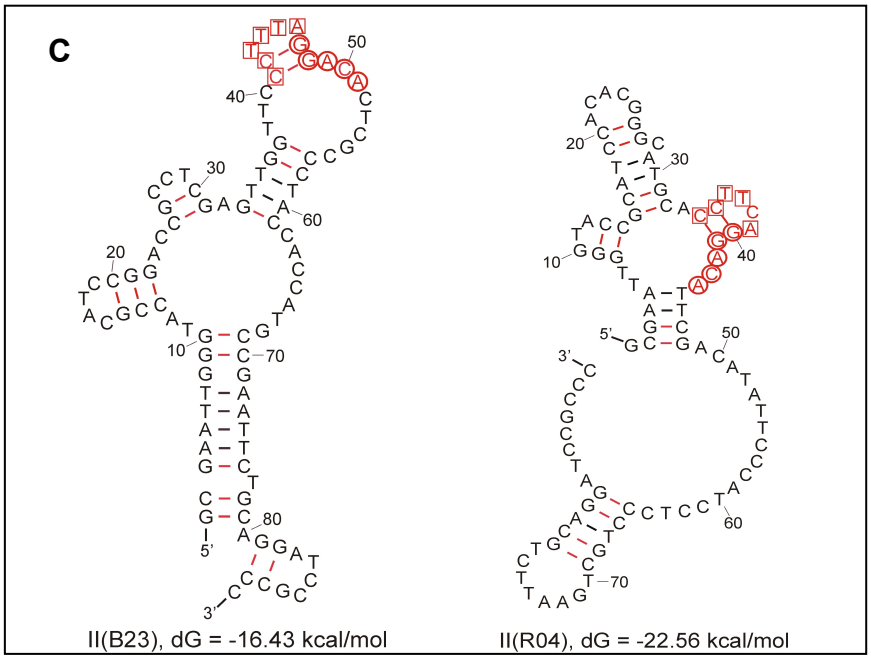


***Figure 4-15 The secondary structures of clones in (A) group 3, (B) group 4, and (C) group 5 as predicted by the Zuker program.*** *The conserved nucleotides in this group are indicated in red, those of which in the conserved motif CM-1 are marked by cycles; in the conserved motif CM-3 by squares.*

The analyses of the secondary structures as predicted by the *Zuker* program provide valuable information about the possible binding motifs of these aptamers. In groups 1, 2 and 3, the highly conserved motif CM-1 and CM-2 are located in the two hairpins with the short loop in-between. In groups 4 and 5 the conserved motifs CM-1 and CM-3 are involved in the hairpin region followed by the loop downstream, in a similar manner as in group 1.These motifs might be important for the GLI binding.

### 4.4.5 Characterization of GLI-Binding

To study the DNA-GLI interaction, the best binders from groups 1 and 2, II(R09) and II(R16), were characterized in detail. The binding constants of these aptamers to GLI were determined by the nitrocellulose filter assays as described in the methods section. The filters were alkali-treated to reduce the non-specific binding of DNA. Figure 4-16 presents that the fractional saturation was plotted as a function of GLI concentration with the program *SigmaPlot*. The $K_D$s for these two aptamers are (1.05 ± 0.08) x $10^{-6}$ M for II(R09) and (1.66 ± 0.10) x $10^{-6}$ M for II(R16). Since not all of DNA molecules are active or in correct conformation to be able to bind to the target (Gold *et al*., 1995), even by saturation the fraction of bound ssDNA is much less than 100%.

Truncation analysis of the GLI-bound sequences could assess the possible binding motif of the DNA aptamer. A minimal sequence (33 nt) with the conserved motifs of CM-1 and CM-2 was designed, based on the primary and secondary structures of the clones in groups 1 and 2 (Fig. 4-17), and this minimal motif might be responsible for binding. The secondary structure analysis of this minimal motif as predicted by the *Zuker* program reveals the conserved two stem-loops (positions 6-14 and 19-28) and an internal loop (positions 15-18). The 5'- and 3'-ends of this minimal motif form a stem by successive five-times G-C pairs (positions 1-5 and 29-33). This stem enhances the chemical stability of this minimal sequence and permitted that the conserved nucleotides in the center may form two hairpins as identified in the predictions of the full-length structures. This minimal motif was analyzed for binding to the GLI peptide by the nitrocellulose filter assays. However, its binding affinity to GLI was too low to be observed.

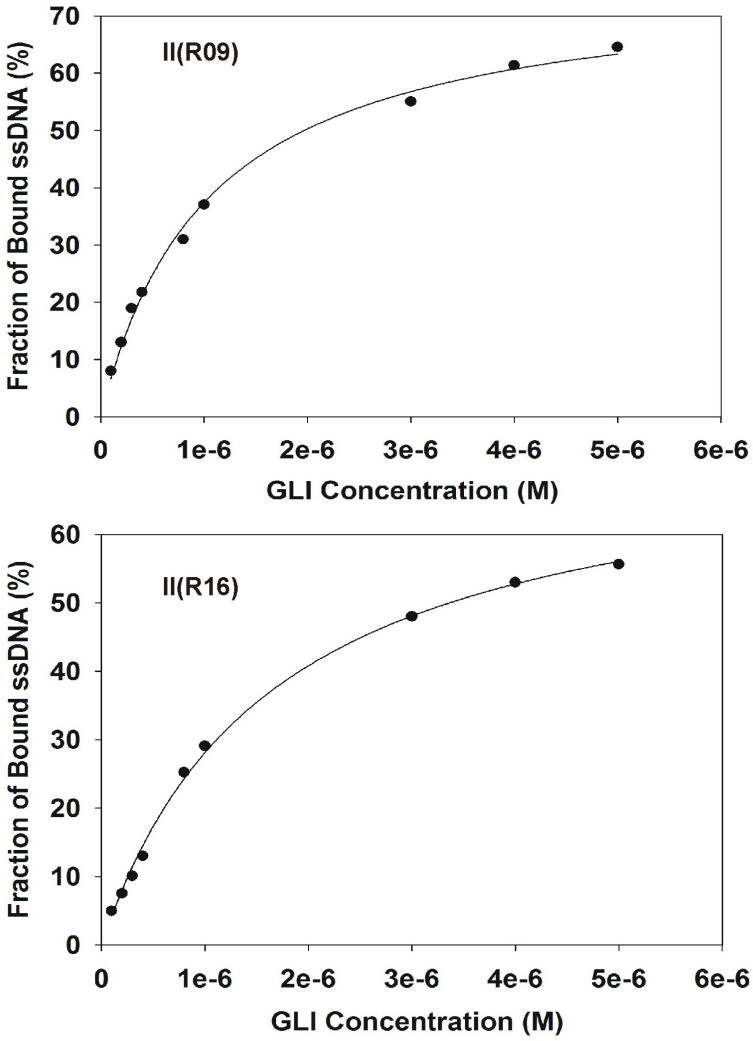


***Figure 4-16 Plots of the binding affinity for aptamers II(R09) and II(R16) to GLI using the fraction of bound ssDNA fitted to the concentration of GLI.*** *Each line represents the best fit for formation of a simple biomolecular complex (R values of 0.9994 and 0.9996).*

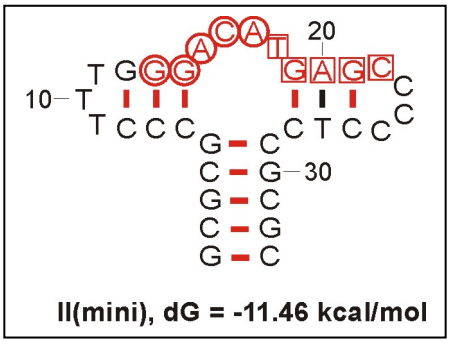


***Figure 4-17***

***Predicted secondary structure of the minimal sequence by the Zuker program.*** *The conserved nucleotides in the motif CM-1 are indicated by red cycles and those in the motif CM-2 by red squares.*

### 4.4.6 Cross-Reactivity of Aptamers

The binding affinity of the aptamer II(R09) to its own peptide target GLI was compared with that to the other *zf* peptide target ZFY. ZFY (30-residue) is the *zf* peptide used in the second *SELEX* experiment of this thesis (Fig. 4-1). Each of these two peptides contains a zinc finger motif of the classical $Cys_2His_2$ type and two peptides have 43% sequence identity. The binding of II(R09) to ZFY was investigated by the nitrocellulose filter binding assays (Fig. 4-18). Interestingly aptamer II(R09) from *SELEX* against GLI has cross-reaction with ZFY, but its binding affinity to GLI was higher than to ZFY.

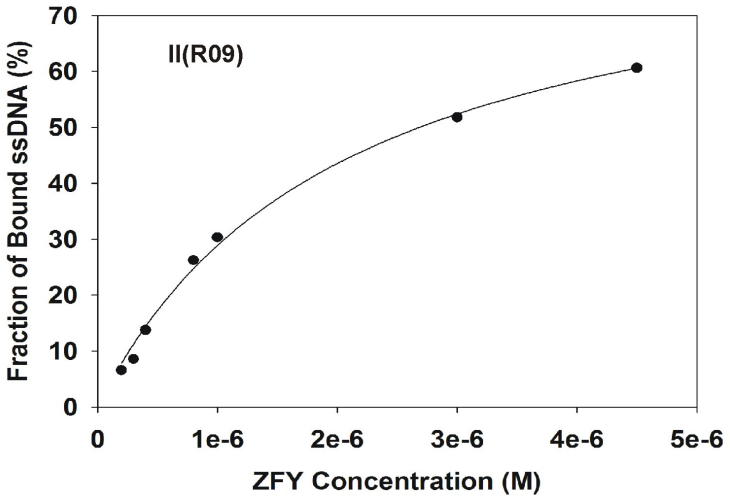


***Figure 4-18 Plot of the binding affinity for aptamer II(R09) to ZFY using the fraction of bound ssDNA fitted to the concentration of ZFY.***
*The line represents the best fit for formation of a simple bimolecular complex (R values of 0.9992).*

In addition, the binding constants of the enriched pool to both ZFY and GLI peptides were also determined by the nitrocellulose filter binding assays. The random ssDNA pool served as a control. The enriched pool against GLI was observed to cross-react with ZFY (Fig. 4-19). It bound to ZFY with even higher affinity than to its own target GLI. However, as controls the binding constants of the random pool to both ZFY and GLI were too low to be measured accurately under these conditions (peptide concentration < 5 μM). They were estimated to be much higher than 20 μM. The $K_D$s of the aptamer II(R09), the enriched pool and the random pool, to ZFY and GLI, are calculated by the *Sigmablot* as summarized in Table 4-4.

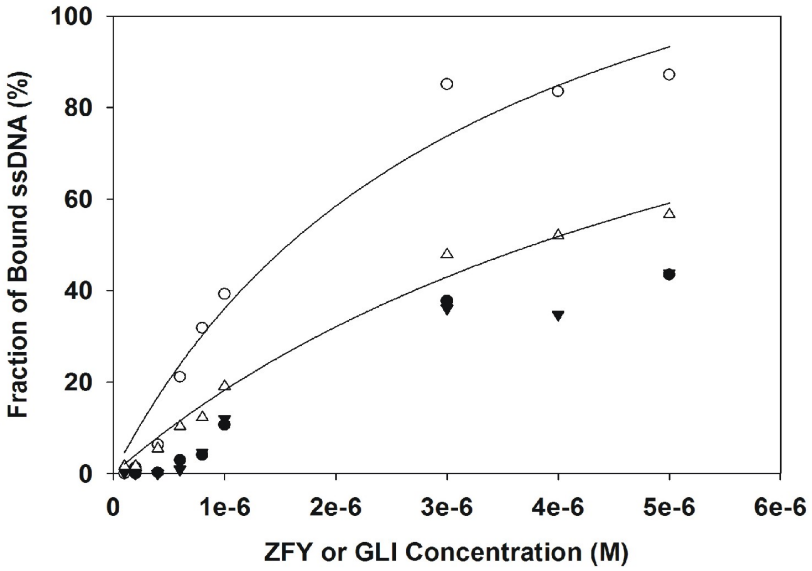


***Figure 4-19 Binding affinities of the random ssDNAs and enriched pool, to ZFY or GLI.*** *The fractional saturation is plotted as a function of protein concentration, for the random ssDNAs to ZFY (●), the enriched pool to ZFY (○), the random ssDNAs to GLI (▼) and enriched pool to GLI (△). The line represents the best fit for formation of a simple bimolecular complex of the enriched pool with ZFY or GLI (R values of 0.9924 to ZFY and 0.9971, from top to bottom).*

***Table 4-4 Comparison of calculated binding constants to ZFY and GLI.***

| Clones | $K_D$ ( x $10^{-6}$M) to ZFY | $K_D$ ( x $10^{-6}$M) to GLI |
|---|---|---|
| II(R09) | 2.05 ± 0.23 | 1.05 ± 0.08 |
| Enriched pool vs. GLI | 3.30 ± 1.18 | 6.43 ± 2.04 |
| Random ssDNA pool | > 20 μM * | > 20 μM * |

** The binding affinity was too low to be determined accurately.*

## 4.5 Aptamers against Peptide ZFY

### 4.5.1 Selection of ZFY-Bound Sequences

The other target, the ZFY peptide, was used for a second *SELEX* experiment. The selection against ZFY was performed for fourteen rounds. The magnetic bead binding assays were performed comparing the DNA pools before round one and after round fourteen. The DNA pools were incubated with the ZFY peptide in a 1:1 molar

ratio of DNA and target (0.25 µM for each). A control peptide containing 23-residue, which is derived from the sequence (residue 136-158) of prion protein in golden hamster, was used as a control for demonstrating the ZFY-specific binding of the enriched DNA pool. BSA and the matrix served also as negative controls. The binding results revealed a very clear enrichment for specific ZFY-bound DNA sequences (Fig. 4-20).

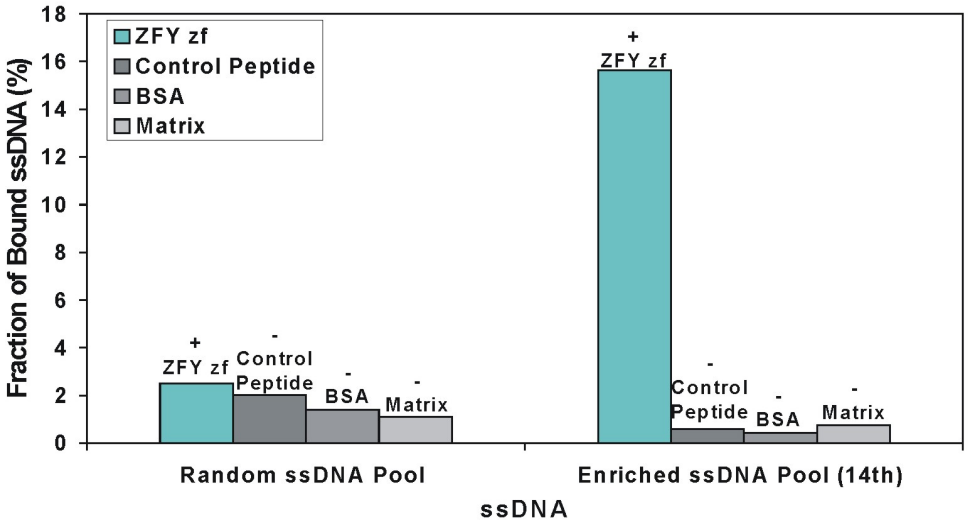


***Figure 4-20 Selection of ZFY ssDNA aptamers from a random ssDNA pool.*** *The random ssDNA pool before round one and the ZFY-bound sequences enriched after round fourteen were compared for binding in the magnetic bead binding assays as described under 3.4.3. The fractions of bound ssDNA (%) in the random pool (left) and enriched pool (right) to the ZFY peptides (+) are indicated by green columns. As controls, the fractions of bound ssDNA (-) to the 23 amino-acids peptide, BSA and the matrix are indicated by grey columns.*

### 4.5.2 Effects of Different Metal Ions on Binding to the ZFY Peptide

Folding of an individual zinc finger domain is achieved through coordination, by cysteine or histidine side chains, of one $Zn^{2+}$ atom. However, it is known from *in vitro* studies that, in some instances, metals other than $Zn^{2+}$ are capable of functioning or competing with $Zn^{2+}$ in metal coordination. The effects of different metal ions on the binding of the ZFY peptides were demonstrated by the nitrocellulose filter binding assays (Fig. 4-21). The ZFY peptides were coordinated with $Zn^{2+}$, $Cd^{2+}$, $Co^{2+}$ ions or without metal ion, respectively. Radioactively-labeled ZFY ssDNA aptamers (final conc. <1 nM) were incubated with ZFY coordinated with different metal ions (final conc. 500 nM) for 30 min. The binding buffers include

traces of different metal ions (50 µM) according to each peptide target to protect the metal ion-coordination. The data demonstrate that the binding affinity of the metal-free peptides to the enriched DNA pool decreased by 42% compared with that of the $Zn^{2+}$-coordicated peptides. $Co^{2+}$- and $Cd^{2+}$-coordinated peptides exhibit binding affinities to the enriched DNA molecules with 14% and 37% reduction.

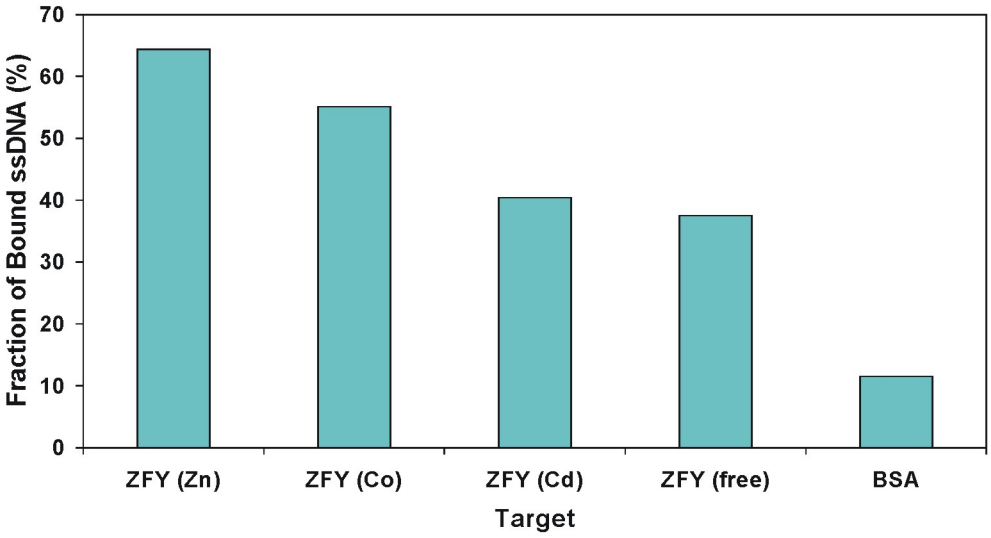


***Figure 4-21 Binding affinities of the ZFY ($Zn^{2+}$) ssDNA aptamers to $Zn^{2+}$-, $Co^{2+}$, $Cd^{2+}$-coordinated and metal-free ZFY peptides.*** *BSA served as control. The fractions of bound ssDNA (%) are indicated by columns.*

### 4.5.3 Primary Structures

The eluted fraction of the ZFY-bound ssDNAs was cloned after round fourteen in *SELEX* against ZFY. DNA sequencing was performed by Sequence Laboratories Göttingen GmbH. Thirty-two clones were sequenced from the enriched pool. The primary structures in the former random region (50 nt) were compared and aligned by *BioEdit* and *ClustalW.* Sequence analysis shows that there are sixteen clones with different sequences (Tab. 4-5). Some clones are observed as guanine-rich. Besides the normal random length of 50 bases, clone I(B15) was isolated with a random region of 51 bases, whereas clone I(B22) and I(B05) have a random region of 49 bases. These changes can be attributed to erroneous DNA replication.

| Nr. | Sequence (5′-3′) | Numbers of Clones | Frequency of Sequence | Portion of Guanine |
|---|---|---|---|---|
| I(R18) | TGTGGCGAATAGCGGGGAAGGGAAGTCGAAGGGTTAGTGGCGTCCTCCCC | | | |
| I(R10) | TGTGGCGAATAGCGGGGAAGGGAAGTCGAAGGGTTAGTGGCGTCCTCCCC | | | |
| I(B16) | TGTGGCGAATAGCGGGGAAGGGAAGTCGAAGGGTTAGTGGCGTCCTCCCC | 5 | 15.6% | 42.0% |
| I(R04) | TGTGGCGAATAGCGGGGAAGGGAAGTCGAAGGGTTAGTGGCGTCCTCCCC | | | |
| I(B25) | TGTGGCGAATAGCGGGGAAGGGAAGTCGAAGGGTTAGTGGCGTCCTCCCC | | | |
| I(B12) | GGCACGTCTCGATCTGCGGATTGCACCTTCTGTATCACCTGGCAGTGCCC | | | |
| I(R09) | GGCACGTCTCGATCTGCGGATTGCACCTTCTGTATCACCTGGCAGTGCCC | | | |
| I(R06) | GGCACGTCTCGATCTGCGGATTGCACCTTCTGTATCACCTGGCAGTGCCC | 5 | 15.6% | 26.0% |
| I(R08) | GGCACGTCTCGATCTGCGGATTGCACCTTCTGTATCACCTGGCAGTGCCC | | | |
| I(R19) | GGCACGTCTCGATCTGCGGATTGCACCTTCTGTATCACCTGGCAGTGCCC | | | |
| I(R14) | ACAACTGCCCGGGTAGGCCAGGGGGAGGAGGCATTTGTATACTATGCGGG | | | |
| I(R03) | ACAACTGCCCGGGTAGGCCAGGGGGAGGAGGCATTTGTATACTATGCGGG | 4 | 12.5% | 40.0% |
| I(R12) | ACAACTGCCCGGGTAGGCCAGGGGGAGGAGGCATTTGTATACTATGCGGG | | | |
| I(B01) | ACAACTGCCCGGGTAGGCCAGGGGGAGGAGGCATTTGTATACTATGCGGG | | | |
| I(R21) | CCATCGGGCAACCTCTACGCACCATCTTGAGTGGTGGATGACGGTTCGCC | | | |
| I(B10) | CCATCGGGCAACCTCTACGCACCATCTTGAGTGGTGGATGACGGTTCGCC | | | |
| I(R01) | CCATCGGGCAACCTCTACGCACCATCTTGAGTGGTGGATGACGGTTCGCC | 4 | 12.5% | 28.0% |
| I(R13) | CCATCGGGCAACCTCTACGCACCATCTTGAGTGGTGGATGACGGTTCGCC | | | |
| I(B19) | CGCAACACGGTCAGGTCAGGGCTAGGATGTTGCGTCAGACAGGTCAAGTG | 2 | 6.3% | 36.0% |
| I(R05) | CGCAACACGGTCAGGTCAGGGCTAGGATGTTGCGTCAGACAGGTCAAGTG | | | |
| I(B04) | CAACGGGGGGCGTGGGCTCCCTCAGGGTGATCTGTTGATCCTTAGTTCCC | 2 | 6.3% | 34.0% |
| I(R23) | CAACGGGGGGCGTGGGCTCCCTCAGGGTGATCTGTTGATCCTTAGTTCCC | | | |
| I(B15) | CTACGCACCGGTCTCGCGCGGTTGTTGTTTACAAACGGTACTCCTCCACTG | 1 | 3.1% | 23.5% |
| I(B22) | GGCAGCGACTGGCTTGGGTCAGGGCATGGAGTCGTGCGGTGCGTGGACG | 1 | 3.1% | 49.0% |
| I(B14) | CAGCGGCTATGGGCTAGGGTATGGACTGGTATGCGACTCAGTGCCCCTCA | 1 | 3.1% | 34.0% |
| I(B08) | CGCAGGGCCTCTCCACGCAATTTCCTCGAGAATGGATACGGTCCCCCTTC | 1 | 3.1% | 22.0% |
| I(B24) | ACACGCCCTCTGGGACATGAGCAAACGCCCTCCACTCTCTCCACTAACCC | 1 | 3.1% | 14.0% |
| I(R25) | CACCCCACCGACCGCGCCCTCTGGGACATGAGCAATGGCACCCCACCTGG | 1 | 3.1% | 24.0% |
| I(B05) | ACACAGCCCCTCGATGCGCCTCCTGGGACATGAGCACACACAGCTCTCC | 1 | 3.1% | 20.4% |
| I(B20) | CACCAAGCGTTAGCTATCCTAGCCTCCTGTGGTTACACGCTCGTGAATGC | 1 | 3.1% | 22.0% |
| I(R07) | CACACCCGTGGTATCCCCCGTCATGGTCTCATGAGATGCCCACCGCTTGG | 1 | 3.1% | 24.0% |
| I(B09) | GGCACACGTCTTCACCATCCCGGGGAATATACAGTCACTGTGTGCTGGTG | 1 | 3.1% | 28.0% |

***Table 4-5 Alignment of ZFY-bound clones based on the sequences in random region.*** *Sequences of thirty-two PCR clones encoding ssDNA ligands from SELEX against ZFY are shown on the left. The number of identical sequences, frequency of sequence, and portion of guanines in each sequence are indicated on the right side of the sequences.*

All sequences were analyzed on primary structures in the random region as for those in *SELEX* against GLI (see 4.4.2). Sequences analysis of these twenty-two clones failed to identify an overall conserved motif, however, revealed that they could be classified into six groups based on nucleotide conservation at specific residues (Tab. 4-6). The sequences in groups 2 and 3 could form possibly G-quadruplexes

based on the G-rich region. Interestingly, clone I(B24) in group 5 presents identical sequence with aptamer II(R09) from *SELEX* against GLI. In addition, the conserved nucleotides of other sequences in group 5 are also similar with those in the enriched pool against GLI (Tab. 4-3).

```
GROUP 1
        I(B15)      CTACGCACCGGTCTCG--C-GCGG-TTGTTGTTTACAAACGGTACT-CCTC-CACTG
        I(B12)         GGCA-CG-TCTCGATCTGCGGATTGCACCTTCT-----GTATCACCTGGCAGTGCCC
Consensus:              GCA CG TCTCG  C GCGG TTG              GTA   CCT  CA TG

GROUP 2
        I(R18)      TGTGGCGAATAGCGGGG-AAGGGAAGTCGAAGGGTTAGTGGCGTCCTCCCC
        I(B04)             CAACGGGGGGCGTGGGCTCCCTCAGGGTGATCTGTTGATCCTTAGTTCCC
Consensus:                    GGGG   GGG         GGG      G

GROUP 3
        I(R14)     ACAACTGCCCGGG-T--AGGCC-AGGGGGAGGA--GGCATTTGTATACTATGCGGG
        I(B14)           CAGCGGCTAT-GGGCTAGGGTATGGACTGGTATGCGACTCAGTGCCCCTCA
        I(B19)        CGCAACACGG-T-CAGGTC-AGGGCTAGGA-TGTTGCGTCAGACAGGTCAAGTG
        I(B22)      GGCAGCGACTGGCT-TGGGTC-AGGGCATGGAGTCGTGCGGTGCGT-GGACG
Consensus:                 GG     GG   AGGG   GGA

GROUP 4
        I(R21)      CCATCGGGCAACCTCTACGCACCATCTTGAGTGGTGGATGACGGTTCGCC
        I(B08)       CGCAGGGCC-TCTCCACGCAATTTCCTCGAGAATGGAT-ACGGTCCCCCTTC
Consensus:             GGGC   CTC ACGCA   TC T      TGGAT ACGGT

GROUP 5
        I(B24)                  ACACGCCCTCTGGGACATGAGCAAACGCCCTCCACTCTCTCCACTAACCC
        I(R25)        CACCCCACCGACCGCGCCCTCTGGGACATGAGCA-ATGGCACCCCACCTGG
        I(B05)      ACACAGCCCCTCGATGCGCCTCCTGGGACATGAGCACACACA------GCTCTCC
Consensus:                     CGCC  CTGGGACATGAGCA             CTC

GROUP 6
        I(B20)        CACCAAGCGTTAGCTATCCTAGCCTCCTGTGGTTACACGCTCGTGAATGC
        I(R07)        CACACCCGTGGTATCCCCCGTCATGGTCTCATGAGATGCCCACCGCTTGG
        I(B09)      GGCACACGTCTTCACCATCCCGGGGAATATACAGTCACTGTGTGCTGGTG
Consensus:            CAC
```

***Table 4-6 Comparison of the sequences of the ZFY-bound ssDNAs.*** *Four nucleotides are shown with different colors. The gaps are indicated by hyphens. Conserved identical nucleotides are shown below each group of the ssDNA ligands, where the positions with mutations are presented by italic letters.*

### 4.5.4 Binding Affinities of Single Clones

The binding affinities of the clones with different sequences were tested with the magnetic bead binding assays as described in the methods section. The ssDNA pool containing random sequences was used as a control. Each binding assay was performed as a mean of triple independent experiments. All clones showed specific binding when incubated with 250 nM peptides, however, with different affinities (Fig. 4-22). Binding of the ssDNA pool containing random sequences to the peptides was very weak, which excluded the possibility of unspecific binding between

aptamers and peptides. Clone I(B22) bound to the matrix even in the absence of target peptides, however, neither of the other clones did.

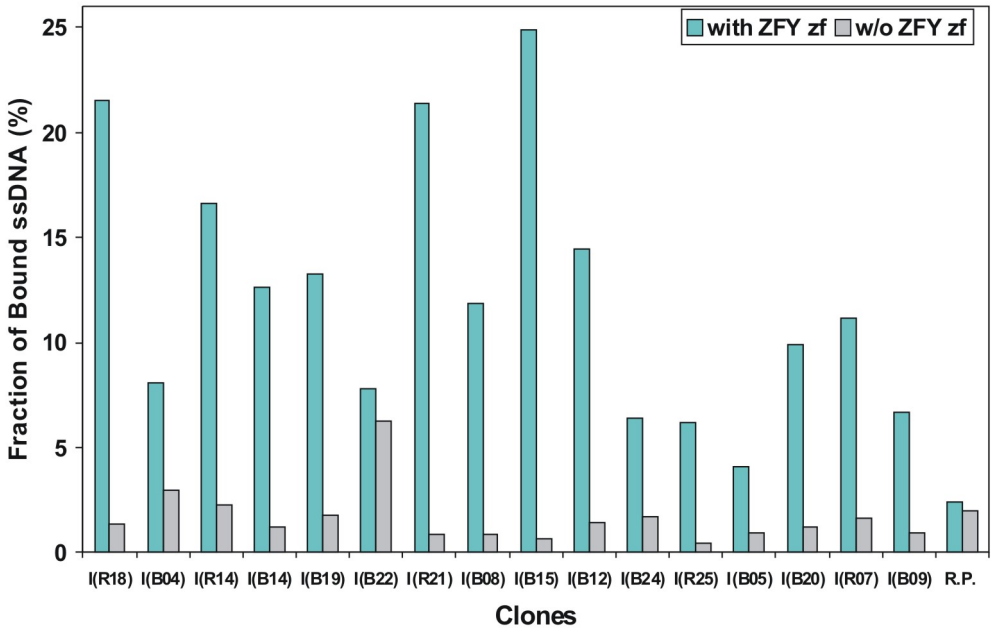


***Figure 4-22 Magnetic bead screens of clones obtained from the fourteen rounds of SELEX against ZFY.*** *The binding in the presence of ZFY is indicated by a green column, whereas, matrix binding by a grey column. The ssDNA clone is indicated below the column. The random ssDNA pool (R. P.) was applied as a control.*

### 4.5.5 Secondary Structures

As described for the GLI-bound sequences under 4.4.4, computer analysis using the *Zuker mfold* program version 3.2 predicted stable secondary structures for these ZFY-bound ssDNAs. Only the structures with highest energies are shown. Furthermore, the secondary structures of the clones were compared with each other in each group, e.g., by positions of conserved nucleotides. The clones in group 6 were not analyzed because of the lack of conserved nucleotides. It seems that more conserved nucleotides are involved in base pairs (especially G-C pairs), stronger is the binding ability.

Group 1

The predicted secondary structures of the two sequences in group 1 are shown in Figure 4-23. Clone I(B15) has an inner loop of 16 nucleotides, from which two short and one long helical regions are diverged. Both of the two short helical

regions (positions 24-40 and positions 42-54) form hairpins, in which one of them is intermitted by a bulge. The long helical region contains the primer regions. It has two hairpins in the end (positions 82-90) and middle (positions 63-72). The conserved nucleotides TCTCGCGCG in both I(B15) and I(B12) are located in one side of the hairpin region, of which CG and GCG are involved in stable G-C pairs. TCT are located in a tetra-loop and C is in the small bulge of the hairpin. This conserved hairpin region might be important for ZFY binding.

A further analysis revealed that eighteen conserved nucleotides in clone I(B15) are located in base pairs, of which fourteen are part of G-C pairs, however, only nine conserved nucleotides in clone I(B12) are involved in base pairing, of which eight form G-C pairs. In the binding tests, I(B15) demonstrated much stronger binding to ZFY than I(B12).

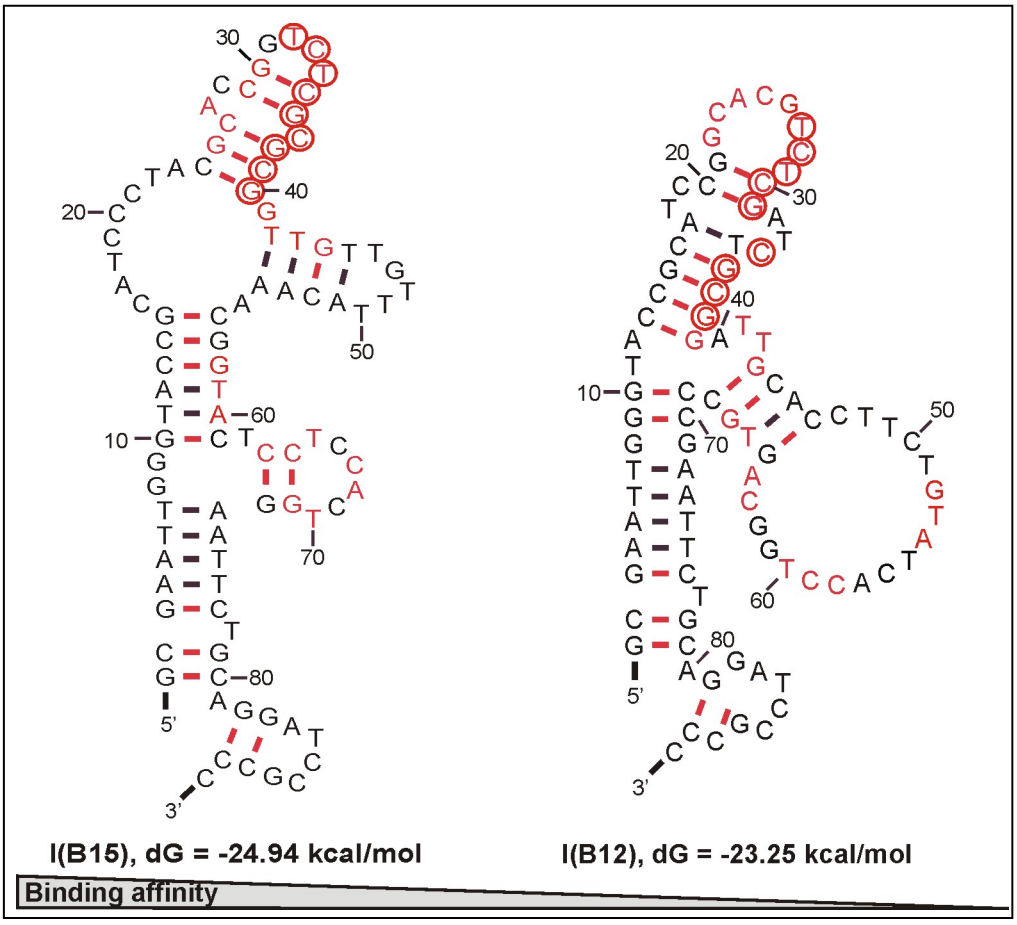


***Figure 4-23 Secondary structures of the clones in group 1 as predicted by the Zuker mfold program.*** *The conserved sequences in primary structures are indicated in red. The nucleotides, which are also conserved in secondary structures, are marked in red cycles. The free energies and the trend of binding affinities (decreases from left to right) in the binding tests (Fig. 4-22) are shown under the figures.*

Group 2

There are two different sequences in seven clones in group 2. The predicted secondary structures of clones I(R18) and I(B04) by the *Zuker* program are shown in Figure 4-24 A. Clone I(R18) forms a long helical region (positions 17-84) with a loop on the top and three bulges. The conserved guanines are located either on the stem (positions 33-46 to positions 60-71), which is purine-rich, or the loop (positions 47-59). However, it failed to identify highly conserved motifs in these structures.

Moreover, Clone I(R18) is G-rich and could form a G-quadruplex structure. However, such structure can not be predicted by available algorithm of secondary structure analysis (SantaLucia, 1998; Saito and Tomida, 2005). G-quadruplex can form a lipophilic four-stranded structure by two vertical arrangements of multiple guanine tetrads. The tetrads are stabilized by Hoogsteen hydrogen bonds. G-quadruplex in clone I(R18) was predicted by the *QuadFinder* and *QGRS* mapper programs. A minimal G-rich sequence could form a G-quadruplex with a length of 27 nucleotides ($G_2N_5G_2N_8G_2N_6G_2$). Normally shorter loops are more common than longer loops. G-quadruplexes tend to have loops roughly equal in size. The greater the numbers of guanine tetrads, the more stable the quadruplex (Kikin *et al.,* 2006). Two of the possible schematic representations of these G-quadruplexes are outlined in Figure 4-24 B (Padmanabhan and Tulinsky, 1995; Burge *et al.*, 2006). Both of them have two guanine tetrads connected by three loops and the two structures differ in the tetrad grooves, which span the loops. Such a G-quadruplex in clone I(R18) might be important for ZFY binding.

A further analysis revealed that seven conserved nucleotides of clone I(R18) are all involved in G-C base pairs. For clone I(B04) six conserved nucleotides are all located in G-C base pairs. However, I(B04) could not form the similar G-quadruplex structure as I(R18). In the binding tests (Fig. 4-22), clone I(B04) has a much weaker binding to ZFY than clone I(R18).

Group 3

In group 3 eight clones exhibit four different sequences. Figure 4-25 illustrates secondary structures as predicted by the *Zuker* program of the clones from group 3, except matrix-binder I(B22). It failed to identify overall conserved motif in these structures. Having a close analysis at the conserved sequences in clone I(R14), five

of six conserved nucleotides, which are located in stems, are part of G-C pairs. In clone I(B19) there are four from six and in clone I(B14) four from five.

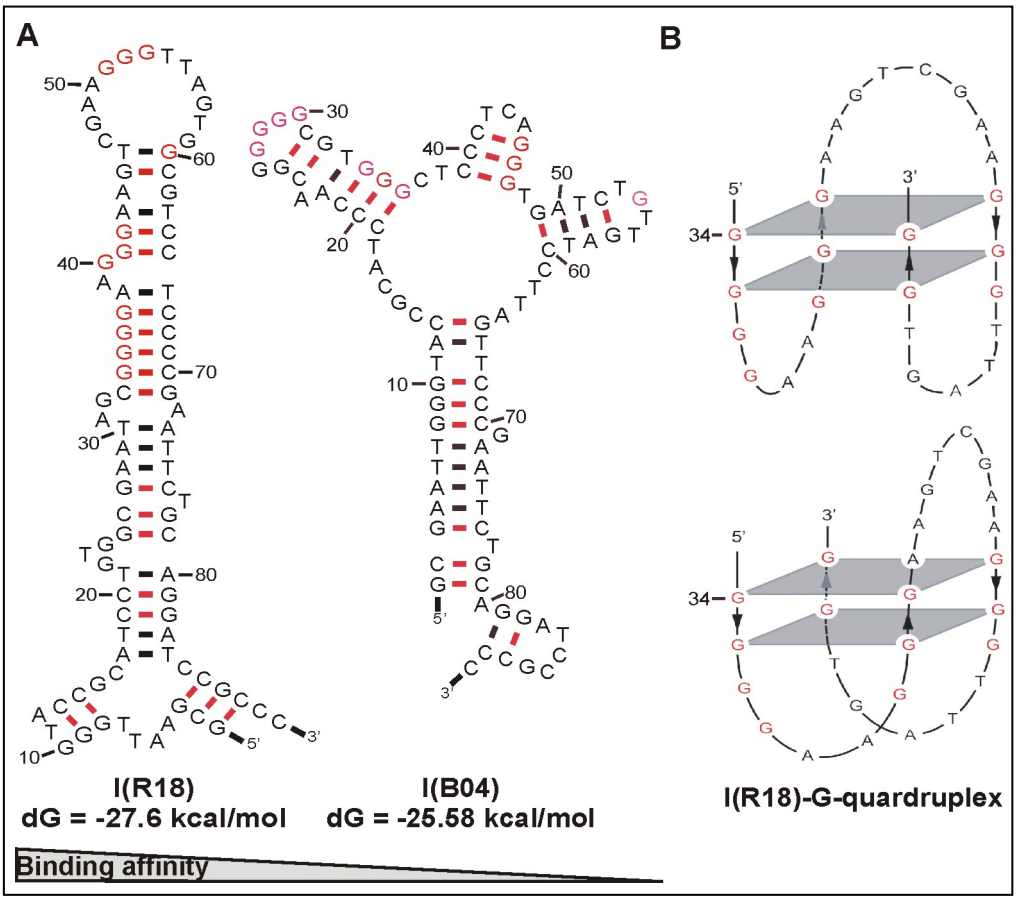


***Figure 4-24 (A) Secondary structures of the clones in group 2 as predicted by the Zuker mfold program.*** *The description is same as in Figure 4-23.* ***(B) Schematic presentations of the predicted G-quardruplex structures of clone I(R18).*** *The conserved nucleotides are indicated with red letters. The guanine tetrads are marked by dark squares.*

Moreover, these clones are also G-rich and the conserved G-rich region might form a G-quadruplex (Fig. 4-26 A). Clone I(R14) could form the shortest loops (Fig. 4-26 B) compared to the other clones, therefore, it might present a more stable secondary structure. In the binding tests (Fig. 4-22), clone I(R14) showed the strongest binding to ZFY in this group.

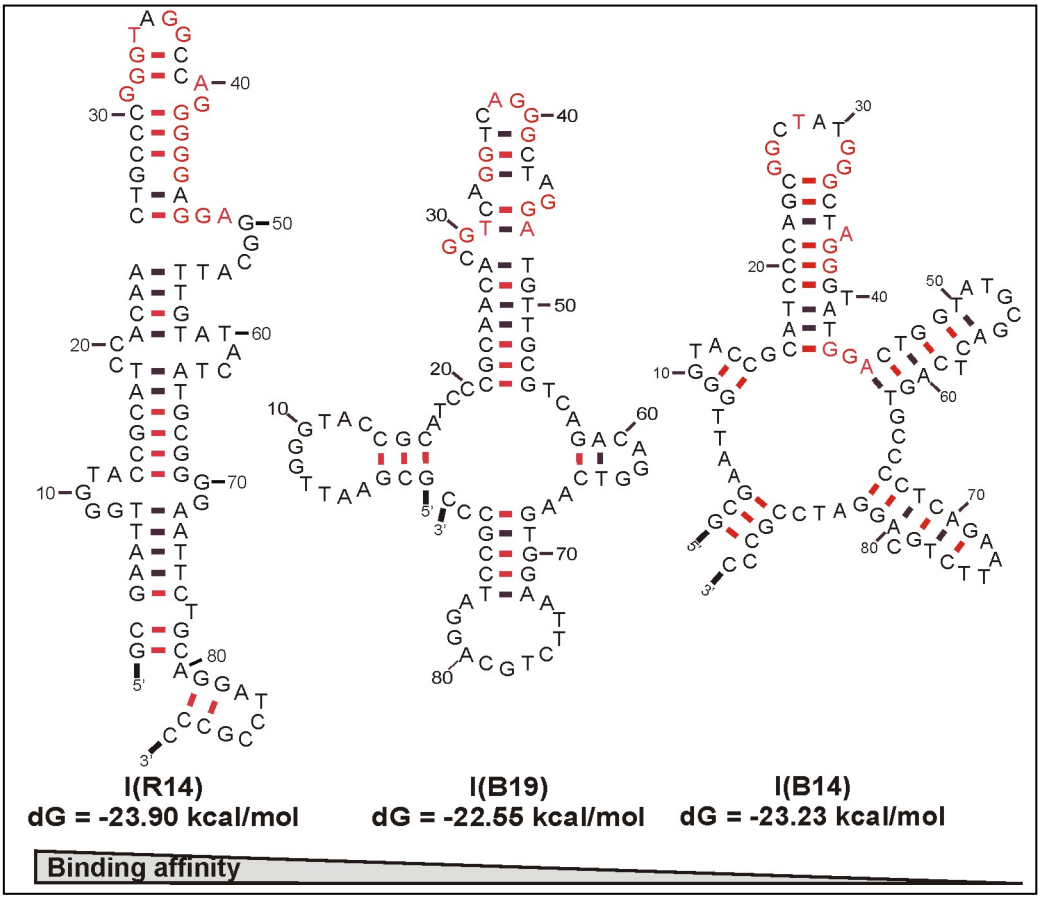


***Figure 4-25 Secondary structures of the clones in group 3 as predicted by the Zuker mfold program.*** *The description is the same as in Figure 4-23*

**A**

| Clone | G-rich region |
|---|---|
| I(R14) | $G_2N_2G_2N_3G_2N_4G_2$ |
| I(B19) | $G_2N_3G_2N_3G_2N_4G_2$ |
| I(B14) | $G_2N_4G_2N_4G_2N_4G_2$ |

**B**

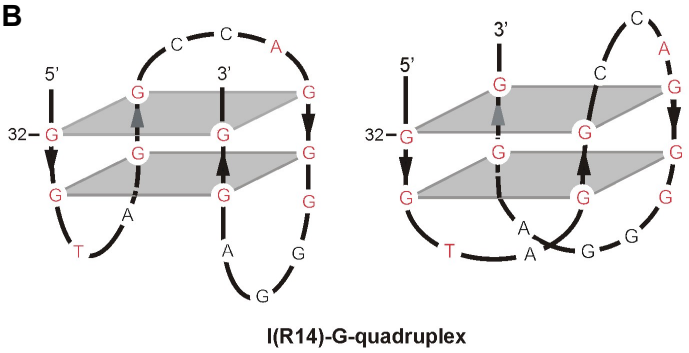


***Figure 4-26 (A) The predicted conserved G-rich regions in the sequences of group 2.*** *The guanines which contribute to G-quadruplex are marked by red colour. The nucleotides located in loops are indicated with N.* ***(B) Schematic presentations of G-quardruplex structures of I(R14).*** *The description is the same as in Figure 4-24 B.*

Group 4

Group 4 contains two different sequences from five clones. Their secondary structures as predicted by the *Zuker* program are shown in Figure 4-27. Both of the clones were predicted for very similar secondary structures. The conserved nucleotides TGGAT ACGGT [positions 55-65 in clone I(R21) and 53-62 in clone I(B08)] are highly conserved in both structures. The nucleotides GGAT and CGGT pair with the nucleotides in the primer region (positions 12-15 and 17-20). T and A are located in single strands. This conserved region might be important for ZFY binding.

Out of the conserved nucleotides of clone I(R21), seventeen are part of base pairs, of which eleven locate in stable G-C pairs. In clone I(B08) fifteen conserved nucleotides are located in base pairs, of which ten are part of G-C pairs. In the binding tests (Fig. 4-22), clone I(R21) has a stronger binding ability to ZFY than clone I(B08).

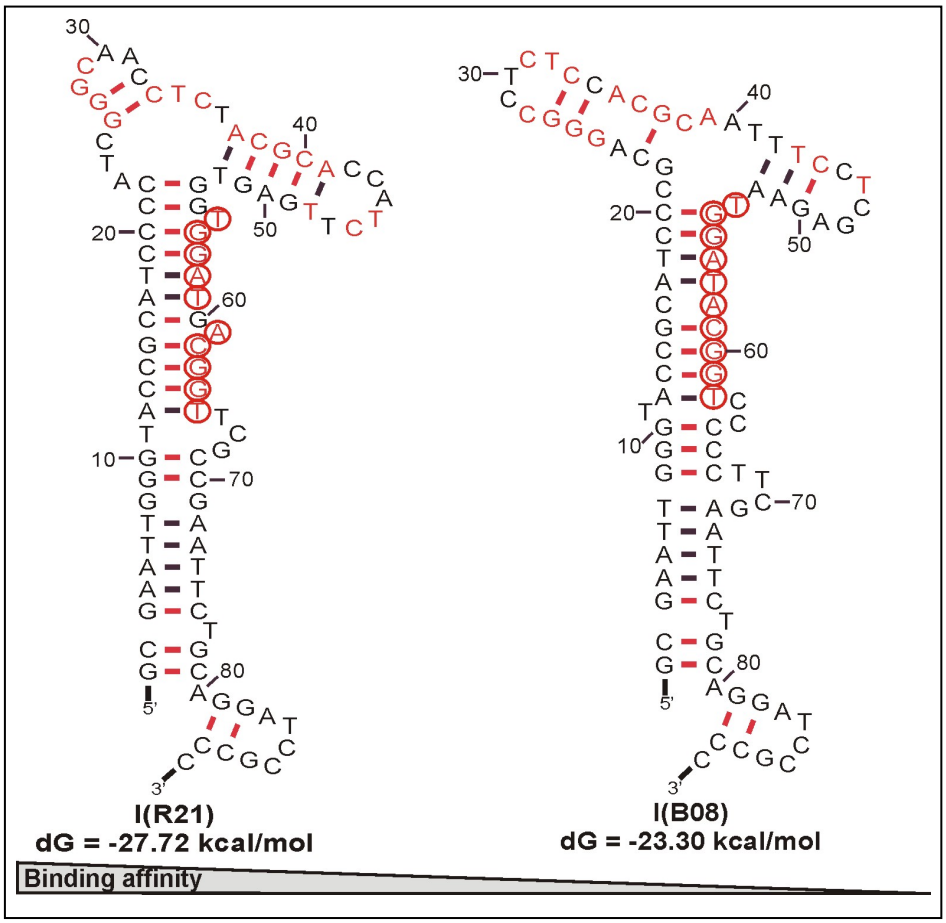


***Figure 4-27 Secondary structures of the clones in group 4 as predicted by the Zuker mfold program.*** *The description is the same as in Figure 4-23.*

Group 5

The three clones in group 5 have similar secondary structures (data not shown) as the GLI-bound sequences. Clone I(B24) is identical with II(R09) from the *SELEX* against GLI (Fig. 4-14). The cross-reactivity of the identical binder from these two independent selections was discussed under 4.4.6.

### 4.5.6 Characterization of ZFY-Binding

To characterize the aptamer-ZFY interaction, the dissociation constants of the best binders from groups 1-5 were further determined by SPR and the nitrocellulose filter binding assays. Aptamer I(B15), which showed the highest binding to ZFY in the previous binding tests, was first quantified by SPR spectroscopy on a BIAcore instrument. Figure 4-28 illustrates the sensorgrams of a concentration series of aptamer I(B15) injected over ZFY immobilized on a sensor chip (A), and the binding curve (B). The association and dissociation of the aptamer to the peptides were observed by the increase and decrease of the RU values. As the concentrations of the aptamer increase (from bottom to top), the saturation (at ~280 RU) of the DNA sites is approached and the association reaction rate increases. The experimental results confirm the high affinity binding between aptamer I(B15) and ZFY observed in the magnetic bead binding assays (Fig. 4-22). The binding constant $K_D$ was calculated by the *Sigmablot* program (version 9.0) as (1.54 ± 0.41) x $10^{-7}$ M.

As discussed above, ZFY peptides could fold into tetrahedral $Zn^{2+}$-coordination only in the presence of $Zn^{2+}$ ions, whereas metal-free ZFY peptides have a high content of random coil. The effect of $Zn^{2+}$ ions on the binding of aptamer I(B15) was demonstrated by the magnetic bead binding assays. Radioactively labeled I(B15) (250 nM) was incubated with $Zn^{2+}$-coordicated ZFY (2.5 µM) or metal-free ZFY (2.5 µM) for 40 min. The experimental data in Figure 4-29 demonstrate that aptamer I(B15) binds to ZFY in the presence of $Zn^{2+}$ ions and the metal-free ZFY peptides exhibit much weaker binding affinity to the aptamer.

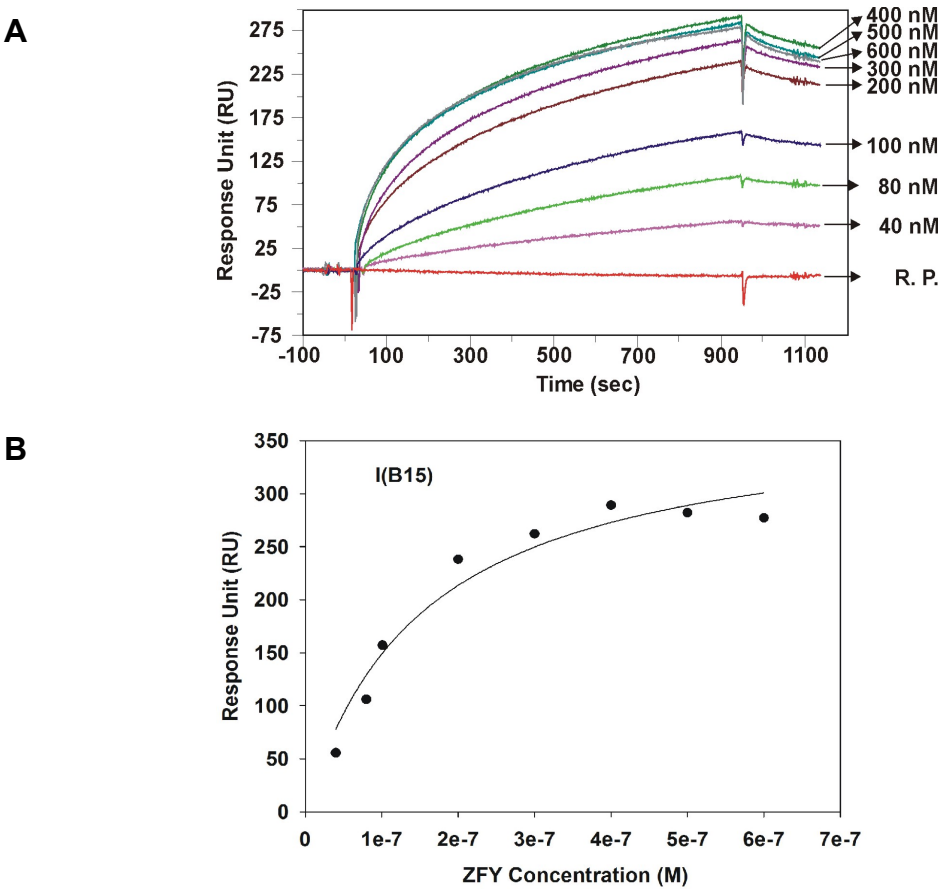


***Figure 4-28 (A) SPR-sensorgramms for the interaction of aptamer I(B15) with ZFY.*** *A 400 nM random ssDNA pool (R. P.) served as a negative control. The response units (RU) are blotted against times (sec).* ***(B) Plot of the binding affinity for aptamer I(B15) to ZFY.*** *The line represents the best fit for formation of a simple bimolecular complex (R values of 0.9966).*

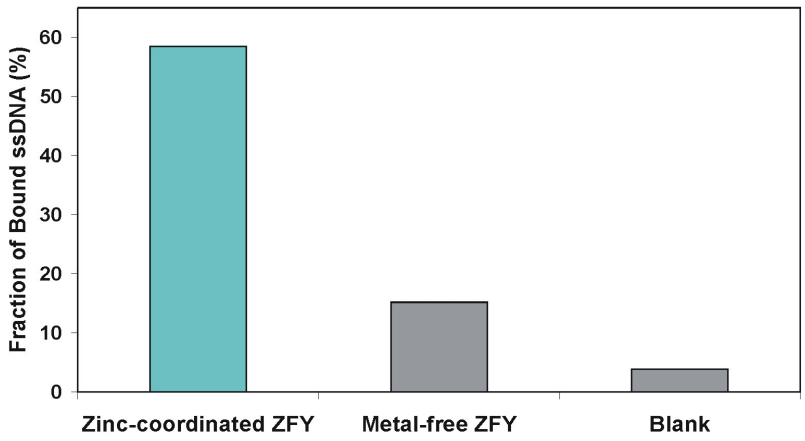


***Figure 4-29 Binding affinities of aptamer I(B15) to $Zn^{2+}$-coordicated and metal-free ZFY.*** *The fractions of bound ssDNA (%) are presented by columns. The target is indicated below the column. The blank sample contains only matrix in the absence of peptides.*

The binding specificity of aptamer I(B15) to ZFY peptides in comparison with GLI peptides were evaluated by the magnetic bead binding assay. GLI (29-residue) is the *zf* peptide target used in *SELEX* against GLI (Fig. 4-1). The radioactively labeled aptamer I(B15) (100 nM) was incubated in a molar ratio of 1:1 with ZFY, GLI, the control protein BSA, and the matrix, respectively. The experimental data in Figure 4-30 indicate that aptamer I(B15) shows no cross-reaction with GLI under this condition. Moreover, it binds neither to BSA nor to the matrix.

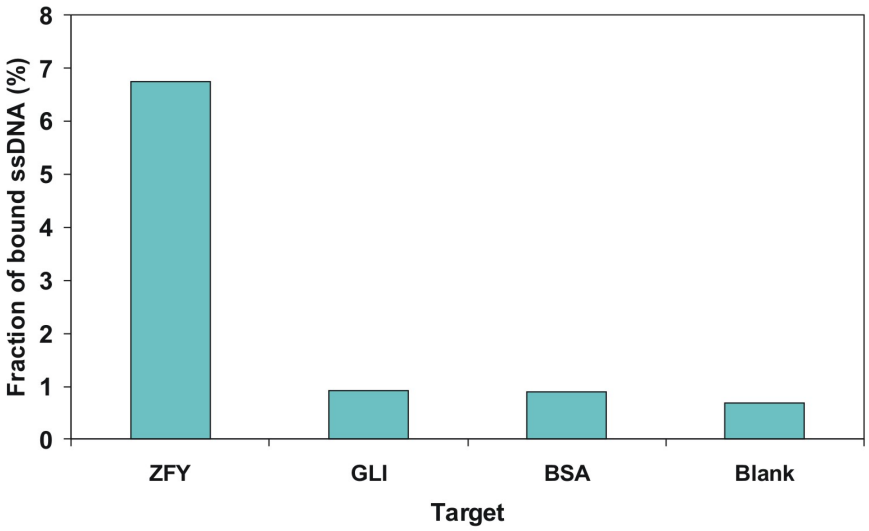


***Figure 4-30 Binding tests of aptamer I(B15) to ZFY and GLI.*** *The fractions of bound ssDNA (%) are presented by columns. BSA and the matrix served as controls.*

In addition, the binding constants of the best binders from other groups (except group 6) were determined by the nitrocellulose filter binding assays. The fraction of bound ssDNA was plotted against the concentration of ZFY with the program *Sigmaplot*. The binding curves for aptamers I(R18), I(R14), I(R21) and I(R24) are shown in Figure 4-31. The $K_D$s for these aptamers were determined to be in the nM range, except for clone I(B24), which has a $K_D$ in the µM range (Tab. 4-7). As mentioned above, aptamer I(B24) is identical with aptamer II(R09) found in the other enriched pool against GLI and the $K_D$ of aptamer II(R09) to GLI was determined to be (10.5 ± 0.8) x $10^{-7}$ M (see under 4.4.6).

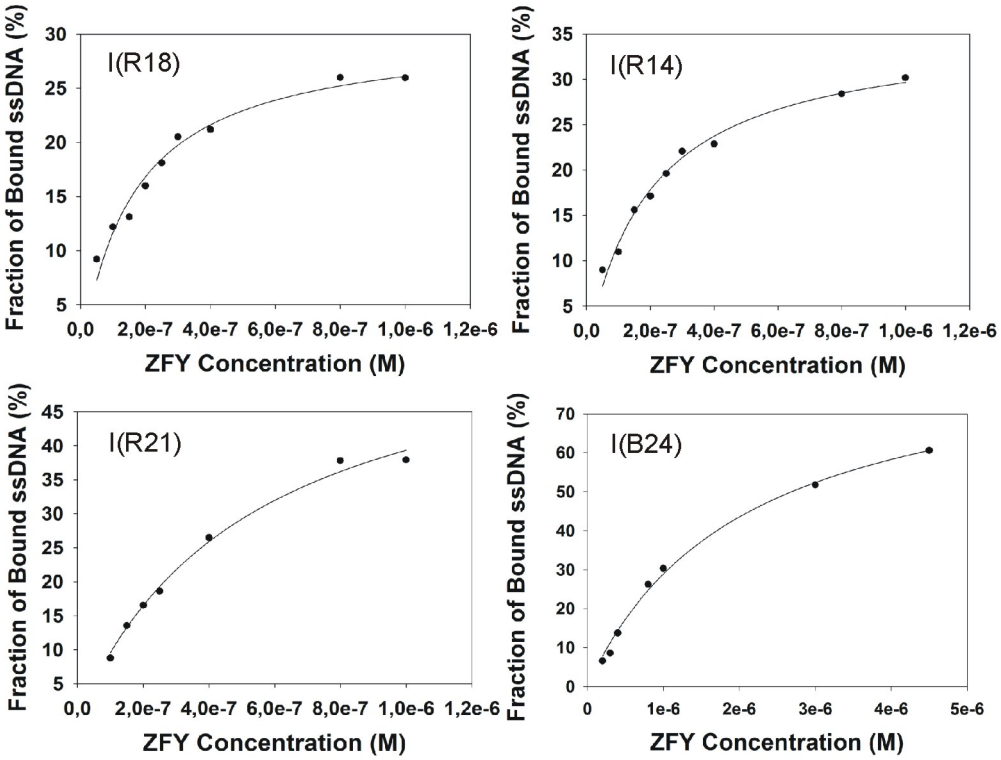


***Figure 4-31 Plot of the binding affinity for the aptamers to ZFY using the fraction of bound ssDNA value fitted to the concentration of ZFY.*** *Each line represents the best fit for formation of a simple bimolecular complex (R values of 0.9986, 0.9992, 0.9993 and 0.9992).*

***Table 4-7 Calculated binding constants of several aptamers to ZFY.***

| Clones | $K_D$ ( x $10^{-7}$ M) |
|---|---|
| I(R18) | 1.60 ± 0.22 |
| I(R14) | 2.00 ± 0.21 |
| I(R21) | 5.30 ± 0.60 |
| I(B24) | 20.54 ± 2.28 |

One of the best binders, aptamer I(R18), is G-rich, and have potential to form a G-quadruplex as discussed under 4.5.5 (Gr. 2). To probe the nucleotide sequence or structural requirements for aptamer I(R18)-ZFY interaction, three truncated aptamers were designed as outlined in Table 4-8. Variant T1 (30 nt) was truncated based on stem-loop as predicted by the *Zuker* program*;* variant T2 (27 nt) is designed based on G-quadruplex as predicted by the *QuadFinder*, whereas variant

T3 (20 nt) contains only one strand of the purine-rich polynucleotide in stem-loop region of T1.

***Table 4-8 Primary structures of aptamer I(R18) and its three truncated variants.***

| Name | Sequence (5'-3') | N |
|---|---|---|
| I(R18) | GCGAATTGGGTACCGCATCCTGTGGCGAATAGCGGGGAAGGGAAGTCGAAGGGTTAGTGGCGTCCTCCCCGAATTCTGCAGGATCCGCCC | 90 |
| I(R18)-T1 | CGGGGAAGGGAAGTCGAAGGGTTAGTGGCGTCCTCCCCG | 39 |
| I(R18)-T2 | GGGGAAGGGAAGTCGAAGGGTTAGTGG | 27 |
| I(R18)-T3 | GGGGAAGGGAAGTCGAAGGG | 20 |

These three truncated variants were measured for binding to ZFY. The binding curves of variants T1 and T2 are shown in Figure 4-32. The $K_D$s were calculated by the program *SigmaPlot* as (5.20 ± 0.95) x $10^{-7}$ M for variant T1 and (7.08 ± 0.95) x $10^{-7}$ M for variant T2. The effects of the truncation analyses of aptamer I(R18) on interaction with ZFY are outlined in Figure 4-33. The truncated variant T1 (39 nt), which is predicted by the *Zuker* program containing a hairpin with a G-rich region, binds to ZFY with a better affinity than the truncated variant T2 (27 nt) with only the G-rich region. Both of them exhibit affinity binding to ZFY, but weaker than that of the full-length aptamer I(R18). However, the shortest purine-rich truncated variant T3 (20 nt) was not observed to bind to ZFY.

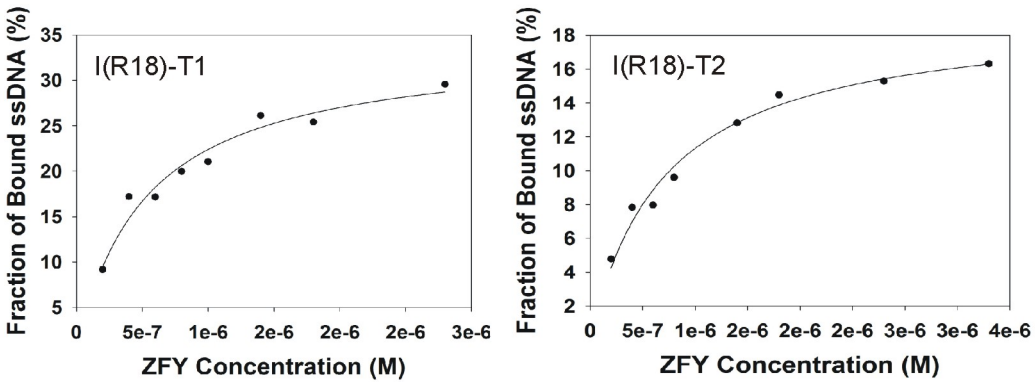


***Figure 4-32 Plot of the affinities for truncated I(R18)-T1 and -T2 to ZFY using the fraction of bound ssDNA value fitted to the concentration of ZFY.*** *Each line represents the best fit for formation of a simple bimolecular complex (R values of 0.9983 and 0.9988).*

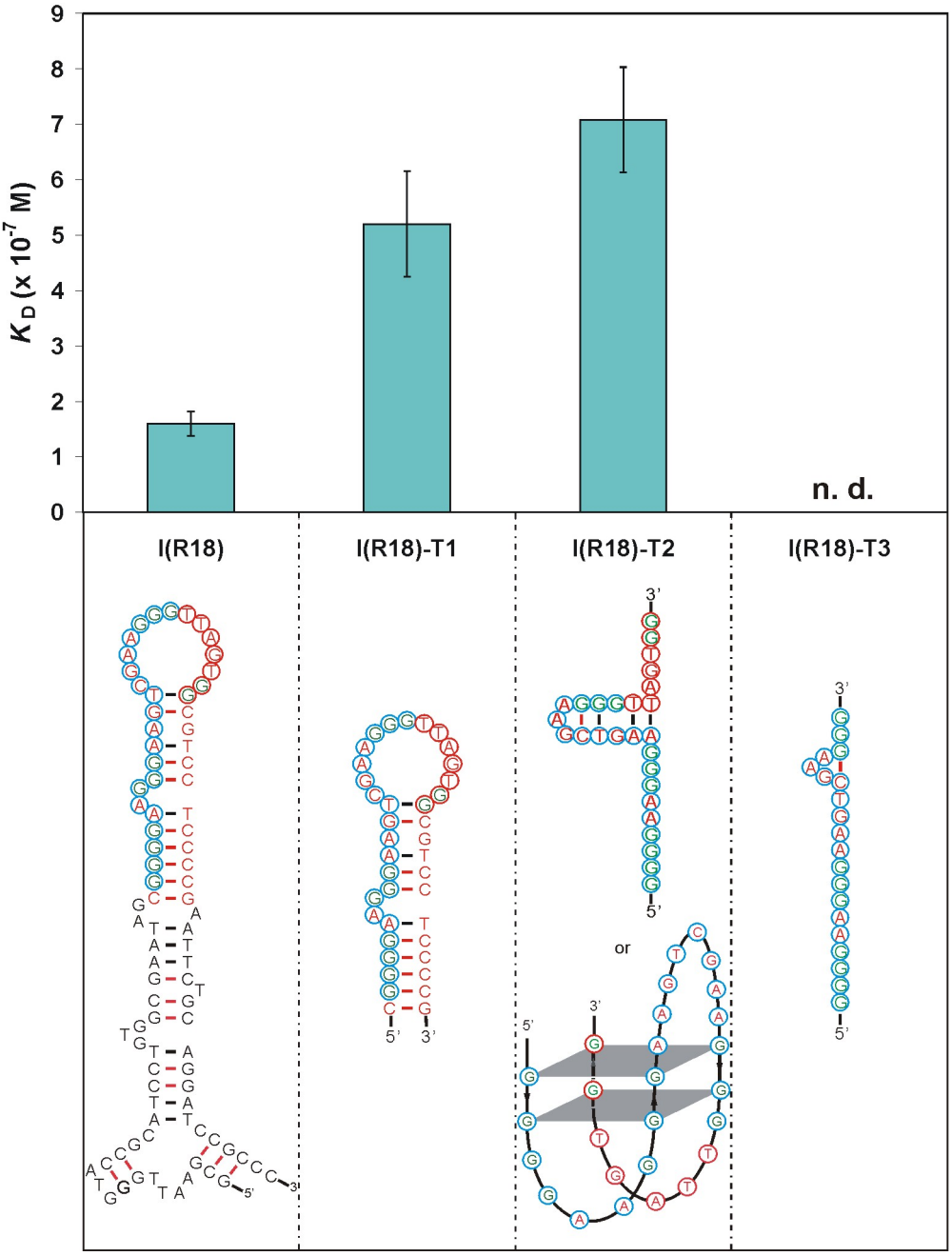


***Figure 4-33 Comparison of the binding affinities of ZFY to aptamer I(R18),and the truncated variants I(R18)-T1, I(R18)-T2 and I(R18)-T3.*** *The calculated binding constants ($K_D$) are shown by columns. n. d. stands for not detectable. The predicted secondary structures of these variants (by the Zuker or QGRS program as discussed under 4.5.5 (Gr. 2) are given under each column.*

## 4.6 Binding against Zinc Finger Protein (ZNF593)

Once aptamers are raised against a zinc finger structure, there is a fair chance that the *zf* structure will also be recognized within the whole protein structure. In the selection experiments against peptide targets, aptamers were raised against two zinc finger peptides, ZFY and GLI, respectively. Aptamers raised against GLI have overall conserved nucleotides and cross-react with ZFY. The binding affinities of the aptamers to both peptides are, however, relative low in the μM range. In contrast, aptamers raised against ZFY have significantly higher affinities to ZFY in the nM range. Therefore, only the aptamers against ZFY are further studied for protein binding.

The ZFY peptide was used as the target in the *SELEX* experiment. However, the attempt to overexpress the ZFY transcription factor containing thirteen zinc fingers failed probably due to the complexity and large number of *zf*s. In order to obtain a proof of principle, ZNF593 protein containing a single $Cys_2His_2$ zinc finger, which is highly similar to the ZFY peptide, was used for binding tests to the ZFY-aptamers.

ZNF593 protein was found by Terunuma and his co-workers (1997) to negatively modulate the DNA-binding activity of the Oct-2 transcription factor. Oct-2 is the member of the POU domain family of transcription factors. The inhibitory pathway of ZNF593 remains unknown. However, it has been speculated that protein ZNF593 could act either by binding to the DNA octamer sequence or by interacting with the Oct-2 protein (Phillips *et al.,* 2007). ZNF593 shares more than 40% sequence identity (over 30 residues in the *zf* domain) with ZFY peptide (Fig. 4-34). Moreover, the tertiary structure of its zinc finger domain resolved by NMR spectroscopy (Hayes *et al*., 2008) is very similar to that of the ZFY peptide (Kochoyan *et al*., 1991b). Both of them have the ββα-helix topology common to the classical $Cys_2His_2$ *zf*. Due to the high similarity between the ZFY peptide and the *zf* domain of the ZNF593 protein, not only in sequences but also tertiary structures, there was a fair chance that the aptamers raised against the ZFY peptide could also recognize the similar *zf* domain in the ZNF593 protein.

The ZNF593 protein was purchased from Geneway (USA) as his-tagged fusion protein. Purity and integrity of the protein was evaluated by SDS-PAGE on a 15% gel (Fig. 4-35). ZNF593 migrated slightly slower than expected, but corresponded to the approximate size of 17 kD according to the manufacturer's

instruction. Purity of ZNF593 protein was estimated based on the SDS gel image by *Quantity One* (BioRad) and was assessed to be > 86% homogeneous.

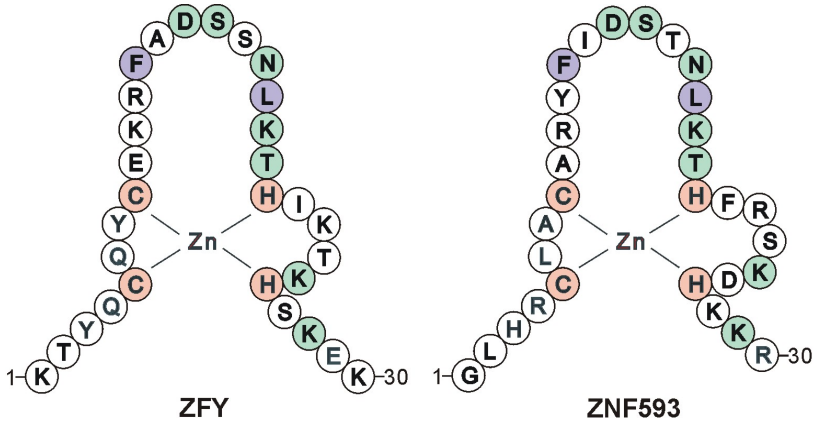


***Figure 4-34 Sequence Comparison in the zf domains of ZFY and ZNF593.*** *Conserved positions are colored where the metal-coordinated residues (red) and hydrophobic residues (purple) are located. Other identical amino acids are indicated in green cycles.*

Binding studies were performed by the nitrocellulose filter binding assays. First of all, binding of the ZNF593 protein to the nitrocellulose filters was evaluated qualitatively. The nitrocellulose filter (0.45 μM) loaded with ZNF593 protein (36 pmol) was washed three times with binding buffer and finally eluted by SDS loading buffer with heating. The result in Figure 4-35 shows that the ZNF593 protein was not present in any of the washing fractions. It was only detected in the fraction which was eluted by SDS from the resultant filter. This indicates that the ZNF593 protein bound to the filters successfully.

Binding affinities of the best ZFY-binders I(B15), I(R18) and I(R14) were determined to the ZNF593 protein. In comparison, the enriched pool against ZFY and random ssDNA pool served as controls. The binding curves of aptamers I(B15), I(R18), I(R14), enriched pool and random ssDNA pool are shown in Figure 4-36. The results of their binding constants to the ZNF593 protein are compared in Table 4-9 with those to the ZFY peptide.

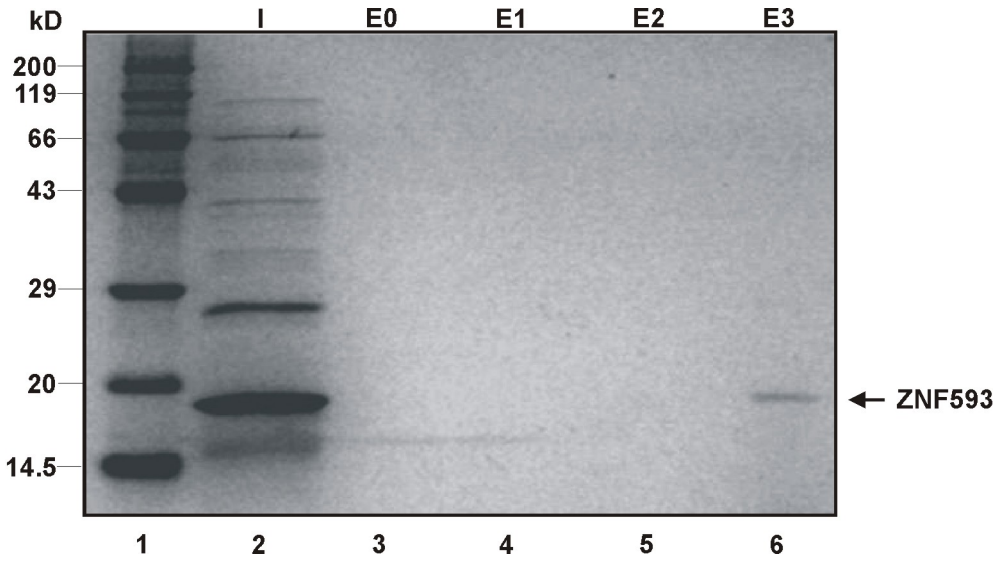


***Figure 4-35 Analysis of fusion ZNF593 protein and the determination of its binding to nitrocellulose filter.*** *Lane 1: protein ladder. The sizes of the molecular mass standards (Roth) are indicated on the left of the figure. Lane 2: fusion ZNF593 proteins (0.5 µg). Lane 3-5: E0, E1 and E2 are the washing fractions. Lane 6: E3 is the eluted fraction from filter by SDS. The samples were resolved on a 15% SDS-PAGE gel and the gel was stained with Coomassie Blue.*

As mentioned above, aptamer I(B15) was determined to be one of the best binders to the ZFY peptide and did not bind to the GLI peptide or BSA. It exhibits a $K_D$ of 154 nM to the ZFY peptide. The results here show that aptamer I(B15) bound to the ZFY-related ZNF593 protein with a $K_D$ of 290 nM. Interestingly, it was observed that the random ssDNA pool bound also to ZNF593 protein with a $K_D$ of 908 nM. Variant I(R14) and the enriched pool exhibited affinities with $K_D$s of 863 nM and 644 nM to ZNF593, lower than that of the random pool. Another of the best peptide binders, I(R18), bound to ZFY peptide with a $K_D$ of 160 nM, however, bound to the ZNF593 protein with a much lower affinity ($K_D$ of ~3.5 µM). Therefore, aptamer I(B15) is the only variant, which exhibits high and comparable binding affinities to both the ZFY peptides and also the ZNF593 protein. It has clearly improved affinity to ZNF593, than the bulk of the random sequences in the library.

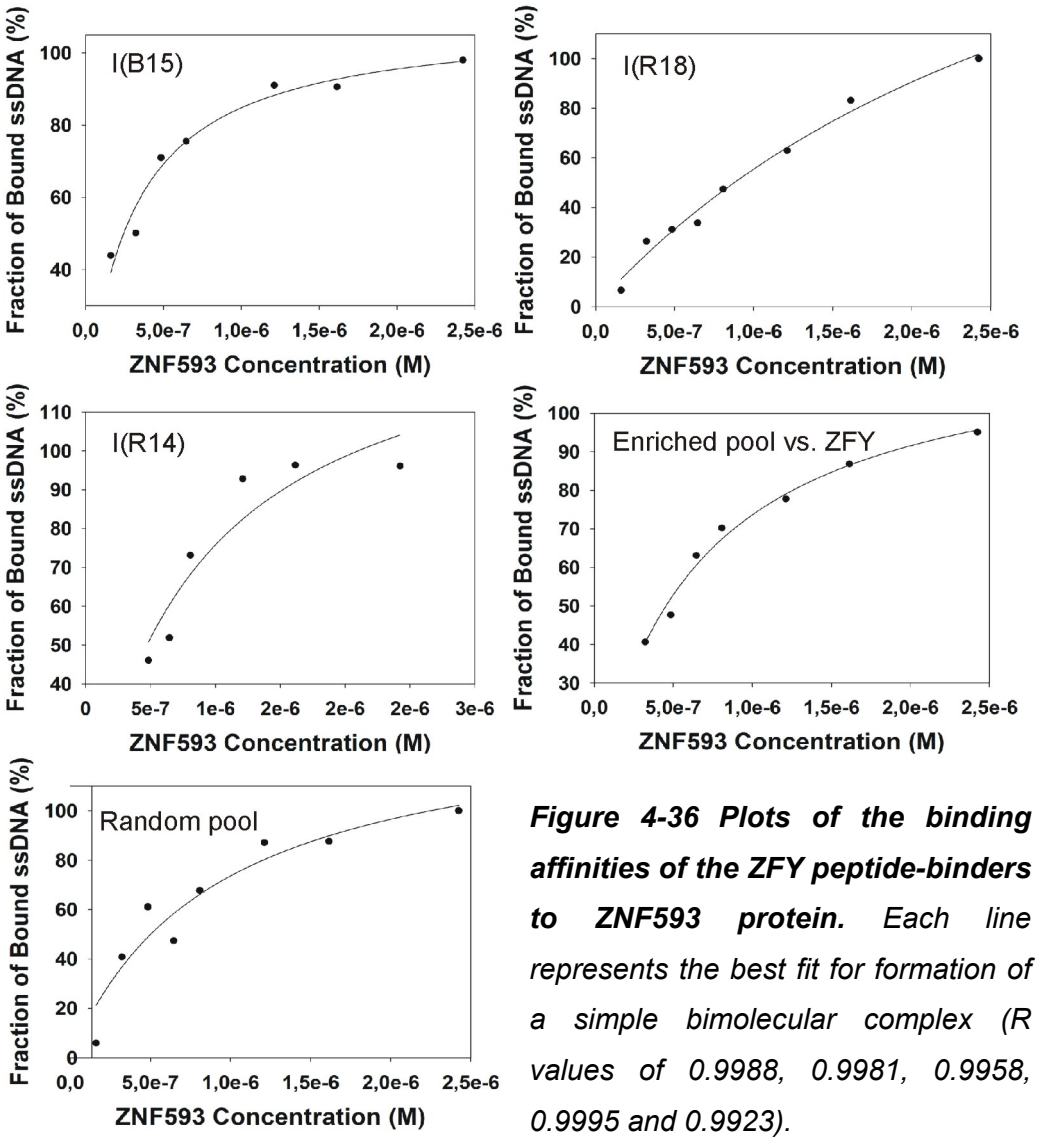


***Figure 4-36 Plots of the binding affinities of the ZFY peptide-binders to ZNF593 protein.*** *Each line represents the best fit for formation of a simple bimolecular complex (R values of 0.9988, 0.9981, 0.9958, 0.9995 and 0.9923).*

***Table 4-9 Summary of the binding affinities to ZNF593 protein in comparison with those to ZFY peptide.***

| Clones | $K_D$ to ZFY (x$10^{-7}$ M) | $K_D$ to ZNF593 (x$10^{-7}$ M) |
|---|---|---|
| I(B15) | 1.54 ± 0.41 | 2.90 ± 0.47 |
| I(R18) | 1.60 ± 0.22 | ~34.53 ± 8.90 |
| I(R14) | 2.00 ± 0.21 | ~8.63 ± 3.29 |
| Enriched pool against ZFY | -* | 6.44 ± 0.69 |
| Random ssDNA pool | n. d. * | ~9.08 ± 3.31 |

* '-': not measured; n. d.: not detectable.

## 4.7 Employment of Selected Aptamer

In the later application of the aptamers against *zf* proteins, it could be very useful to apply them as specific molecular DNA probes for the recognition of *zf* targets from a more complex mixture, *e.g.* a cell extract. The diagnosis of *zf* targets in cell extract will distinguish different types of cells, such as normal vs. tumor cells. In this work the aptamer I(B15) served as a model for affinity captures of *zf* proteins from HeLa cell extracts. The aptamer-bound fragments were analyzed by western blotting and MALDI-TOF-MS.

### 4.7.1 Designs of Aptamer Affinity Capture Assays

Affinity capture assays by aptamer I(B15) were designed for nuclear and cellular extracts of HeLa cells. Aptamer I(B15) was immobilized on a Neutravidin affinity column, in order to partition the bound proteins from the cell extracts. Two affinity capture assays, methods No. 1 and 2, were designed for nuclear extracts as discussed in the methods section. A brief schematic description of the affinity captures is illustrated in Figure 4-37.

In the direct capture (method No. 1) from nuclear extract of HeLa cells, the aptamer-bound proteins were eluted by SDS loading buffer. A short oligonucleotide (20 nt) instead of aptamer I(B15) served as a parallel control. In the competitive capture (method No. 2) from nuclear extract, the chances to capture specific binding proteins were raised using excess DNA probes to ensure a complete pull-down. The binding buffer contained 0.125 µg/µl poly(dI-dC) to reduce unspecific binding between proteins and polynucleotides. To occupy unspecific binding sites on the matrix 0.6 µg/µl BSA was used in the binding buffer. In addition, pre-incubation was performed to exclude matrix-binding proteins. After incubation and wash, the aptamer-bound proteins were eluted with a biotin solution.

Cell extracts of HeLa cells were also utilized as a protein mixture for affinity captures by the aptamer. Since cell extracts have more unspecific binding proteins than nuclear extracts, only the competitive capture assay (method No. 2) was applied to cell extracts. Additionally, the binding buffer contained 0.1 µg/µl poly(dI-dC), 0.05 µg/µl random ssDNA pool and 0.6 µg/µl BSA as competitors.

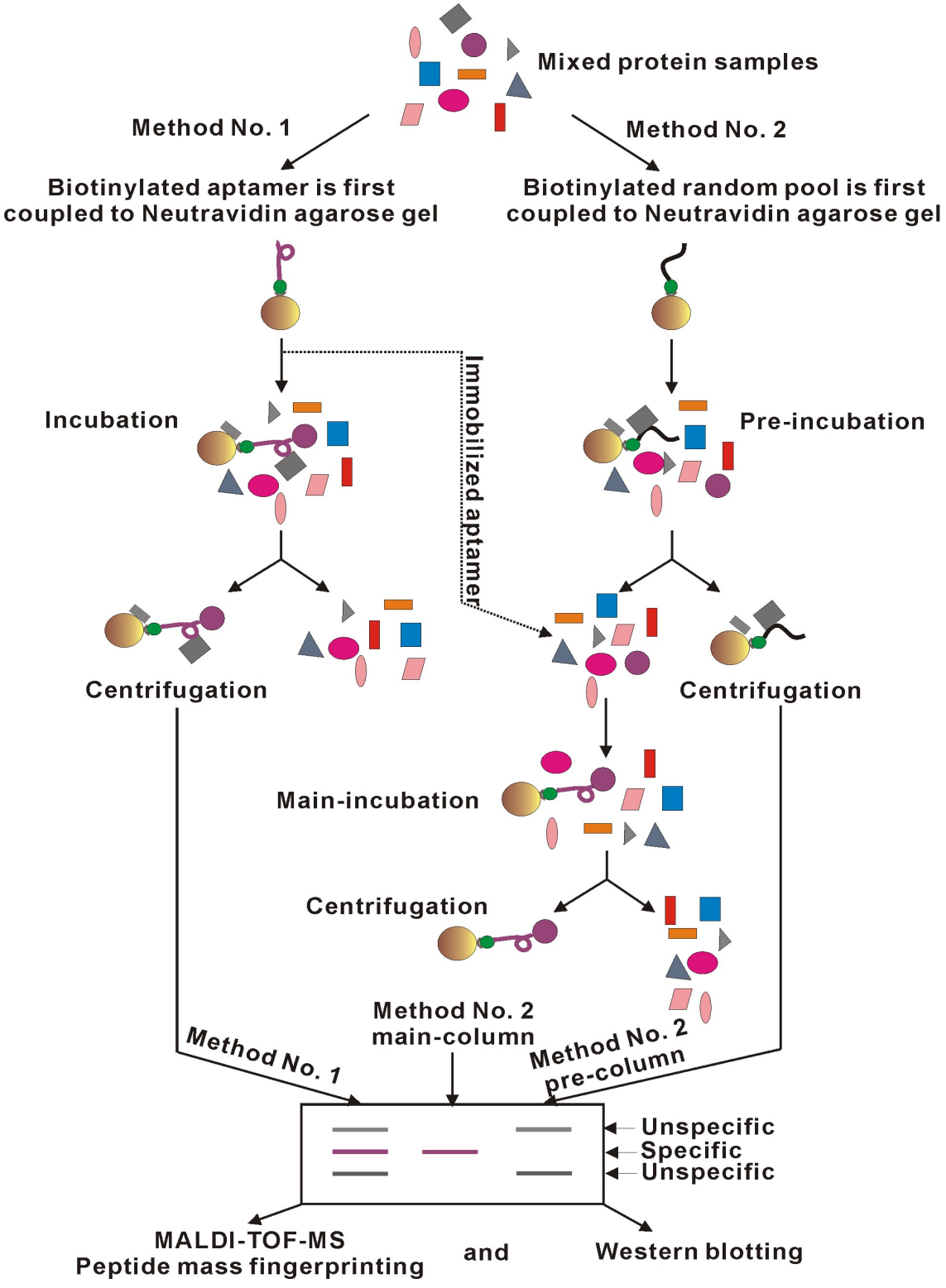


***Fig. 4-37 Schematic description of the designs of the affinity capture assays.***

### 4.7.2 Protein Preparation, Immobilization and Elution of Biotinylated ssDNA

Nuclear and cell extracts of HeLa cells were prepared as described in the methods section and Figure 4-38 illustrates their electrophoretic profiles.

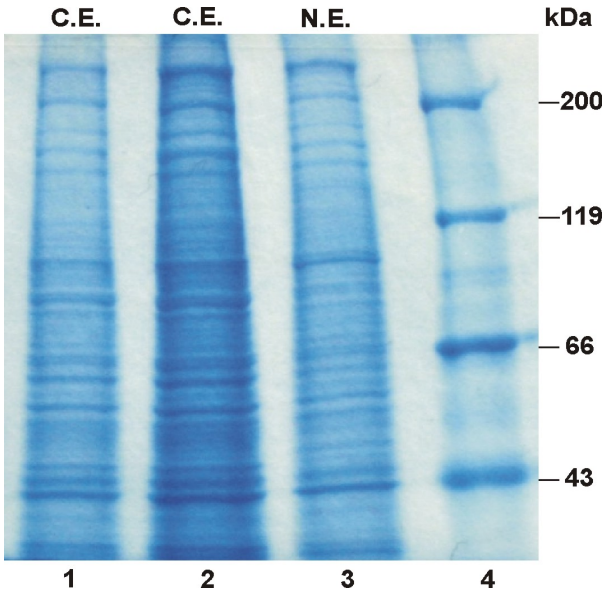


***Figure 4-38 Electrophoretic profiles of nuclear extract (NE) and cell extract (CE) of HeLa cells.*** *Proteins were separated on 8% SDS gel and stained with Coomassie Blue. Lane 1: ~7 µg CE; Lane 2: ~21 µg CE; Lane 3: ~5 µg NE; Lane 4: protein ladder. The sizes of the molecular mass standards (Roth) are marked on the right of the figure.*

The affinity capture assays were performed using Neutravidin agarose gels to immobilize biotinylated ssDNAs. The immobilization efficiency was evaluated to load 80 pmol DNA pool on 120 µl gels. The wash fractions were analyzed on a 10% denaturing polyacrylamide gel (Fig. 4-39). The result shows that no ssDNAs was detected in any of the wash fractions. It indicates that all the ssDNAs were immobilized successfully on the Neutravidin agarose gels.

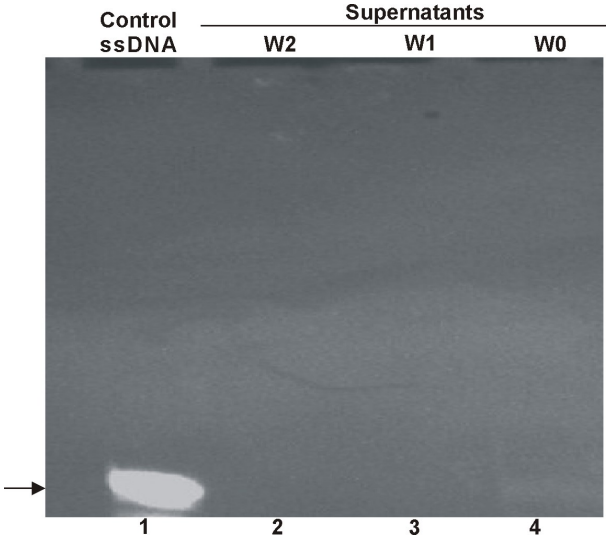


***Figure 4-39 Immobilization of ssDNA on Neutravidin agarose gel.*** *Lane 1: input of ssDNA pool (80 pmol); Lane 2: third supernatant after wash; Lane 3: second supernatant after wash; Lane 4: first supernatant directly after incubation. The gel was stained with ethidium bromide and the position of the ssDNA (90 nt) is marked by an arrow.*

Subsequently, the elution efficiency of biotinylated aptamers from the Neutravidin agarose gels was evaluated by an affinity capture assay. The biotinylated I(B15) (10 pmol) was incubated with 16 µg nuclear extract. Finally, aptamer I(B15) was eluted consecutively with 1.9 mM biotin solution, SDS loading buffer and 5 M urea. In the first elution, the competition between the excess biotins and the

biotinylated ssDNAs led to the release of the biotinylated aptamers from the Neutravidin gels. Proteins that bound to ssDNA aptamers were eluted together with the biotinylated aptamers; whereas proteins bound unspecifically to the matrix material could still retain on the gels. This mild elution method reduces the number of unspecific binding proteins. Afterwards SDS and urea denatured and eluted all retained proteins including unspecific binding proteins. The result in Figure 4-40 shows that the majority of the immobilized ssDNAs were eluted successfully by excess biotin (lane 2). Moreover, degradation of ssDNAs by nucleases could not be observed in the assays. Therefore, these results indicate that the aptamer I(B15) can be used as a model in the affinity capture assays for cell or nuclear extracts of HeLa cells.

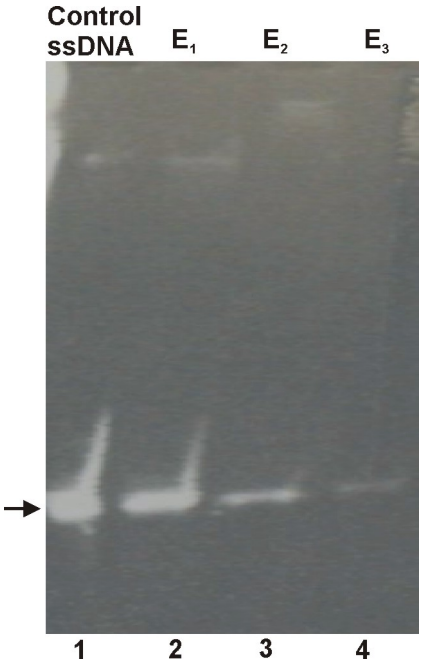


***Figure 4-40 The elution efficiency of the biotinylated ssDNA aptamer from the Neutravidin agarose gel.*** *Lane 1: 10 pmol aptamer I(B15); Lane 2: first elution from aptamer I(B15) resin by biotin; Lane 3: second elution by SDS; Lane 4: third elution by urea. The samples were analyzed on a 10% denaturing polyacrylamide gel and the gel was stained by ethidium bromide. The position of the aptamer I(B15) is marked by an*

### 4.7.3 Identification of ZFX Transcription Factor by Western Blotting

Aptamer I(B15) binds to the ZFY peptide, which is derived from the domain 6 of the ZFY transcription factor. ZFX is a homologue of ZFY on the X chromosome. In the acidic domain there is 87% sequence identity between ZFY and ZFX, while in the *zf* domain this value rises to 97% (Palmer *et al*., 1990). In the domain 6, there is only one amino acid difference. If aptamer is raised to bind the ZFY peptide of domain 6, it has a fair chance that it binds to the whole ZFY protein. Because of the high similarity of ZFY and ZFX, the aptamer can be expected to bind to the ZFX protein as well.

Since ZFX is expressed in a very low amount in HeLa cells, the aptamer-bound proteins in the affinity capture assays were first analyzed on an SDS-gel followed by western blotting with ZFX-specific serum.

To confirm the expression and extraction of the ZFX, the native nuclear and cell extracts were analyzed by western blotting with the anti-ZFX antibodies in the presence of a positive control of denatured cell total lysate. Anti-ZFX serum was obtained from Dr. Boris Reizis (CUMC, USA). It was raised in rabbit against the ZFX N-terminal acidic transcriptional activation domain (AD). The western blot in Figure 4-41 confirms the expression of ZFX in HeLa cells and the extractions of ZFX in the native nuclear and cell extracts used for the affinity captures. However, the efficiencies of the extractions of ZFX are low, especially for the cell extracts.

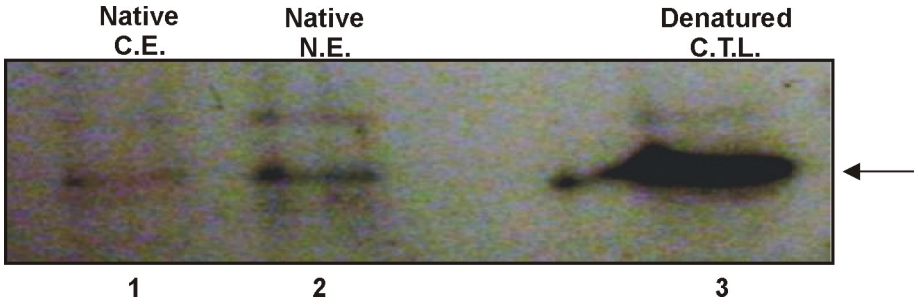


***Figure 4-41 The expression and extraction of ZFX transcription factor analyzed by western blotting with anti-ZFX antibodies.*** *Lane 3: denatured cell total lysate (CTL); Lane 1: native cell extract (CE); Lane 2: native nuclear extract (NE). The position of ZFX is indicated by an arrow*.

The aptamer-bound fractions of nuclear proteins in the direct and also competitive affinity captures were blotted by the anti-ZFX antibodies to analyze if ZFX was isolated from the nuclear extracts. The blot was incubated with anti-ZFX overnight (1:15000 dilution) and with a secondary GAR-HRP antibody (1:10000 dilution) for another 1 h. However, ZFX was identified in neither of the aptamer-bound fractions of nuclear proteins (data not shown). Even employing higher concentrations of the both antibodies up to 1:5000 dilution, no ZFX was detected in any fraction of aptamer-bound proteins (Fig. 4-42).

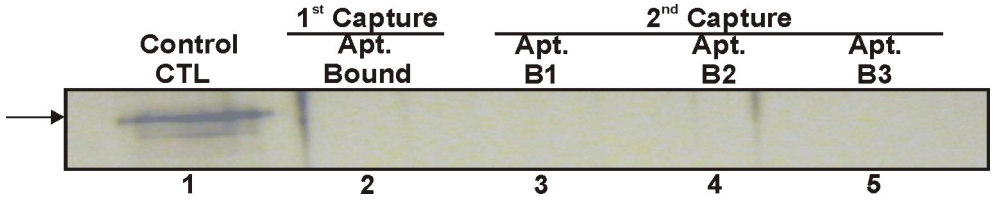


***Figure 4-42 Western blotting of aptamer-bound proteins obtained from the affinity captures of nuclear proteins from HeLa cells using anti-ZFX serum.*** *Lane 1: denatured cell total lysate (CTL); Lane 2: aptamer-bound proteins in the direct capture (method No.1); Lane 3-5: aptamer-bound proteins (first, second, third eluted fractions) in the competitive capture (method No. 2). The blot was incubated by increased concentrations of the both first and secondary antibodies (1:5000). The position of ZFX is marked by an arrow.*

The detection of ZFX by western blotting in the aptamer-bound nuclear proteins might have been unsuccessful because of inefficient extraction and low abundance of ZFX. For the affinity capture assays by aptamer, cell or nuclear proteins were prepared as native proteins. The amount of ZFX extracted is limited by numbers of cells and the efficiency depends on the extraction methods. In general, it is very difficult to withdraw such small amount of proteins from cell debris. The cell pellets after nuclear extraction and cell total extraction were analyzed by western blotting using anti-ZFX serum. The result in Figure 4-43 demonstrates that ZFX proteins were not extracted completely and large parts were retained in cell pellets. Many efforts were made to increase the extraction efficiency of native ZFX proteins from HeLa cells. However, they failed to obtain a better yield (data not shown).

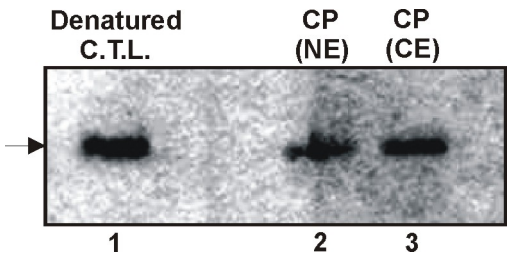


***Figure 4-43 The presence of ZFX in resultant cell pellets.*** *Lane 1: denatured cell total lysate (CTL); Lane 2: cell pellet (CP) after nuclear extraction (NE); Lane 3: cell pellet (CP) after cell total extraction (CE). The position of ZFX is indicated by an arrow.*

### 4.7.4 Identification of Aptamer-Bound Proteins by MALDI-TOF-MS

Cell extract of HeLa cells was used for the affinity capture assays by the aptamer I(B15) as described in the methods section. HeLa cell extract (1 mg) was pre-incubated with the random ssDNA pool-resin. Subsequently, the supernatant was added to the aptamer I(B15)-resin. Several major bands from the main elution by biotin were excised and identified by MALDI-TOF -MS as nucleolin, restin and SND1 (Fig. 4-44). However, no *zf* protein was found in this affinity capture assay with cell total extract.

**A**

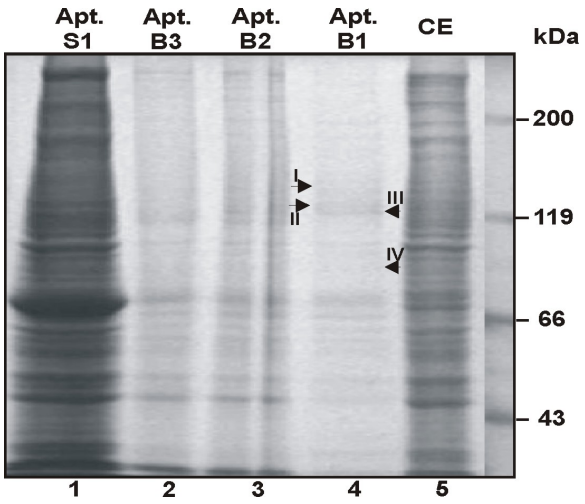


**B**

| Nr. | Protein | Mcal (kDa) | Mapp (kDa) |
|---|---|---|---|
| I | Restin | 161 | ~150 |
| II | SND1 | 103 | ~120 |
| III | Nucleolin | 77 | ~115 |
| IV | n. i.* | - | ~80 |

***Figure 4-44 (A) Affinity capture of cellular proteins by aptamer I(B15).*** *Electrophoretic profiles of the proteins are shown, which were captured on the Neutravidin agrose gels in aptamer-'column' (Lane 2-4 correspond to the third, second and first elution of bound proteins from aptamer I(B15) resin by urea, SDS and biotin). Lane 1: supernatant direct after the incubation in aptamer-'column'; Lane 5: 23 µg cell extract. Molecular weight marker is shown and the selected proteins (I, II, III, IV) were indicated by arrows.* ***(B) Identification of the selected proteins in the affinity capture from cell extracts by MALDI-TOF-MS.*** *The calculated ($M_{cal.}$) and the apparent molecular masses ($M_{app}$) are given.* * n.i.: not identified

The direct affinity capture (method No. 1) from nuclear extracts of HeLa cells was also performed using aptamer I(B15). The bound proteins on the Neutravidin agrose gels containing the aptamer or the control oligonucleotide (20 nt) were separated on a 8% SDS gel (Fig. 4-45 A). Several major bands from the aptamer-bound proteins were excised, digested by trypsin, and identified by MALDI-TOF-MS. Data were used for peptide mass fingerprintings (PMF). Fragment ion spectra were

taken for a *Mascot* program search of the *Swissprot* databases. The identified proteins are listed in Figure 4-45 B. Two of them are zinc finger proteins. However, most of the other identified proteins are unspecific nucleic acids binding proteins. The *Mascot* scores calculated for Matrin-3 and TAFII68 are 140 and 88 respectively, which indicate that the searches matched significantly. The MS spectra for peptide mass fingerprintings of *zf* proteins, matrin-3 and TAFII68, are shown in Figure 4-46.

**A**

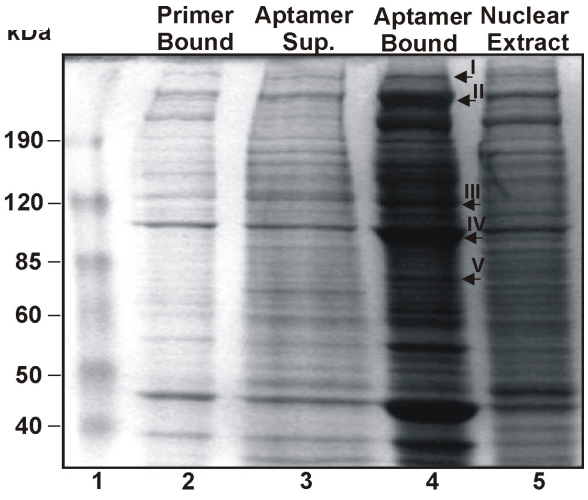


**B**

| Nr. | Protein | Mcal (kDa) | Mapp (kDa) |
|---|---|---|---|
| I | DNA-PK | 474 | > 250 |
| II | Filamin-A | 283 | > 250 |
| | Spectrin | 285/275 | |
| III | Matrin-3 | 95 | ~105 |
| IV | α-Actinin-4 | 105 | ~100 |
| | Splicing factor | 76 | |
| V | TAFII68 | 62 | ~80 |

***Figure 4-45 (A) The direct affinity capture (method No. 1) of nuclear proteins by aptamer I(B15).*** *Electrophoretic profiles of the proteins are shown, which were captured on the Neutravidin agrose gels with aptamer I(B15) (lane 4) and an oligonucleotide control (lane 2). Lane 1: molcecular weight marker; Lane 3: 10 µl unbound nuclear proteins in the first supernatant (sup.). Lane 5: ~15 µg nuclear extract. The selected proteins (I, II, III, IV, V) were indicated by arrows. (**B) Identification of the selected proteins in the direct affinity capture (method No. 1) from nuclear extract by MALDI-TOF-MS.** The calculated ($M_{cal}$) and apparent molecular masses ($M_{app}$) are given. The zf proteins identified are underlined.*

In the competitive affinity capture (method No. 2) from the nuclear extracts of HeLa cells, the bound proteins on the Neutravidin agrose gels containing aptamer I(B15) or random ssDNA pool were separated on a 8% SDS gel. The electrophoretic profiles of the eluted proteins are shown in Figure 4-47 A. The background proteins were much less, which indicates that unspecific binding was reduced by the improved conditions mentioned under 4.7.1. Several major bands from the eluted fractions by biotin and SDS were excised and identified by MS. Subsequently, data were used for peptide mass fingerprinting. The results are given in Figure 4-47 B.

Two proteins were identified as zinc finger proteins. The MS spectra for peptide mass fingerprintings of proteins TAFII68 and TLS are shown in Figure 4-48 and the *Mascot* scores were 163 and 86 respectively, which indicate the searches matched significantly. The *zf* protein TAFII68 was also identified in the direct affinity capture (method No. 1) from the nuclear extract. In comparison, two bands (V and VI) were excised from the bound fraction of random ssDNA pool-'column' (Fig. 4-47 lane 8). These bands are in the corresponding positions where the two *zf* proteins were identified from aptamer I(B15)-'column' (lane 4 and 5). However, no *zf* proteins were detected from this control capture assay using the random ssDNA pool.

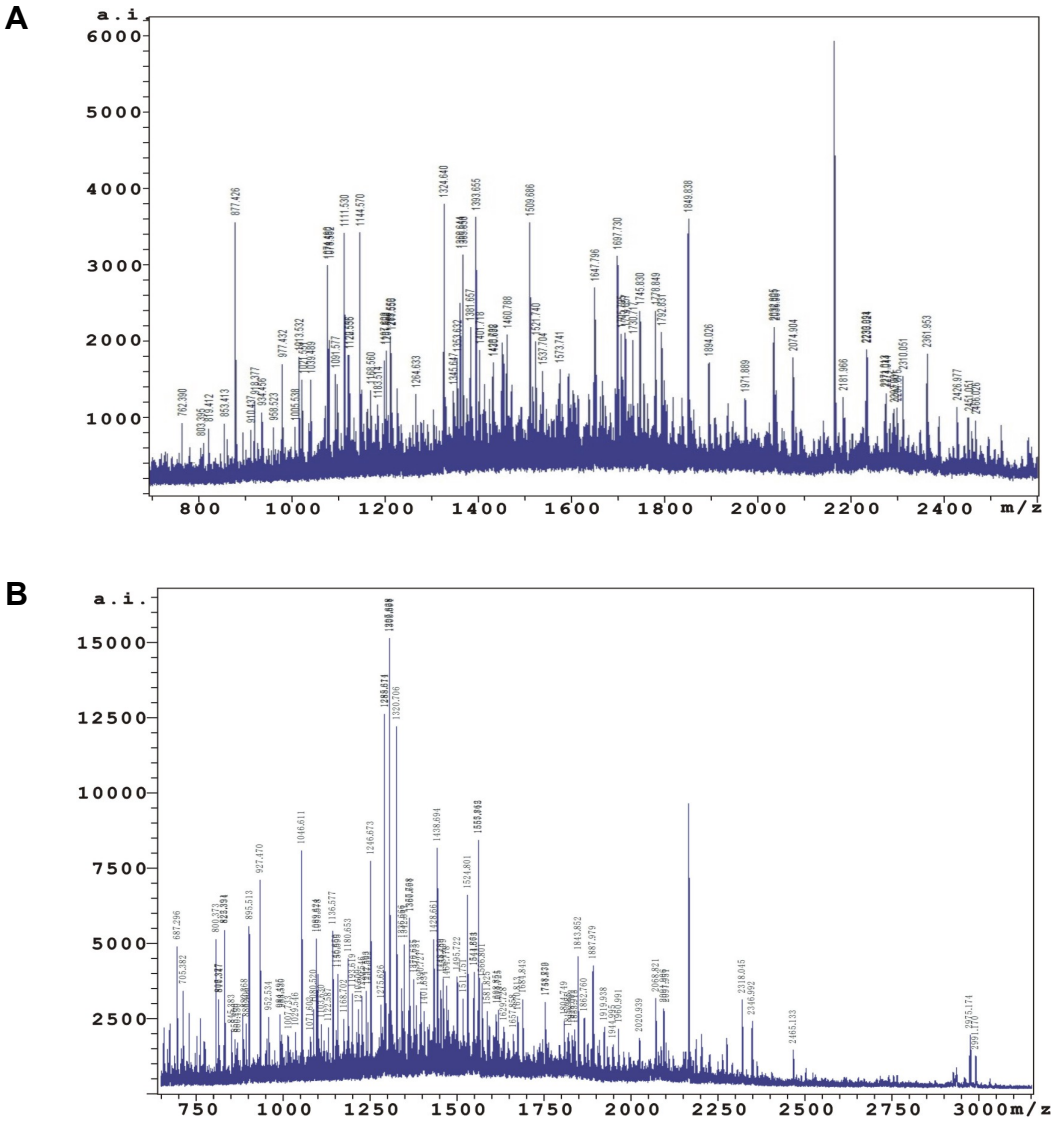


***Figure 4-46 (A) MALDI-TOF-MS identification of Matrin-3.*** *Protein band III (Fig. 4-45) was identified as Matrin-3 (Mass: 95 kD) with a Mascot score of 140.* ***(B) MALDI-TOF-MS identification of TAFII68.*** *Protein band V (Fig. 4-45) was identified as TAFII68 (Mass: 62 kD) with a Mascot score of 88.*

**A**

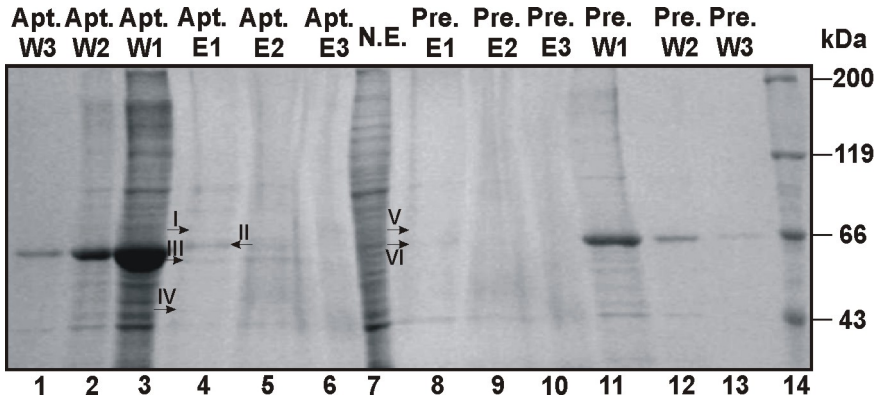


**B**

| Nr. | Protein | Mcal (kDa) | Mapp (kDa) |
|---|---|---|---|
| I | TAFII68 | 62 | ~80 |
| II | TLS | 54 | ~60 |
| III | hnRNP K | 51 | ~56 |
| IV | DBPB | 36 | ~40 |
| V | n. i.* | - | ~70 |
| VI | BSA | 66 | ~60 |

***Figure 4-47 (A) The competitive affinity capture (method No. 2) of nuclear proteins by aptamer I(B15).*** *Electrophoretic profiles of the proteins are shown, which were captured on the Neutravidin agarose gels in aptamer-'column' (Lanes 4-6 correspond to the first, second and third eluted fractions by biotin, SDS and urea) and in random pool-'column' (Lanes 8-10 show the corresponding elution fractions). Lane 1-3: unbound fractions washed from aptamer-'column'; Lane 7: 10 µg nuclear extract of HeLa cells; Lane 11-13: washed fractions from random pool-'column'; Lane 14: molecular weight marker; The selected proteins (I, II, III, IV, V, VI) were indicated by arrows.* ***(B) Identification of the selected proteins in the competitive affinity capture (method No. 2) from nuclear extracts by MALDI-TOF-MS.*** *The calculated ($M_{cal}$) and apparent molecular masses in gel ($M_{app}$) are given. The zinc finger proteins are underlined.* n. i.: not identified.*

Several zinc finger proteins were identified by the affinity captures of nuclear proteins from HeLa cells, using aptamer I(B15) as a model. Two *zf* proteins were identified in the direct affinity capture assay (method No. 1). One of them was protein Matrin-3. It has the classical $Cys_2His_2$-type *zf*. The other identified *zf* protein was the TATA-binding protein-associated factor 2N (also called TAFII68 or RBP56). It belongs to the $Cys_2Cys_2$-type zinc finger of RanBP2 family. Furthermore, two *zf* proteins were identified in the competitive affinity capture assay (method No. 2) by

aptamer I(B15). One was again protein TAFII68. The other one was protein TLS. TLS has a similar $Cys_2Cys_2$-type zinc finger of RanBP2 family as the protein TAFII68.

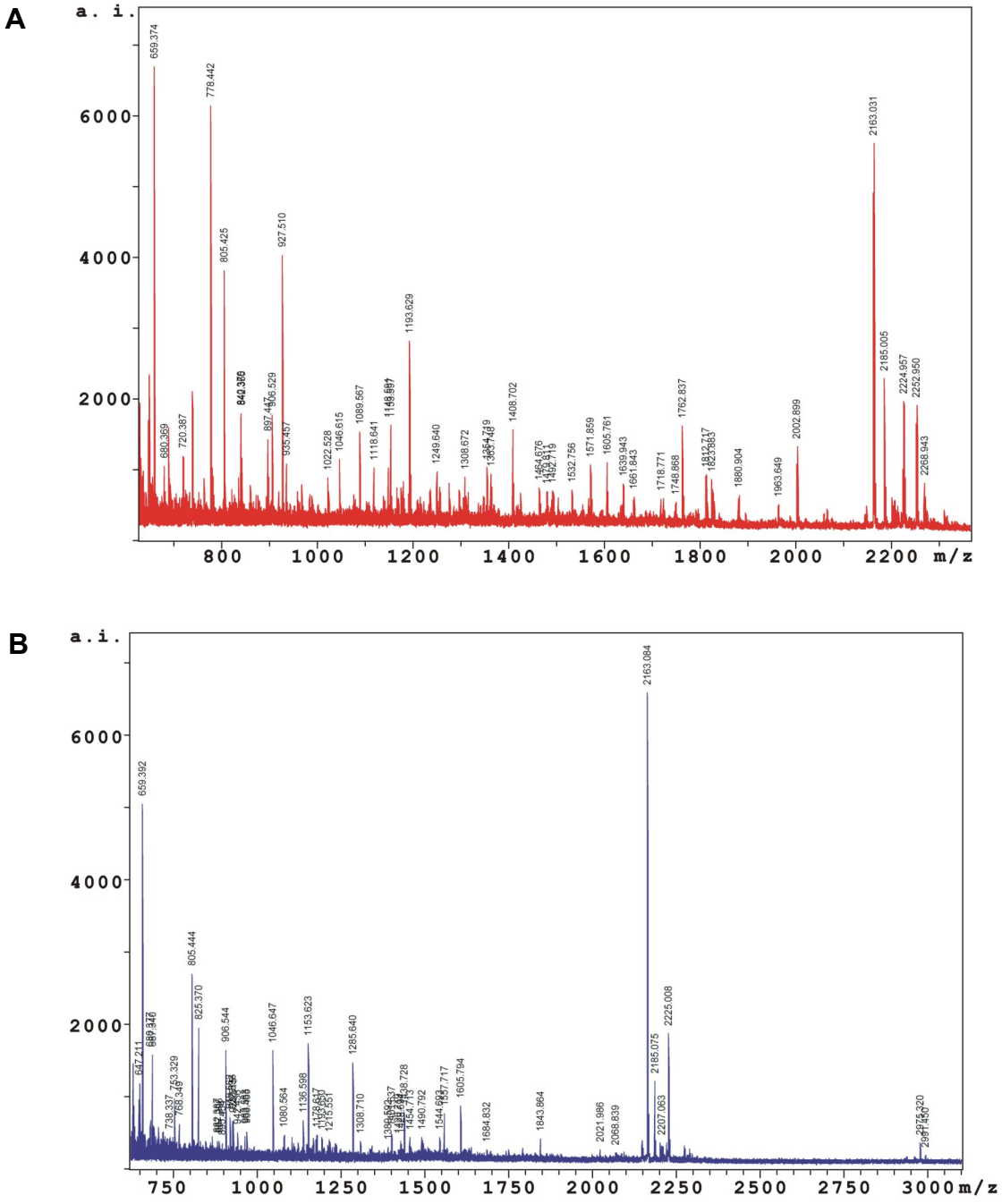


***Figure 4-48 (A) MALDI-TOF-MS identification of TLS.*** *Protein band II (Fig. 4-47) was identified as TLS (Mass: 54 kD) with a Mascot score of 86.* ***(B) MALDI-TOF-MS identification of TAFII68.*** *Protein band I (Fig. 4-47) was identified as TAFII68 (Mass: 62 kD) with a Mascot score of 166.*

These three *zf* proteins were mentioned in the introduction section under 1.1.3. The primary structures of the *zf* domains in proteins TAFII68 and TLS share extensive 62.5% sequence similarity. Their degree of homology with the zinc finger domain in protein Matrin-3 is low. However, the zinc binding residues in all three sequences are highly conserved. In addition, they all have a hydrophobic residue (phenylalanine) flanking the metal binding site (Fig. 4-49 A). In comparison with ZFY, against which aptamer I(B15) was selected, the zinc finger domain in the identified nuclear protein, Matrin-3, has more than 30% sequence identity. The other two *zf* domains in proteins TAFII68 and TLS, have ~20 % sequence identity with ZFY (Fig. 4-49 B).

**A**

```
Matrin-3 zf          FYCK--LCS--LFYTNEEVAKNTHCSSLPHYQKLKK
TAFII68 zf       KSGDWVCPNPSCGNMNFARRNS-----CN---QCNEPRPE
TLS zf           RAGDWKCPNPTCENMNFSWRNE-----CN---QCKAPKPD
```

**B**

```
ZFY zf              KTYQCQYCEKRFADSSNL-K-THIK-TKHS-KEK
Matrin-3 zf          FY-CKLCSL-FYTNEEVAKNTHCSSLPHYQKLKK
Consensus             Y C  C   F       K TH     H  K K

ZFY zf           KT---YQCQY--C-EKRFADS-SNLKTHIK-TKHS-KEK
TAFII68 zf       KSGDWV-CPNPSCGNMNFARRNS----CNQ---CNEPRPE
Consensus        K      C    C    FA   S

ZFY zf              KTYQCQY--CEKR-FADS-SNLKTHIK-TKHSKE-K
TLS zf            RAGDWKCPNPTCENMNFSWRNE----CNQ---C-KAPKPD
Consensus               C    CE   F                K  K
```

***Figure 4-49 (A) Sequence comparison of the zf domains of the proteins identified in the affinity capture assays by aptamer I(B15) from nuclear extracts of HeLa cells.*** *The nucleotides in bold are conserved in all three sequences. The underlined nucleotides are identical in proteins TAFII68 and TLS.* ***(B) Sequence analyses of the zf domains in proteins Matrin-3, TAFII68 and TLS in comparison with ZFY respectively.*** *Consensus amino acids are indicated.*

# 5 Discussion

Early detections of tumors are perhaps the most promising and feasible means to reduce disease and cancer deaths in a foreseeable future, since the development of new therapeutic strategies remains challenging. Researchers are on the way to develop efficient diagnostic tests targeting potential biomarkers. Over the past decades, many multifunctional transcription factors containing zinc fingers have been found to be implicated in human diseases including cancer. Zinc finger transcription factors dosage is critical at certain times in development and they are often overexpressed or underexpressed in tumors. Therefore, employing zinc finger-specific diagnostic tests will certainly make early detection approaches feasible. Some efforts had already been made to achieve specific molecular probes for recognizing zinc finger proteins, e.g. using different antibodies. However, as discussed in the introduction section, high-affinity oligonucleotides for zinc fingers had not been paid much attention till now, although they may be more suitable candidates as diagnostic tools due to their multiple advantages.

## 5.1 Analysis and Characterization of Targets

In this work two variants of the single $Cys_2His_2$ *zf* motifs, ZFY and GLI, were chosen as targets of interest. Both of them belong to the Krüppel family of the $Cys_2His_2$–type zinc finger protein. To date, a selection of oligonucleotides binding with high affinities against a single zinc finger has not been demonstrated yet. In addition, the comparison of these two different selection results could be helpful to understand the binding mechanisms of *zf* structures in general.

An important point for a successful enrichment of DNA molecules is the homogeneity and the proper conformation of target peptides. Cys thiol groups in proteins in general and zinc finger domains in particular are sensitive to oxidative damage and readily form disulfide bonds. In this work, the reagent Tris(2-carboxyethyl)phosphine (TCEP) was used to reduce oxidized peptides (Burns *et al.*, 1991; Han and Han, 1994; Getz *et al.*, 1999). The HPLC results show that the single *zf* is susceptible to be oxidized due to the disulfide bonds and the reduction of *zf*

could be successfully achieved by TCEP. Care still had to be taken to prevent re-oxidation of reduced peptides after preparative HPLC.

The integrity of the *zf* peptides was confirmed by MALDI-TOF-MS. The experimentally found monoisotopic mass corresponded to the calculated monoisotopic average mass. To examine cys redox reactions, it was necessary to perform isotope cluster analysis using the mass accuracy and resolution of the TOF mass analyzer. These results demonstrate that the peptides had the expected masses; they were reduced successfully by incubation with 10-fold molar excess of TCEP for 1 hr at room temperature and they were then ready for metal coordination.

To confirm the tetrahedral metal coordination, the conformation of the peptides was determined by CD in the presence or absence of $Zn^{2+}$ ions. When the cys-containing finger structure folds around the $Zn^{2+}$ ion, a protective pocket is formed resulting in no added redox stress on the cys residues. Metals with filled d-orbitals such as $Zn^{2+}$ ions do not exhibit redox chemistry and are excellent metals for stabilizing the fold of domains containing cys residues (Larabee *et al.*, 2005). The dissociation constants of $Zn^{2+}$-binding could be demonstrated in the picomolar to nanomalar ranges (Pedone *et al.*, 1996; Kägi, 2001; Maret, 2002)**.** In the present study the spectra of metal-free ZFY and GLI peptides were characterized as unstructured polypeptide backbones. Upon adding $Zn^{2+}$ ions, dramatic changes could be observed in ZFY peptides, characteristic for α-helixes. These CD spectra were in agreement with the results described for *zf* peptides in many other studies (Weiss and Keutmann, 1990b; Omichinski *et al.*, 1993; McColl *et al.*, 1999; Bertola *et al.*, 2000; Bal *et al.*, 2002; Kopera *et al.*, 2004). The spectra of $Zn^{2+}$-coordinated GLI were characterized as a relatively weak CD band. However, this was similar to what was reported in the literature for the second finger in TFIIIA and Xfin-31 $Zn^{2+}$-coordinated domain (Frankel *et al.*, 1987; Nedved and Moe, 1994). The CD spectra characteristics of secondary structure of helical conformation were not apparent. Presumably, contribution to the CD spectrum of reverse turns, the cluster of aromatic amino acids and the zinc complex, decreased the apparent magnitude of helical CD spectrum. However, there were significant changes at 200 nm and 205 nm.

The peptide secondary structure deconvolution was calculated by the *PEPFIT* program (Poschner *et al.*, 2007). It is well known that CD spectra of polypeptide backbone could be distorted by unknown contributions of various side chains. Even the unstructured polypeptides are more far away being random. The intensity of the

helical CD spectrum is also length-dependent. Therefore, such calculation is referred to as an estimation. However, we could observe the trend of the $Zn^{2+}$-denpendent folding transitions. The estimated secondary structure contents of metal-free peptides ZFY and GLI were very similar, characteristic of unstructured polypeptide backbones. Upon adding $Zn^{2+}$ ions, the secondary structure contents of $Zn^{2+}$-coordinated ZFY peptides exhibited significant changes, characteristic of helical conformations. This trend was less pronounced for GLI peptides, but it still could be observed.

All these characterization results demonstrate that $Zn^{2+}$-coordination led to a proper folding of the peptides. Just prior to each selection, $Zn^{2+}$-coordinated peptides were prepared freshly. Care had to be taken when adding excess reducing reagent, adding excess zinc ions, reducing air-exposure time and keeping low temperature to avoid re-oxidation. A 10-fold molar excess of TCEP was used to reduce peptides and $Zn^{2+}$ ions were added in a 2.5-fold molar excess to the reduced target peptides. In addition, micromolar to millimmolar ranges of $Zn^{2+}$ ions and the proteins that bind them are found in cells, which also contain small pools of free $Zn^{2+}$ (Larabee *et al.*, 2005). Therefore, $Zn^{2+}$ ions (50 μM) were used in the *SELEX* buffer during selection. All reduced peptides should have formed correct tetrahedral ββα-structures in the presence of an excess of $Zn^{2+}$ ions. Moreover, cells are known to have many proteins which have the ability to act as reducing agents (thioredoxins, metallothioneins, and other cys-rich *zf* proteins). Therefore, TCEP (0.6 mM) was also applied to the *SELEX* buffer for providing a reducing environment during the whole selection. The use of TCEP in *in vitro* studies may aid in mimicking the reducing environment present in cells (Larabee *et al.*, 2005). These efforts could thus enhance the integrity of the target peptide and therefore the likelihood of successful selections.

## 5.2 *In vitro* Selection

In this work, the *in vitro* selection conditions were designed and optimized. First of all, the diversity of an oligonucleotide library is very important for the selection, because increasing numbers of different oligonucleotides enhance the likelihood of the presence of molecules with high affinities to the targets. The diversity is determined by the length of the randomized domain and the number of molecules present in the library (Gold *et al.,* 1995). The original DNA template generated in this

work by chemical synthesis was 90 nucleotides, with a random region of 50 nucleotides ($N_{50}$). After the amplification 4.86 nmol ssDNA molecules containing 1.45 x $10^{15}$ different sequences were applied for selection.

In addition to pool complexity, stringency of the selection is certainly an important point. Typically, in an *in vitro* selection experiment, stringency is progressively increased in the course of a *SELEX* process (Stoltenburg *et al.*, 2007). It was achieved by several ways in this work. Firstly, the molar ratio of ssDNAs to target peptides started with 2:1 in the first two rounds and increased to 4:1 in later cycles. Since the fraction of strong binders increases with the number of selection rounds, the risk of eliminating them is greatest in the early rounds of the procedure. It is therefore common to start with a higher protein to oligonucleotide ratio at the beginning of the experiment, but then decreases this ratio as the number of performed rounds increases (Djordjevic, 2007). Secondly, pre-selection against the matrix alone was performed from the second cycle, since counter-*SELEX* against the partitioning matrix can be important (Gold *et al.*, 1995). This helped to reduce the number of the background binders, which partition without facilitation by the protein target. Thirdly, the partitioning matrix was changed from Neutravidin agarose gels to Streptavidin magnetic beads from round eight, since an alternative partitioning protocol could be also very helpful to reduce the target-nonspecific sequences (Gold *et al.*, 1995). Fourthly, the concentration of potassium ions in the *SELEX* buffer was increased in the last several cycles. It is well known that proteins can interact with nucleic acids either specifically, or non-specifically. Specific interactions are based on hydrogen bonds and Van der Waals interactions, while unspecific interactions are due to electrostatic interactions alone (Djordjevic, 2007). This strategy of changing the concentration of potassium ions increased the stringency and reduced the number of unspecific binders.

## 5.3 Characterization of Aptamers against Peptides

In the first *SELEX* experiment, the GLI-binding sequences were enriched successfully after fourteen rounds of selection. From twenty-three sequenced clones there were seventeen with different sequences. The highly conserved common motif CM-1 (5'-GGACA-3') appeared in all sequences. By detail analysis, these sequences

could be classified into five groups based on the conserved nucleotides, which are partly overlapping. Two further conserved motifs CM-2 (5'-TGAGC-3') and CM-3 (5'-CCTTTA-3') occur each in three groups.

Secondary structure predictions according to the *Zuker* algorithm provided stable structures. The conserved residues similarly folded in each group. Nevertheless, there are high homologies in the secondary structures of the conserved motifs among these groups. For instance, in all sequences the highly conserved GG nucleotides in the CM-1 motif are positioned in strong G-C base-pairs in stems of small hairpins and ACA are located in loops downstream. Out of the conserved motif CM-2 in almost all sequences of groups 1, 2 and 3, the nucleotides GAG are involved in base pairings in stems of the other small hairpins. In addition, the conserved motif CM-3 forms a small stem-loop with GG of the CM-1 motif in all sequences of groups 1, 4 and 5. In summary, the highly conserved motifs CM-1 and CM-2 in groups 1, 2 and 3 are located in the two stem-loop regions with the short loop in-between. In groups 4 and 5 the conserved motifs CM-1 and CM-3 are located in the small hairpin region followed by the loop and fold similarly as in group 1. These conserved common motifs in the secondary structures might be important for GLI binding.

The binding constants of two of the best binders II(R09) and II (R16) to GLI were determined to be $1.0 \times 10^{-6}$ and $1.7 \times 10^{-6}$ M. However, the five zfs in GLI were characterized to bind to a 45-bp DNA fragment that contained the natural binding site with a binding constant of approximately 20 nM (Pavletich and Pabo, 1993). Therefore, the binding affinities of the aptamers in the present work are comparable with those of the peptide-binding aptamers in the literature, but much lower than those of the natural binding sites.

In addition, the minimal motif (33 nt) designed on the basis of the highly conserved nucleotides in the predicted secondary structures did not bind to GLI specifically. This result might indicate that the binding sites of GLI aptamers might be multiple and not be able to be simplified in such a minimal motif containing only conserved nucleotides. It might also be possible that the long G-C stem makes the two small stem-loops in the minimal motif near each other much more tightly than in the full-length structures. This reason might thus lead to the loss of binding activity.

Furthermore, the aptamer II(R09) and the enriched pool against GLI cross-reacted with the other *zf* peptide target ZFY. The cross-reactivity to ZFY indicates

that these highly conserved GLI-binding sequences may not distinguish two different, but similar *zf* peptides. Such kind of cross-reactivity was also found by Ellington and his coworkers (1990) who identified some RNA ligands, which bound to different organic dyes. The authors guessed that these ligands might fail to discriminate between the different dyes or they bound to the matrix itself. In this work, the interaction between aptamers and GLI may possibly be sequence-dependent. The cross-reactivity might be due to the sequence-homology of ZFY and GLI. Another possibility may be that they bind to some conserved region in these *zf* peptide targets of the secondary or tertiary structures. As demonstrated by the characterization of the GLI peptide, the spectra of $Zn^{2+}$-coordinated GLI showed a weak CD band. It may indicate that the GLI peptide was somehow less structured in the presence of $Zn^{2+}$ and did not provide enough homologous conformational elements in solution. It was therefore difficult for DNA molecules to recognize an overall conserved binding site. This may have led to the aptamers with relative lower affinities but cross-reactivities to the other *zf* peptide ZFY.

Moreover, the random ssDNA pool was observed to bind more weakly to the peptide when the concentration of the target peptide was increased to several micromolars (< 5 μM). The binding constant could not be measured accurately due to the low affinity and was therefore estimated to be more than 20 μM under these conditions. However, it is not surprising because it is well known that many zinc finger proteins interact with DNA or RNA unspecifically, for example, the binding constant of unspecific RNA binding to T4 DNA polymerase was reported to be about 30 μM (Tuerk and Gold, 1990). Therefore, the estimated binding constants of the random pool to the peptides of this work are quite normal for unspecific DNA-protein interactions.

In the second *SELEX* experiment, the ZFY-binding sequences were enriched successfully by fourteen rounds of selection. From thirty-three clones, sixteen different sequences were observed. Sequence analysis failed to give an overall conserved motif; however, it is not unusual for an *SELEX* procedure to yield sets of sequence unrelated high affinity ligands, because there are many completely different ways of creating specific binding sites for any given ligand (Ellington and Szostak, 1990; Bardeesy and Pelletier, 1998). These sequences observed in this study could be classified into six groups based on nucleotide conservation at specific residues. Among them, the sequences in group 5 were similar to those in the

enriched pool against GLI. The clone I(B24) was even identical with clone II(R09). The cross-reactivity of these sequences to both peptide targets has already been discussed above.

The binding results of different metal ions on the enriched aptamers to ZFY showed that metal ion replacements in zinc fingers can lead to a number of effects of aptamers binding to the ZFY peptides. Effects of other heavy metal ion substitutions on other zinc finger domains have been observed with several other studies (Predki and Sarkar, 1994; Berg and Shi, 1996). Interestingly, Omichinski and his coworkers (1993) demonstrated that addition of $Co^{2+}$ or $Cd^{2+}$ ions to a small single-finger peptide from the ETF GATA-1, produced actively binding peptide-metal ion complexes with binding constants very similar to those obtained with the $Zn^{2+}$ complex. In the present study, the results demonstrate that the binding of an enriched ssDNA aptamers to $Zn^{2+}$-coordinated ZFY decreased to $Co^{2+}$- or $Cd^{2+}$-cooridnated or also metal-free peptides. This indicates that metal-binding is critical for the interaction. The binding affinity to the $Co^{2+}$-coordianted peptides was only a little lower than that to the $Zn^{2+}$-coordinated peptides. This observation is in agreement with other studies that $Co^{2+}$ folds the peptide in a fashion very similar to that of $Zn^{2+}$ as determined by CD spectra, NMR analysis and EXAFS structural studies of XPA and XPA-MBD substituted with $Zn^{2+}$ and $Co^{2+}$ (Kopera *et al.*. 2004). However, the difference in binding to the $Cd^{2+}$-coordinated and metal-free peptides was not so large in the present binding study. The reason might be that the $Cd^{2+}$ complex was somehow less structured and $Cd^{2+}$ may in addition also deform the zinc finger structure (Kopera *et al.*, 2004). The CD spectra of $Cd^{2+}$ complex had a decreased content of α-helix, as compared to $Zn^{2+}$ and $Co^{2+}$ complexes. These factors might be the reasons that the binding of the enriched pool to the $Cd^{2+}$-coordinated peptides was weaker than that to the $Zn^{2+}$- or $Co^{2+}$-coordinated peptides. Therefore, the effects of metal ion replacements on the enriched aptamers to ZFY indicate that the tetrahedral metal binding of the peptides is important for the high affinity binding.

The secondary structures of the ZFY-binding sequences were predicted by the *Zuker* mfold program. Consensus secondary structures were analyzed in each group. In group 1, the conserved nucleotides TCTCGCGCG in both clones I(B15) and I(B12) are located on one side of a stem-loop region, of which CG and GCG are involved in stable G-C pairs. In addition, TCT are located in the loop and C is in the

small bulge in both structures. This conserved hairpin region might be component for ZFY binding. In group 2 it failed to identify consensus secondary structure on the basis of structure predictions by the *Zuker* mfold program. A further analysis on the conserved nucleotides in clone I(R18) reveals that they could form a G-quadruplex structure, which can not be predicted by available algorithm of secondary structure analysis. It can form two guanine tetrads connected by three loops. The G-quadruplex might play an important role in ZFY-binding to clone I(R18), which was later analyzed by truncation studies. The sequences in group 3 are also G-rich and the conserved G-rich region might form a G-quadruplex. Moreover, both of the clones in group 4 were predicted to have very similar secondary structures. The nucleotides TGGAT ACGGT are highly conserved in the secondary structures, of which GGAT and CGGT pair with the nucleotides in 5'-primer region. In addition, the three clones in group 5 have similar secondary structures as the GLI-binding sequences. Interestingly, by further analysis of the positions of conserved residues on predicted secondary structures, a trend might be found in each group. That is, the ligand, in which more conserved residues are located in stems contributed by base-pairs and especially strong G-C base-pairs, has often higher binding affinity to ZFY in the binding tests.

The further characterization of the ZFY-binding sequences revealed that they have much higher binding affinities to ZFY, than the GLI-binding sequences to GLI. The binding constants of the best binders from each group were determined to be 154-2000 nM. It has repeatedly been reported that peptide binders with high affinities were difficult to obtain (Nieuwlandt *et al.,* 1995; Bardeesy and Pelletier, 1998; Beuckelaer *et al.,* 1999; Kawakami *et al*., 2000). Even though small peptides are attractive therapeutic targets, few peptides have been successfully used as target molecules for selections. Peptides are difficult targets for molecular recognition because they often adopt different conformations and lose their entropy upon binding to the aptamer (Gold *et al.,* 1995). Therefore, the binding affinities of the ZFY-binding aptamers are comparable to those reported for other aptamer-peptide interactions.

Two of the best binders identified in the present study, I(B15) and I(R18), were characterized in further detail. Aptamer I(B15) bind to ZFY with a $K_D$ of 1.5 x $10^{-7}$ M. As discussed above, the conserved hairpin region (positions 24-40) as predicted by the *Zuker* mfold program may be component of the aptamer I(B15), which binds to the ZFY. Furthermore, the study of the effect of $Zn^{2+}$ ions on the aptamer I(B15)-ZFY

interaction demonstrates that the binding was zinc-dependent. Such zinc-dependent binding was also found in several other studies between *zf*s and dsDNA (Sakaguchi *et al.*, 1991; Predki and Sarkar, 1994; Pedone *et al.*, 1996). Moreover, Jeong (2008) showed that the selected RNA aptamers can bind specifically to the nucleocapsid (NC) protein of the HIV-1 in a zinc finger motif dependent manner. These reports support the results in this work that the conformation of the zinc finger structure was critical for aptamer interaction.

Another of the best binders, I(R18) from group 2, was determined to bind to ZFY with a $K_D$ of 1.6 x $10^{-7}$ M and was studied by truncation experiments. A 39-nt variant was truncated from the full-length sequence based on the stem-loop (including the G-rich region) as predicted by the *Zuker* program. A 27-nt variant was truncated based on the minimal G-quadruplex as predicted by the *QuadFinder.* The binding results demonstrate that both of these variants bind to ZFY, with weaker but comparable affinities as the full-length aptamer. However, the shorter purine-rich variant truncated from the 27-nt sequence did not exhibit any specific binding any more. These results suggest that the G-quadruplex structure might be necessary and important, but not sufficient for aptamer I(R18)-ZFY interaction.

## 5.4 Functional Studies

The aptamers were selected in this work against two peptides each containing a single zinc finger of ZFY and GLI transcription factors. Although the GLI-binding sequences have highly conserved nucleotides, they exhibit relatively lower binding affinities in the µM range. However, the binding affinities of the aptamers against ZFY were significantly higher (in the nM range). Therefore, the later functional studies were focused mainly on the ZFY-binding aptamers.

Firstly, the peptide-binding aptamers were evaluated for protein binding. The attempt to overexpress the ZFY protein containing thirteen zinc fingers, however, failed, probably due to the complexity and large number of *zf*s. Still, within peptide-binding sequences, some might recognize ZFY in a very specific way, while others might bind to conserved regions of similar zinc fingers. Therefore, as a proof of principle, ZFY-binding aptamers were tested whether some of them bound to a protein with the related $Cys_2His_2$ zinc finger, namely ZNF593. It shares more than

40% sequence identity in *zf* domain with ZFY. Hayes and his coworkers (2008) solved the solution structure of ZNF593 and the inspection of the analysis of 3D coordinates with other proteins in databases revealed significant identity with the ZFY peptide (Fig. 5-1). Therefore, ZNF593 protein is a proper target to be chosen as a related protein with a ZFY-similar zinc finger for binding studies.

The results revealed that the aptamer I(B15) bound to the fusion protein ZNF593 with a $K_D$ of 2.9 x $10^{-7}$ M, which was comparable with that to the ZFY peptide. The another aptamer I(R18) had a much weaker interaction with a $K_D$ of 3.5 x $10^{-6}$ M and this interaction with protein ZNF593 was significantly weaker than that to ZFY. The binding results indicate that the aptamer I(R18) would recognize ZFY specifically and that aptamer I(B15) may be able to recognize both peptide ZFY and protein ZNF593, and even other very related zinc finger proteins. As discussed in the introduction section, in nature TFIIIA binds to DNA in a primary sequence-specific manner, but binds to RNA based on conserved secondary/tertiary structure independent of the primary RNA sequence (Pieler *et al*., 1984; Pieler *et al*., 1986; Theunissen *et al.*, 1992). Therefore, it is not surprising that *in vitro* selection leads to either sequence-dependent or structure-dependent high affinity molecules. However, aptamer I(B15) did not bind to the other zinc finger peptide GLI. The explanation may be that GLI may have a less ordered *zf* structure as was discussed in CD analysis under 5.1.

Interestingly, under the buffer and salt conditions in this work a random ssDNA pool bound to ZNF593 protein unspecifically with a binding constant of approximately 1 μM. The unspecific interaction is apparent, although 0.05 μg/μl tRNA was used in the binding buffer as non-specific competitor. However, there are several studies which reported that zinc finger proteins bind to polynucleotides non-specifically with binding constants of around 1 μM or less (Gauss *et al.* 1987; Lee *et al*., 1991; Schneider *et al.,* 1992; Schneider *et al.,* 1993; Kim *et al*. 2002; Kirthi and Savithri, 2003; Djordjevic, 2007). In this work, aptamer I(B15) had clearly, but not significantly, improved affinity to protein ZNF593, than the bulk of the random sequences in the library.

For later possible applications of selected aptamers, such as in diagnosis, a more complex mixture of proteins has to be analyzed. For example, it would be very useful to analyze cell extracts using aptamers for distinguishing different cell types, *e.g.* normal and tumor cells, by recognizing zinc finger proteins. This is, however, a

big challenge. Many efforts have already been described in the literature to capture and identify dsDNA-binding proteins from cell extract or nuclear extract (Nordhoff *et al.*, 1999, Drewett *et al.*, 2001; Gadgil *et al.*, 2001, Forde and McCutchen-Maloney, 2002; Deng *et al.*, 2003; Yaneva and Tempst, 2003; Park *et al.*, 2005). However, interactions of proteins with single-stranded oligonucleotides are more complex than protein-dsDNA interactions. This is due to the fact that interactions of proteins with single-stranded oligonucleotides in general significantly depend on secondary and tertiary structures. In addition, aptamer affinity chromatography has been described for the purification of a protein from conditioned cell culture media (Romig *et. al.,* 1999). Murphy and his co-workers (2003) describe first the successful application of aptamer affinity chromatography for one-step purification of the recombinant TTF1 protein from *E.coli* lysate. However, no assay has been described till now for aptamer affinity capture of zinc finger proteins or transcription factors directly from eukaryotic cell extract or nuclear extract. In this work aptamer affinity capture assays were established for a complex mixture of proteins in cell extracts or nuclear extracts of HeLa cells, using biotinylated aptamer I(B15) immobilized on Neutravidin agarose gel.

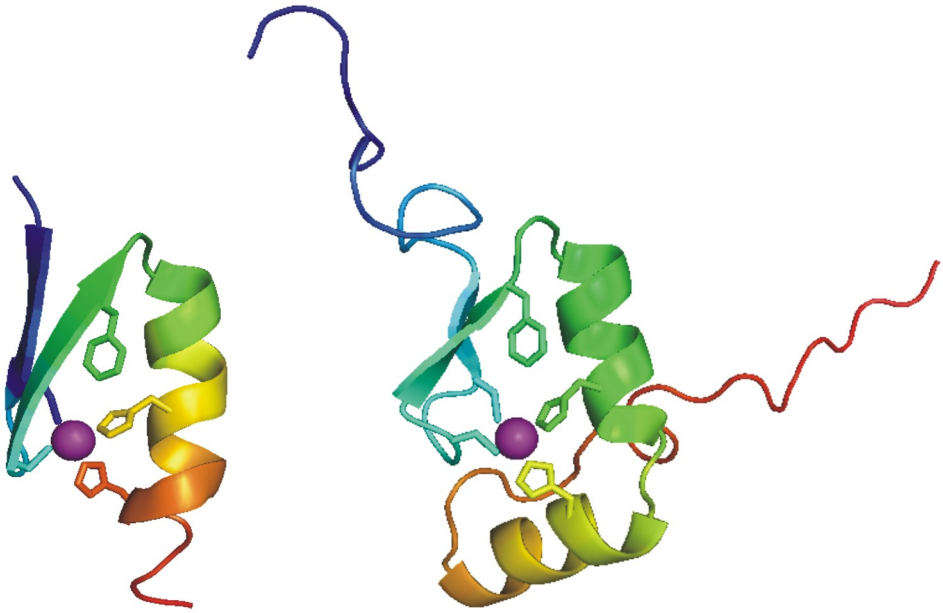

***Figure 5-1 Ribbon diagrams of ZFY target peptide (PDB code 7znf) and ZNF593 protein (PDB code 1zr9).*** *Two cysteines and histidines coordinate with zinc ion. Hydrophobic residue (phenylalanine) flanks the zinc binding site.*

It is assumed that transcription factors represent only 0.01-0.001% of the total cellular protein mass and that approximately 2000 genes encoding different transcription factor proteins are believed to be required by a functional human cell. Within the cell, or the nucleus of eukaryotic cells, the concentration of DNA is so high that the transcription factor proteins will be bound to DNA essentially all the times (see in Stormo and Fields, 1998). Thus to obtain a maximum amount of the transcription factor proteins from cell extracts, a high salt of 420 mM sodium chloride solution was used in the lysis buffer for dissociating DNA binding proteins from chromosomal DNAs.

Firstly, ZFX transcription factor was expected to be captured by the ZFY-aptamer I(B15) from the nuclear extract of HeLa cells. ZFY and ZFX proteins are very similar and nearly equal in size. In domain 6, from which the ZFY peptide used in this thesis was derived, there is only one amino acid difference between ZFY and ZFX. In this study the expression of the ZFX transcription factor in HeLa cells was confirmed by western blotting with anti-ZFX serum. However, no ZFX could be identified in the aptamer-bound proteins by affinity capture assays of the nuclear extracts of HeLa cells. The western blotting results show that ZFX retained largely in cell debris. It was quite a challenge to capture ZFX in the nuclear extract, since it existed only in a very tiny amount and faced also the competition by a large number of unspecific binding proteins. Identification of ZFX transcription factor by affinity capture directly from crude extract of cells has therefore proven to be very difficult.

Secondly, the aptamer-bound proteins were partly identified by gel electrophoresis, followed by MALDI-TOF-MS. The captured proteins include usual abundant unspecific binding proteins as well as specific binding proteins. Two zinc finger proteins (TAFII68 and Matrin-3) were identified in a direct capture assay (method No. 1). However, the background of unspecific binding proteins was quite dominant. Since non-specific binding proteins were abundantly present and the stringency of the affinity capture was relatively low, it is not surprising that proteins that bind to nucleic acids in a non-specific manner may dominate on the DNA-binding site of the aptamer. Although it was impossible to completely avoid the unspecific binding of proteins, some means should be devised, to decrease the interaction level of unspecific binding proteins, and at the same time increase the detection level of specific binding proteins (Park *et.al*., 2005).

Subsequently, the unspecific-binding proteins were removed or reduced by adding unspecific competitors like 0.125 µg/µl poly(dI-dC), pre-incubating with immobilized random ssDNAs, and eluting with excess biotin solution. Indeed it was noticed that the background decreased clearly after such treatments were performed. Although the background proteins could be significantly reduced it was still not enough to permit the isolation of zinc finger proteins from the total cellular extracts. Therefore, the work was next concentrated on the nuclear extracts from HeLa cells. Indeed it was possible that two *zf* proteins could be identified in a competitive capture assay (method No. 2). For comparison, no *zf* proteins were identified in the control column immobilized with the random ssDNA pool. Thus the results indicate that the interactions of these zinc finger proteins with the aptamer exhibited some specificity. It is clear that the results obtained are encouraging enough to be continued.

It is very interesting if one takes a closer look at the proteins which had bound to the aptamers generated in this study. The zinc finger proteins captured with the affinity experiments are Matrin-3, TAFII68 and TLS proteins. As already discussed in the introduction section under 1.1.3, protein Matrin-3 belongs to classical $Cys_2His_2$ type *zf* (Matsushima *et al.*, 1997) as ZFY, ZFX and ZNF593 proteins. Proteins TAFII68 and TLS belong to non-classical $Cys_2Cys_2$ type *zf* of RanBP2 family and share extensive sequence similarity of 74%. The sequences of these *zf* domains comparing with the ZFY peptide, against which the aptamer I(B15) was isolated, were analyzed as homologous common zinc fingers, but not with identical residues (Fig. 5-2). However, they all have at least two conserved cysteines in metal-binding residues and conserved hydrophobic residues flanking the metal-binding site. These residues and the zinc-coordinated complex might be necessary and important for interaction of the aptamer with zinc fingers. Moreover, structure alignments of proteins are more informative than alignments based on sequence only. Some proteins showed the great structural similarity even though they share few sequence identities. As discussed above, the experimental data (Kochoyan *et al.*, 1991b; Hayes *et al.*, 2008) revealed the highly similarity in tertiary structures between the *zf* domains of the ZFY peptide and the ZNF593 protein. However, the 3D structures of the *zf* domains in the Matrin-3, TAFII68 and TLS proteins have not been solved experimentally yet. Although the primary structures of these *zf* domains are not highly homologous to that of the ZFY peptide, these sequences might present very similar

secondary and tertiary structures. It is quite possible that the aptamer may recognize some structural features common to the zinc finger motif used in this study.

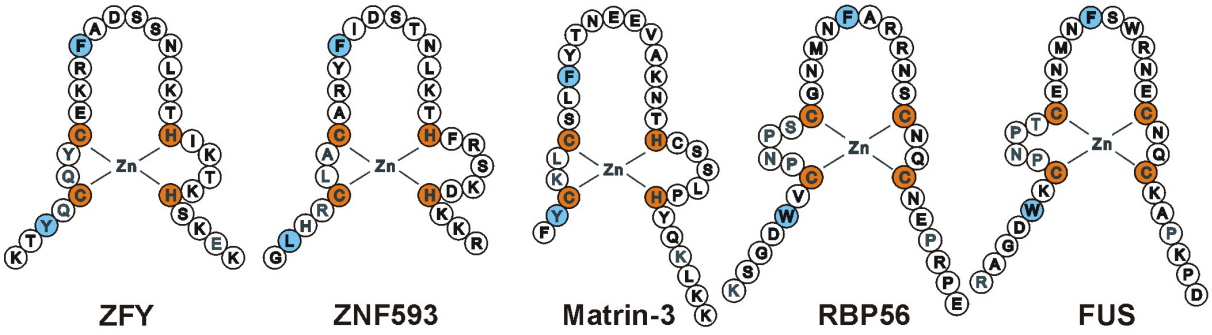


***Figure 5-2 Schematic diagram of the zf domains in the aptamer I(B15)-binding ZFY, ZNF593, Matrin-3, RBP56 and FUS.*** *Conserved positions are marked that contain metal-binding residues (orange) and the hydrophobic residues (blue).*

## 5.5 Applications and Outlook

The aptamers selected in this thesis could be valuable new agent against zinc finger targets for diagnostic and even therapeutic applications. They could be employed to recognize zinc finger targets by affinity captures from extracts of different cell types, *e.g.* normal and cancer cells, followed by two-dimensional gel analysis and then protein identification. The zinc finger targets that may have different dosages in altered cells could be identified by aptamers and further studied as valuable biomarkers.

Although dsDNA-*zf*s interactions are well understood, little is known about *zf*s-RNA or –ssDNA interactions. In particular, the binding mechanism between a single zinc finger motif and ssDNA has so far not been investigated yet. Therefore, it would be better understood if the molecular structure of the complex of the isolated high affinity ssDNA ligand to zinc finger is solved by X-ray crystallography or NMR.

In addition, the isolated ZFY or GLI binding sequences can be subjected in further experiments to another selection, to obtain zinc finger-binding aptamers with higher affinity and selectivity. A library of mutagenized DNAs could be constructed and additional variation can be introduced by error-prone PCR during the selection

rounds. Aptamers could be selected against other transcription factor containing a similar *zf* motif or a *zf* protein mixture. The selected aptamers with higher affinity can then serve as therapeutic probes for targeting the zinc finger transcription factors.

Based on the proof of principle described in the present aptamer selection procedure, Spiegelmers with higher biostability can be designed for zinc finger target, since the mirror image of a small peptide can be synthesized chemically with unnatural building blocks. This may result in stable zinc finger-binding Spiegelmers for a variety of medical and diagnostic applications related to gene activity profiling.

# 6 Summary

Zinc finger (*zf*) transcription factors are primarily involved in human diseases including cancer. Specific molecular probes that target zinc finger transcription factors may be useful for early detection and treatment of diseases. The high affinity and specificity of aptamers selected since the early 1990s have clearly demonstrated that these molecules have great potentials to meet these challenges.

This work demonstrates for the first time that high affinity DNA aptamers can be isolated successfully to recognize a single zinc finger motif. They were selected against two zinc-coordinated peptides, each of which contains a single $Cys_2His_2$-type zinc finger motif of ZFY and GLI transcription factors, in two independent *SELEX* experiments respectively. The ZFY-aptamers have high affinities with $K_D$s in nanomolar range to the ZFY peptide, while the GLI-aptamers exhibit binding activities with $K_D$s of the micromolar range to the GLI peptide. Interestingly enough they show also significant binding affinities to the ZFY peptide. The binding motifs of these aptamers were defined by primary and secondary structural analyses, as well as by truncation experiments. Moreover, studies on the binding effects of metal ion replacements show that the zinc-coordinated tetrahedral structure is critical for the interaction. Subsequently, the aptamer I(B15) was determined to bind to the ZNF593 protein containing a single zinc finger motif, which is highly similar to the ZFY peptide used in the *in vitro* selection. The binding affinity of the aptamer to the ZNF593 protein is comparable with that to the ZFY peptide and it exhibits clearly improved affinities when compared to the random sequences of the starting library. Finally, affinity capture assays were established using the aptamer I(B15) for recognizing *zf* proteins from HeLa cell extracts and several zinc finger proteins were identified from the aptamer-bound nuclear proteins by MALDI-TOF-MS. The data presented also indicate that the aptamers may recognize some structural features common to the zinc finger motifs used in this study.

Consequently, these selected DNA aptamers will help to better understand the interaction of single-stranded oligonucleotides with zinc finger proteins. Finally, this

thesis lays the basis for further work involving Spiegelmers or aptamers with higher affinities and biostablities to be used for the diagnosis and therapy of diseases, such as tumor diseases.

# 7 Zusammenfassung

Zinkfinger(zf)-Transkriptionsfaktoren sind an einer Vielzahl von menschlichen Erkrankungen, unter anderem Krebs, beteiligt. Molekulare Wirkstoffe, die spezifisch gegen Zinkfinger-Transkriptionsfaktoren wirken, könnten für die Früherkennung und Behandlung dieser Krankheiten nützlich sein. Aptamere wurden seit den frühen 1990er Jahren gegen eine Vielzahl von Zielstrukturen entwickelt und eigenen sich durch ihre hohe Affinität und Spezifität besonders zur Bewältigung dieser Aufgaben.

Im Rahmen dieser Arbeit wurden erstmalig erfolgreich hochaffine DNA-Aptamere gegen ein einzelnes Zinkfingermotiv generiert. In zwei voneinander unabhängig durchgeführten *SELEX*-Experimenten wurden Aptamere gegen zwei Zink-koordinierte Peptide erzeugt, wobei beide Peptide ein einzelnes $Cys_2His_2$-Typ Zinkfingermotiv der ZFY- und GLI- Transkriptionsfaktoren enthielten. Die ZFY-bindenden Aptamere weisen Dissoziationskonstanten im nanomolaren Bereich auf, während die gegen GLI selektierten Aptamere eine Bindung im mikromolaren Bereich zeigen und auch das ZFY Motiv binden. Mögliche Bindungsmotive der Aptamere wurden sowohl durch Primär- und Sekundärstrukturanalysen, als auch durch Verkürzungsstudien bestimmt. Aus den experimentellen Daten geht weiterhin hervor, dass die Zink-Koordinierten, tetraedrische Strukturen essentiell für die Interaktion sind. Es konnte gezeigt werden, dass das Aptamer I(B15) an das ZNF593-Protein bindet, welches ein dem ZFY ähnliches Zinkfingermotiv enthält. I(B15) hat zu ZNF593 eine vergleichbare Affinität wie zu ZFY und eine deutlich erhöhte Affinität im Vergleich zu den Zufallssequenzen der Ausgangsbibliothek. Ferner wurde ein Verfahren etabliert, bei dem unter Verwendung von dem Aptamer I(B15) zf-Proteine aus HeLa-Zellextrakten isoliert und anschließend durch MALDI-TOF-MS identifiziert werden konnten. Diese Analyse lässt den Schluss zu, dass das Aptamer gemeinsame Strukturelemente der Zinkfingermotive erkennt.

Durch diese Arbeit geben die hier entwickelten Aptamere ein Werkzeug, um ein besseres Verständnis über Wechselwirkungen von einzelsträngigen Oligonukleotiden mit Zinkfingerproteinen zu erlangen. Darüber hinaus können auf Basis dieser Arbeit Spiegelmere oder Aptamere gegen Zinkfinger-Transkriptionsfaktoren mit höherer Affinität und Biostabilität entwickelt werden. Diese würden in der Medizin von hohem Nutzen für diagnostische und therapeutische Anwendung sein.

# 8 References


Allen, P., Worland, S., Gold, L. 1995. Isolation of high-affinity RNA ligands to HIV-1 integrase from a random pool. Virology. 209: 327-336.

Altaba, A. R. 1999. GLI proteins and Hedgehog signaling. TIG. 15 (10): 418-425.

Anderson, W. F., Ohlendorf, D. H., Takeda, Y., Matthews, B. W. 1981. Structure of the cro repressor from bacteriophage lambda and its interaction with DNA.

Andreazzoli, M., Lucchini, S. D., Costa, M., Barsacchi, G. 1993. RNA binding properties and evolutionary conservation of the Xenopus multifinger protein Xfin. Nucleic Acids Res. 21: 4218-4225.

Andreola, M. L., Calmels, C., Michel, J., Toulme, J. J., Litvak, S. 2000. Towards the selection of phosphorothioate aptamers-optimizing *in vitro* selection steps with phophorothioate nucleotides. Eur. J. Biochem. 267: 5032-5040.

Arranz, V., Harper, F., Florentin, Y., Puvion, E., Kress, M., Ernoult-Lange, M. 1997. Human and mouse MOK2 proteins are associated with nuclear ribonucleoprotein components and bind specifically to RNA and DNA through their zinc finger domains. Mol. Cell. Biol. 17(4): 2116-26.

Bal, W., Schwerdtle, T., Hartwig, A. 2002. Mechanism of nickel assault on the zinc finger of DNA repair protein XPA. Chem. Res. Toxicol. 16: 242-248.

Barciszewski, J., Erdmann, V. A. (ed.) 2003. Noncoding RNAs: molecular biology and molecular medicine. Kluwer Academic/Plenum Publischers.

Bardeesy, N., Pelletier, J. 1998. Overlapping RNA and DNA binding domains of the wt1 tumor suppressor gene product. Nucleic Acids Res. 26 (7): 1784-1792.

Beausoleil, S. A., Jedrychowski, M., Schwartz, D., Elias, J. E., Villen, J., Li, J., Cohn, M. A., Cantley, L. C., Gygi, S. P. 2004. Large-scale characterization of HeLa cell nuclear phosphoproteins. PNAS. 101: 12130-12135.

Belgrader, P., Dey, R., Berezney, R. 1991. Molecular cloning of matrin-3. The Journal of Biological Chemistry. 266 (15): 9893-9899.

Berg J. M. 1990. Zinc finger domains : hypotheses and current knowledge. Annu. Rev. Biophys. Biophys. Chem. 19: 405-421.

Berg, J. M., Shi, Y. 1996. The galvanization of biology: a growing appreciation for the roles of zinc. Science. 271: 1081-1085.

Bernert, G., Fountoulakis, M., Lubec, G. 2002. Manifold decreased protein levels of matrin-3, reduced motor protein HMP and hlark in fetal Down's syndrome brain. Proteomics. 2: 1752-1757.

Berntenis, N., Bohrmann, B., Guentert, A., Mueller, B. 2007. Matrin 3 used as biomarker in Alzheimer disease. 06/2007 Patent WO/2007/140974.

Bertola, F., Manigand, C., Picard, P., Belghazi, M., Precigoux, G. 2000. Human T-lymphotrophic virus type I nucleocapsid protein NCp15: structural study and stability of the N-terminal zinc-finger. Biochem. J. 352: 293-300.

Bertolotti, A., Lutz, Y., Heard, D. J., Chambon, P., Tora, L. 1996. The EMBO Journal. 15(18): 5022-5031.

Beuckelaer, A. D., Fürste, J. P., Gruszecka, M., Wittmann-Liebold, B., Erdmann, V. A. 1999. Selection of RNA aptamers that bind to a peptide of the canyon region of human rhinovirus 14. Endocytobiology VII. 565-577.

Biesecker, G., Dihel, L., Enney, K., Bendele, R. A. 1999. Derivation of RNA aptamer inhibitors of human complement C5. Immunopharmacology. 42: 219-230.

Blackstock, W. P., Weir, M. P. 1999. Proteomics: quantitative and physical mapping of cellular proteins. Trends Biotechnol. 17(3): 121-127.

Bock, L. C., Griffin, L. C., Latham, J. A., Vermaas, E. H., Toole, J. J. 1992. Selection of single-stranded DNA molecules that bind and inhibit human thrombin. Nature. 355: 564-566.

Bradford, M. M. 1976. A rapid and sensitive method for the quantitation of microgram quantities of protein utilizing the principle of protein-dye binding. Anal. Biochem. 72: 248-254.

Brennan, P., Donev, R., Hewamana, S., 2008. Targeting transcription factors for therapeutic benefit. Mol. BioSyst. 4: 909-919.

Brown, T. A., 2006. Genomes. Garland Science. London. 3rd edn.

Bunka, D. H. J., Stockley, P. G. 2006. Apatamers come of age-at last. Nature. 4: 588-596.

Burns, J. A., Butler, J. C., Moran, J., Whitesides, G. M. 1991. Selective reduction of disulfides by Tris (2-carboxyethyl)-phosphine. J. Org. Chem. 56: 2648-2650.

Call, K. M., Glaser, T., Ito, C. Y., Buckler, A. J., Pelleitier, J., Haber, D. A., Rose, E. A., Kral, A., Yeger, H., Lewis, W. H., Jones, C., Housman, D. E. 1990. Isolation and characterization of a zinc finger polypeptide gene at the human chromosome 11 Wilm's tumor locus. Cell. 60(3): 509-520.

Caricasole, A., Duarte, A., Larsson, S. H., *et al*. 1996. RNA binding by the Wilms tumor suppressor zinc finger proteins. Proc. Natl. Acad. Sci. USA. 93: 7562-7566.

Cassiday, L. A., Maher III, L. J. 2002. Having it both ways: transcription factors that bind DNA and RNA. Nucleic Acids Res. 30(19): 4118-4126.

Chapman, J. A., Beckey, C. 2006. Pegaptanib: a novel approach to ocular neovascularization. Ann. Pharmacother. 40: 1322-1326.

Chen, T., Brownawell, A. M., Macara, I. G. 2004. Nucleocytoplasmic shuttling of JAZ, a new cargo protein for exportin-5. Mol. Cell. Biol. 24(15): 6608-6619.

Cho, E. J., Collett, J. R., Szafranska, A. E., Ellington, A. D. 2006. Optimization of aptamer microarray technology for multiple protein targets. Analytica Chimica Acta. 564: 82-90.

Clark, J. M. 1988. Novel non-templated nucleotide addition reactions catalyzed by prokaryotic and eukaryotic DNA polymerases. Nucleic Acids Res. 16: 9677-9686.

Clemens, K. R., Wolf, V., McBryant, S. J., Zhang, P., Liao, X., Weight P. E., Gottesfeld, J. M. 1993. Molecular basis for specific recognition of both RNA and DNA by a zinc finger protein. Science. 260 (5107): 530-533.

Collett, J. R., Cho, E. J., Ellington, A. D. 2005. Production and processing of aptamer microarrays. Methods. 37: 4-15.

Crozat, A., Aman, P., Mandahl, N., Ron, D. 1993. Fusion of CHOP to a novel RNA-binding protein in human myxoid liposarcoma. Nature. 363: 640-644.

Dang, C., Jayasena, S. D. 1996. Oligonucleotide inhibitors of Taq DNA polymerase facilitate detection of low copy number targets by PCR. J. Mol. Biol. 264: 268-278.

Daniels, D. A., Sohal, A. K., Rees, S., Grisshammer, R. 2002. Generation of RNA aptamers to the G-protein-coupled receptor for neurotensin, NTS-1. Anal. Biochem. 305: 214-226.

Darfeuille, F., Hansen, J. B., Orum, H., Primo, C. D., Toulme, J. J. 2004. LNA/DNA chimeric oligomers mimic RNA aptamers targeted to the TAR RNA element of HIV-1. Nucleic Acids Res. 32: 3101-3107.

Deng, W. G., Zhu, Y., Montero, A., Wu, K. K. 2003. Quantitative analysis of binding of transcription factor complex to biotinylated DNA probe by a streptavidin-agarose pulldown assay. Analytical Biochemistry. 323: 12-18.

Djordjevic, M. 2007. *SELEX* experiments: new prospects, applications and data analysis in inferring regulatory pathways. Biomolecular Engineering. 24: 179-189.

Dominski, Z., Erkmann, J. A., Yang, X., Sanchez, R., Marzluff, W. F. 2002. A novel zinc finger protein is associated with U7 snRNP and interacts with the stem-loop binding protein in the histone pre-mRNP to stimulate 3'-end processing. Gene. Dev. 16: 58-71.

Doudna, J. A., Cech, T. R. 2002. The chemical repertoire of natural ribozymes. Nature. 418: 222-228.

Dougan, H., Lyster, D. M., Vo, C. V., Stafford, A., Weitz, J. I., Hobbs, J. B. 2000. Extending the lifetime of anticoagulant oligodeoxynucleotide aptamers in blood. Nucl. Med. Biol. 27: 289-297.

Drewett, V., Molina, H., Millar, A., Muller, S., Hesler, F. V., Shaw, P. E. 2001. DNA-bound transcription factor complexes analysed by mass-spectrometry: binding of novel proteins to the human c-fos SRE and related sequences. Nucleic Acids Res. 29 (2): 479-487.

Drolet, D. W., MoonMcDermott, L., Romig, T. S. 1996. An enzyme-linked oligonucleotide assay. Nat. Biotechnol. 14: 1021-1025.

Elise, B. G., Ming X., Tania, C., Roger, C., Paul, R. S. 1999. A comparison between the sulfhydryl reductants Tris(2-carboxyethyl)phosphine and dithiothreitol for use in protein biochemistry. Analytical Biochemistry. 273: 73-80.

Ellington, A. D., Szostak, J. W. 1990. *In vitro* selection of RNA molecules that bind specific ligands. Nature. 346: 818-822.

Ellington, A. D., Szostak, J. W. 1992. Selection *in vitro* of single-stranded DNA molecules that fold into specific ligand-binding structures. Nature. 355: 850-852.

Engelkamp, D., Heyningen, V. V. 1996. Transcription factors in disease. Current Opinion in Generics & Development. 6: 334-342.

Erdmann, V. A., Brosius, J., Barciszewski, J. 2006. RNA towards medicine. Springer.

Erdmann, V. A., Poller, W., Barciszewski, J. 2008. RNA technologies in cardiovascular medicine and research. Springer.

Eulberg, D., Buchner, K., Maasch, C., Klussmann, S. 2005. Development of an automated *in vitro* selection protocol to obtain RNA-based aptamers: identification of a biostable substance P antagonist. Nucleic Acids Res. 33(4): e45.

Fairall, L. *et al*. 1993. The crystal structure of a two zinc-finger peptide reveals an extension to the rules for zinc-finger/DNA recognition. Nature. 366: 482-487.

Fan, X., Shi, H., Adelman, K., Lis, J. T. 2004. Probing TBP interactions in transcription initiation and reinitiation with RNA aptamers that act in distinct modes. PNAS. 101(18): 6934-6939.

Faulhammer, D., Eschgfäller, B., Stark, S., Burgstaller, P., Englberger, W., Erfurth, J., Keinjung, F., Rupp, J., Dan Vulcu, S., Schröder, W., Vonhoff, S., Nawrath, H., Gillen, C., Klussmann, S. 2004. Biostable aptamers with antagonistic properties to the neuropeptide nociceptin/orphanin FQ. RNA. 10(3): 516-527.

Ferreira, C. S. M., Matthews, C. S., Missailidis, S. 2006. DNA aptamers that bind to MUC1 tumour marker : design and characterization of MUC1-binding single-stranded DNA aptamers. Tumor Biol. 27: 289-301.

Forde, C. E., McCutchen-Maloney, S. L. 2002. Characterization of transcription factors by mass spectrometry and the role of SELDI-MS. Mass Spectrometry Reviews. 21: 419-439.

Frankel, A. D., Berg, J. M., Pabo, C. O. 1987. Metal-dependent folding of a single zinc finger from transcription factor IIIA. Proc. Natl. Acad. Sci. USA. 84: 4841-4845.

Friesen, W. J., Darby, M. K. 2001. Specific RNA binding by a single C2H2 zinc finger. J Biol Chem. 276: 1968-1973.

Gadgil, H., Oak, S. A., Jarrett, H. W. 2001. Affinity purification of DNA-binding proteins. J. Biochem. Biophys. Methods. 49: 607-624.

Galan-Caridad, J. M., Harel, S., Arenzana, T. L., Hou, Z. E., Doetsch, F. K., Mirny, L. A., Reizis, B. 2007. Zfx controls the self-renewal of embryonic and hematopoietic stem cells. Cell. 129: 345-357.

Gauss, P., Krassa, K. B., McPheeters, D. S., Nelson, M. A., Gold, L. 1987. Zinc(II) and the single-stranded DNA binding protein of bacteriophage T4. Proc. Natl. Acad. Sci. 84: 8515-8519.

Gessler, M., Poustka, A., Cavenee, W., Neve, R. L., Orkin, S. H., Bruns, G. A. 1990. Homozygous delection in Wilm's tumours of a zinc-finger gene identified by chromosome jumping. Nature. 343(6260): 774-778.

Getz, E. B., Xiao, M., Chakrabarty, T., Cooke, R., Selvin, P. R. 1999. A comparison between the sulfhydryl reductants tris(2-carboxyethyl)phosphine and dithiothreitol for use in protein biochemistry. Analytical Biochemistry. 273: 73-80.

Giangrande, P.H., Zhang, J., Tanner, A., Eckhart, A. D., Rempel, R. E., Andrechek, E. R., Layzer, J. M., Keys, J. R., Hagen, P. O., Nevins, J. R., Koch, W. J., Sullenger, B. A. 2007. Distinct roles of E2F proteins in vascular smooth muscle cell proliferation and intimal hyperplasia. Proc. Natl. Acad. Sci. 104(32): 12988-12993.

Gold, L., Polisky, B., Uhlenbeck, O., Yarus, M. 1995. Diversity of oligonucleotide functions. Annu. Rev. Biochem. 64: 763-797.

Green, L. S., Jellinek, D., Bell, C., Beebe, L. A., Feistner, B. D., Gill, S. C., Jucker, F. M., Janjic, N. 1995. Nuclease-resistant nucleic-acid ligands to vascular-permeability factor vascular endothelial growth-factor. Chem. Biol. 2: 683-695.

Green, L. S., Jellinek, D., Jenison, R., Ostman, A., Heldin, C. H., Janjic, N. 1996. Inhibitory DNA ligands to platelet-derived growth factor B-chain. Biochemistry. 35: 14413-14424.

Hall, T. 2005. Multiple modes of RNA recognition by zinc finger proteins. Current Opinion in Structural Biology. 15: 367-373.

Han, J. C., Han, G. Y. 1994. A procudure for quantitative determination of Tris(2-caboxyethyl)phosphine, an odorless reducing agent more stable and effective than dithiothreitol. Analytical biochemistry. 220: 5-10.

Hanas, J., Hazuda, D. J., *et al*. 1983. Xenopus transcription factor A requires zinc for binding to the 5 S RNA gene. J. Biol. Chem. 258: 14120-14125.

Hanna, J., Wernig, M., Markoulaki, S., Sun, C. W., Meissner, A., Cassady, J. P., Beard, C., Brambrink, T., Wu, L. C., Townes, T. M., Jaenisch, R. 2007. Treatment of sickle cell anemia mouse model with iPS cells generated from autologous skin. Science. 318:1920-1923.

Hannon, G. J. 2002. RNA interference. Nature. 418: 244-251.

Hayes, P. L., Lytle, B. L., Volkmann, B. F., Peterson, F. C. 2008. The solution structure of ZNF593 from Homo sapien reveals a zinc finger in a predominately unstructured protein. Protein Science. 17: 571-576.

Helmling, S., Maasch, C., Eulberg, D., Buchner, K., Schröder, W., Lange, C., Vonhoff, S., Wlotzka, B., Tschöp, M. H., Rosewicz, S., Klussmann, S. 2004. Inhibition of ghrelin action *in vitro* and in vivo by an RNA-Spiegelmer. Proc. Natl. Acad. Sci. USA. 101(36): 13174-13179.

Hermann, T., Patel, D. J. 2000. Adaptive recognition by nucleic acid aptamers. Science. 287(5454): 820-825.

Hicke, B. J., Watson, S. R., Koenig, A., Lynott, C. K., Bargatze, R. F., Chang, Y. F., Ringquist, S., Moon-McDermott, L., Jennings, S., Fitzwater, T., Han, H. L., Warki, N., Albinana, I., Willis, M. C., Varki, A., Parma, D. 1996. DNA aptamers block L-selection function in vivo. Inhibition of human lymphocyte trafficking in SCID mice. J. Clin. Invest. 98: 2688-2692.

Hirau, I., Harada, Y., Nojima, T., Osawa, Y., Masaki, H., Yokoyama, S. 2004. *In vitro* selection of RNA aptamers that bind to colicin E3 and structurally resemble the decoding site of 16S ribosomal RNA. Biochemistry. 43: 3214-3221.

Hisada-Ishii, S., Ebihara, M., Kobayashi, N., Kitagawa, Y. 2007. Bipartite nuclear localization signal of matrin 3 is essential for vertebrate cells. Biochemical and Biophysical Research Communications. 354: 72-76.

Houbaviy, H. B., Usheva, A., Shenk, T., Burley, S. K. 1996. Cocrystal structure of YY1 bound to the adeno-associated virus P5 initiator. Proc. Natl. Acad. Sci. USA. 93: 13577-13582.

Huang, D. B., Vu, D., Cassiday, L. A., Zimmerman, J. M., Maher 3rd, L. J., Ghosh, G. 2003. Crystal structure of NF-kB $(p50)_2$ complexed to a high-affinity RNA aptamer. Proc. Natl. Acad. Sci. 100: 9268-9273.

Ikebukuro, K., Hasegawa, H., Sode, K. 2007. Selection and characterization of DNA aptamers against $VEGF_{165}$ with aptamer blotting method and its application. Nucleic Acids Symposium Series. 51: 399-400.

Ishizaki, J., Nevins, J. R., Sullenger, B. A. 1996. Inhibition of cell proliferation by an RNA ligand that selectively blocks E2F function. Nature Medicine. 2(12): 1386-1389.

Jayasena, S. D. 1999. Aptamers: an emerging class of molecules that rival antibodies in diagnostics. Clinical Chemistry. 45 (9): 1628-1650.

Jellinek, D., Green, L. S., Bell, C., Janjic, N. 1994. Inhibition of receptor binding by high-affinity RNA ligands to vascular endothelial growth factor. Biochemistry. 33: 10450-10456.

Jellinek, D., Green, L. S., Bell, C., Lynott, C. K., Gill, N., Vargeese, C., Kirschenheuter, G., McGee, D. P., Abesinghe, P., Pieken, W. A. *et al*. 1995. Potent 2'-amino-2'-deoxypyrimidine RNA inhibitors of basic fibroblast growth factor. Biochemistry. 34: 11363-11372.

Jenison, R. D., Gill, S. C., Pardi, A., Polisky, B. 1994. High-resolution molecular discrimination by RNA. Science. 263: 1425-1429.

Jenison, R. D., Jennings, S. D., Walker, D. W., Bargatze, R. F., Parma, D. 1998. Oligonucleotide inhibitors of P-selectin-dependent neutrophil-platelet adhesion. Antisense Nucleic Acid Drug Dev. 8(4): 265-279.

Jeong, Y. Y., Kim, S. H., Jang, S. I., You, J. C. 2008. Examination of specific binding activity of aptamer RNAs to the HIV-NC by using a cell-based in vivo assay for protein-RNA interaction. BMB Reports. 41(7): 511-515.

Jhaveri, S., Olwin, B., Ellington, A. D. 1998. *In vitro* selection of phosphorothiolated aptamers. Bioorg. Med. Chem. Lett. 8: 2285-2290.

Jones, L. A., Clancy, L. E., Rawlinson, W. D., White, P. A. 2006. High-affinity aptamers to subtype 3a hepatitis C virus polymerase display genotypic specificity. Antimicrob. Agents Ch. 50: 3019-3027.

John, A. B., James, C. B., John, M., George, M. W. 1991. Selective reduction of disulfides by Tris(2-carboxyethyl)phosphine. J. Org. Chem. 56: 2648-2650.

Joho, K. E., Darby, M. K., Crawford, E. T., Brown, D. D. 1990. A finger protein structurally similar to TFIIIA that binds exclusively to 5S RNA in Xenopus. Cell. 61: 293.

Kägi, J. H. R. 2001. Zinc fingers: ubiquitous modules of gene regulation. The Journal of Trace Elements in Experimental Medicine. 14: 171-175.

Kanaya, E., Nakajima, N., Okada, K. 2002. Non-sequence-specific DNA binding by FILAMENTOUS FLOWER protein from Arabidopsis thaliana is reduced by EDTA. The Journal of Biological Chemistry. 277(14): 11957-11964.

Kasper, M., Regl, G., Frischauf, A. Aberger, F. 2006. GLI transcription factors: mediators of oncogenic Hedgehog signaling. European Journal of Cancer. 42: 437-445.

Katsamba, P. S., Park, S., Laird-Offringa, I. A. 2002. Kinetic studies of RNA-protein interactions using surface plasmon resonance. Methods. 26: 95-104.

Kawakami, J., Imanaka, H., Yokota, Y., Sugimoto, N. 2000. *In vitro* selection of aptamers that act with $Zn^{2+}$. Journal of Inorganic Biochemistry. 82: 197-206.

Keefe, A., D., Szostak, J., W. 2001. Functional proteins from a random-sequence library. Nature. 410(6829): 715-718.

Kikin, O., D' Antonio, L., Bagga, P. S. 2006. QGRS mapper a web-based server for predicting G-quadruplexes in nucleotide sequences. Nucleic Acids Res. 34: 676-682.

Kim, R. J., Moine, S., Reese, D. K., Bullock, P. A. 2002a. Peptides containing cyclin/cdk-nuclear localization signal motifs derived from viral initiator proteins bind to DNA when unphosphorylated. Journal of Virology. 76(23): 11785-11792.

Kim, S. J., Kim, M. Y., Lee, J. H., You, J. C., Jeong, S. 2002b. Selection and stabilization of the RNA aptamers against the human immunodeficiency virus type-1 nucleocapsid protein. Biochemical and Biophysical Research Communications. 291: 925-931.

Kim, M. Y., Jeong, S. 2003. RNA aptamers that bind the nucleocapsid protein contain pseudoknots. Mol. Cells. 16(3): 413-417.

King, D. J., Bassett, S. E., Li, X., Fennewald, S. A., Herzog, N. K., Luxon, B. A., Shope, R., Gorenstein, D. G. 2002. Combinatorial selection and binding of phophorothioate aptamers targeting human NF-kappa B RelA(p65) and p50. Biochemistry. 41: 9696-9706.

Kinzler, K. W., Ruppert, J. M., Bigner, S. H., Vogelstein, B. 1988. The gli gene is a member of the Kruppel family of zinc finger proteins. Nature. 332(24): 371-374.

Kirthi, N., Savithri, H. S. 2003. A conserved zinc finger motif in the coat protein of *Tomato leaf curl Bangalore virus* is responsible for binding to ssDNA. Arch Virol. 148: 2369-2380.

Kleinjung, F., Klussmann, S., Erdmann, V. A., Scheller, F. W., Fuerste, J. P., Bier, F. F. 1998. High-affinity RNAs as a recognition element in a biosensor. Analytical Chemistry. 70(2): 328-331.

Klug A. 1995. Zinc fingers. FASEB J. 9: 597-604.

Klussmann, S. 1996. Spiegel-design: Identifizierung und Charakterisierung Hochaffiner L-RNA-Molecküle. Dissertation zur Erlangung des Doktorgrades am Fachbereich Chemie der Freien Universität Berlin.

Klussmann, S., Nolte, A., Bald, R., Erdmann, V. A., Fürste, J. P. 1996. Mirror-image RNA that binds D-adenosine. Nature Biotechnology. 14: 1112-1115.

Klussmann, S. 2006. The aptamer handbook. Functional oligonucleotides and their applications. 1. Aufl. Wiley-VCH verlag GmbH & Co. KGaA, Weinheim.

Kochoyan, M., Havel, T. F., Nguyen, D. T., Dahl, C. E., Keutmann, H. T., Weiss, M. A. 1991a. Alternating zinc fingers in the human male associated protein ZFY: 2D NMR structure of an even finger and implications for "jumping-linker" DNA recognition. Biochemistry. 30(14): 3371-86.

Kochoyan, M., Keutmann, H. T., Weiss, M. A. 1991b. Architectural rules of the zinc-finger motif: comparative two-dimensional NMR studies of native and ‘’aromatic-swap’’domains define a ‘’weakly polar switch’’. Proc. Natl. Acad. Sci. USA. 88: 8455-8459.

Koopman, P., Ashworth, A., Lovell-Badge, R. 1991. The ZFY gene family in humans and mice. TIG. 7(4): 132-136.

Kopera, E., Schwerdtle, T., Hartwig, A., Bal, W. 2004. Co(II) and Cd(II) substitute for Zn(II) in the zinc finger derived from the DNA repair protein XPA, demonstrating a variety of potential mechanisms of toxicity. Chem. Res. Toxicol. 17: 1452-1458.

Koster, M., Kuhn, U., *et al*. 1991. Structure, expression and *in vitro* functional characterization of a novel RNA binding zinc finger protein from Xenopus. EMBO J. 10(10): 3087-3093.

Kruger, K., Grabowski, P. J., Zaug, A. J., Gottschling, D. E., Cech, T. R. 1982. Self-splicing RNA: autoexcision and autocyclization of the ribosomal RNA intervening sequence of Tetrahymena. Cell. 31 (1): 147-157.

Kubik, M. F., Bell, C., Fitzwater, T., Watson, S. R., Tasset, D. M. 1997. Isolation and characterization of 2’-fluoro-, 2’-amino-, and 2’-fluoro/amino-modified RNA ligands to human IFN-gamma that inhibit receptor binding. J. Immunol. 159: 259-267.

Kumar, P. K. R., Machida, K., Urvil, P. T., Kakiuchi, N., Vishnuvardhan, D., Shimotohno, K., Taira, K., Nishikawa, S. 1997. Isolation of RNA aptamers specific to the NS3 protein of hepatitis C virus from a pool of completely random RNA. Virology. 237: 270-282.

Kurreck, J. 2008. Therapeutic oligonucleotides. Royal Society of Chemistry. Cambridge. UK.

Lachenmann, M. J., Ladbury, J. E., Phillips, N. B., Narayana, N., Qian, X., Weiss, M. A. 2002. The hidden thermodynamics of a zinc finger. J. Mol. BIol. 316: 969-989.

Ladomery, M., Dellaire, G. 2002. Multifunctional zinc finger proteins in development and disease. Ann. Hum. Genet. 66: 331-342.

Lamla, T., Erdmann, V., A. 2003. Searching sequence space for high-affinity binding peptides using ribosome display. J. Mol. Biol. 329(2): 381-388.

Larabee, J. L., Hocker, J. R., Hanas, J. S. 2005. Cys redox reactions and metal binding of a C2H2 zinc finger. Archives of Biochemistry and Biophysics. 434: 139-149.

Law, W. J., Cann, K. L., Hicks, G. G. 2006. TLS, EWS and TAFI5: a model for transcriptional integration of gene expression. Briefings in Functional Genomics and Proteomics. 5(1): 8-14.

Lebruska, L. L., Maher III, L. J. 1999. Selection and characterization of an RNA decoy for transcription factor NF-kB. Biochemistry. 38: 3168-3174.

Lee, M. S., Gottesfeld, J. M., Wright, P. E. 1991. Zinc is required for folding and binding of a single zinc finger to DNA. FEBS. 279(2): 289-294.

Leva, S., Lichte, A., Burmeister, J., Muhn, P., Jahnke, B., Fesser, D., Erfurth, J., Burgstaller, P., Klussmann, S. 2002. GnRH binding RNA and DNA Spiegelmers: a novel approach toward GnRH antagonism. Chem. Biol. 9: 351-359.

Liu, X., Zhang, D., Cao, G., Yang, G., Ding, H., Liu, G., Fan, M., Shen, B., Shao, N. 2003. RNA aptamers specific for bovine thrombin. J. Mol. Recognitt. 16: 23-27.

Liu, J., Lu, Y. 2006. Fast colorimetric sensing of adenosine and cocaine based on a general sensor design involving aptamers and nanoparticles. Angew. Chem. Int. Ed. Engl. 45: 90-94.

Lu, D., Searles, M., A., Klug, A. 2003. Crystal structure of a zinc-finger-RNA complex reveals two modes of molecular recognition. Nature. 426: 96-100.

Maberley, D. 2005. Pegaptanib for neovascular age-related macular degeneration. Issues Emerg. Health Technol. 1-4.

Mallikaratchy, P., Stahelin, R. V., Cao, Z. H., Cho, W. H., Tan, W. H. 2006. Selection of DNA ligands for protein kinase C-delta. Chem. Commun. 30: 3229-3231.

Maret, W. 2002. Optical methods for measuring zinc binding and release, zinc coordination environments in zinc finger proteins, and redox sensitivity and acitivity of zinc-bound thiols. Methods in Enzymology. 348: 230-237.

Marro, M. L., Daniels, D. A., McNamee, A., Andrew, D. P., Chapman, T. D., Jiang, M. S., Wu, Z. N., Smith, J. L., Patel, K. K., Gearing, K. L. 2005. Identification of potent and selective RNA antagonists of the IFN-gamma-inducible CXCL10 chemokine. Biochemistry. 44: 8449-8460.

Matise, M. P., Joyner, A. L. 1999. Gli genes in development and cancer. Oncogene. 18: 7852-7859.

Matsushima, Y., Matsumura, K., Kitagawa, Y. 1997. Zinc finger like motif conserved in a family of RNA binding proteins. Biosci Biotechnol Biochem. 61(5): 905-906.

Matthews, J. M., Sunde, M. 2002. Zinc fingers-folds for many occasions. IUBMB Life. 54: 351-355.

Matthews, J. M., Kowalski, K., Liew, C. K., Sharpe, B. K., Fox, A. H., Crossley, M., Mackay, J. P. 2000. A class of zinc fingers involved in protein-protein interactions. Eur. J. Biochem. 267: 1030-1038.

Mendez-Vidal, C., Wilhelm, M. T., Hellborg, F., Qian, W., Wiman, K. G. 2002. The p53-induced mouse zinc finger protein wig-1 binds double-stranded RNA with high affinity. Nucleic Acids Res. 30(9): 1991-1996.

Mendonsa, S. D., Bowser, M. T. 2004. *In vitro* selection of high-affinity DNA ligands for human IgE using capillary electrophoresis. Anal. Chem. 76: 5387-5392.

McEntee, K., Weinstock, G. M., Lehman, I. R. 1980. RecA protein-catalyzed strand assimilation: stimulation by Escherichia coli single-stranded DNA-binding protein. Proc. Natl. Acad. Sci. 77(2): 857-861.

McColl, D. J., Honchell, C. D., Frankel, A. D. 1999. Structure-based design of an RNA-binding zinc finger. Proc. Natl. Acad. Sci. USA. 96: 9521-9526.

McKay, D. B., Steitz, T. A. 1981. Structure of catabolite gene activator protein at 2.9 A resolution suggests binding to left-handed B-DNA. Nature. 290 (5809): 744-749.

McManus, M. T., Sharp, P. A. 2002. Gene silencing in mammals by small interfering RNAs. Nature. 3: 737-747.

Michael, S. F., Kilfoil, V. J., Schmidt, M. H., Amann, B. T., Berg, J. M. 1992. Metal binding and folding properties of a minimalist $Cys_2His_2$ zinc finger peptide. Proc. Natl. Acad. Sci. USA. 89: 4796-4800.

Michaud, M., Jourdan, E., Villet, A., Ravel, A., Grosset, C., Peyrin, E. 2003. A DNA aptamer as a new target-specific chiral selector for HPLC. J. Am. Chem. Soc. 125: 8672-8679.

Morrison, A., A., Viney, R., L., Ladomery, M., R. 2008. The post-transcriptional roles of WT1, a multifunctional zinc finger protein. Biochim. Biophys. Acta. 1785(1): 55-62.

Mukhopadhyay, R. 2005. Aptamers are ready for the spotlight. Anal. Chem. 77: 114A-118A.

Murphy, M. B., Fuller, S. T., Richardson, P. M., Doyle, S. A. 2003. An improved method for the *in vitro* evolution of aptamers and applications in protein detection and purification. Nucleic Acids Research. 31(18): e110.

Nakamura, C., Kobayashi, T., Miyake, M., Shirai, M., Miyake, J. 2001. Usage of a DNA aptamer as a ligand targeting microcystin. Mol. Cryst. Liquid Cryst. 371: 369-374.

Nedved, M. L., Moe, G. R. 1994. Cooperative, non-specific binding of a zinc figner peptide to DNA. Nucleic Acids Res. 22: 4705-4711.

Nieuwlandt, D., Wecker, M., Gold, L. 1995. *In vitro* selection of RNA ligands to substance P. Biochemistry. 34 (16): 5651-5659.

Nolte, A., Klussmann, S., Bald, R., Erdmann, V. A., Fürste, J. P. 1996. Mirror-design of L-oligonucleotide ligands binding to L-arginine. Nauture Biotechnology. 14: 1116-1119.

Nolte, A. 1996. Mirror design of oligonucleotide ligands. Dissertation zur Erlangung des Doktorgrades am Fachbereich Chemie der Freien Universität Berlin.

Nolte, R., T. *et al*. 1998. Differing roles for zinc fingers in DNA recognition: structure of a six-finger transcription factor IIIA complex. Proc. Natl. Acad. Sci. USA. 95: 2938-2943.

Nordhoff, E., Krogsdam, A. M., Jorgensen, H. F., Kallipolitis, B. H., Clark, B. F. C., Rpepstorff, P., Kristiansen, K. 1999. Rapid identification of DNA-binding proteins by mass spectrometry. Nature Biotechnology. 17: 884-888.

Oehler, S., Alex, R., Barker, A. 1999. Is nitrocellulose filter binding really a universal assay for protein-DNA interactions. Analytical Biochemistry. 268: 330-336.

Oliphant, A. R., Brandl, C. J., Struhl, K. 1989. Defining the sequence specificity of DNA-binding proteins by selecting binding sites from random-sequence oligonucleotides: analysis of yeast GCN4 protein. Molecular and Cellular Biology. 9(7): 2944-2949.

Omichinski, J. G., Trainor, C., Evans, T., Gronenborn, A. M., Clore, G. M., Felsenfeld, G. 1993. A small single-finger peptide from the ETF GATA-1 binds specifically to DNA as a zinc or iron complex. Proc. Natl. Acad. Sci. 90: 1676-1680.

Omichinski, J. G., Pedone, P. V., Felsenfeld, G., Gronenborn, A. M., Clore, G. M. 1997. The solution structure of a specific GAGA factor-DNA complex reveals a modular binding mode. Nat. Struct. Biol. 4(2): 122-132.

Overington, J. P., Al-Lazikani, B., Hopkins, A. L. 2006. How many drug targets are there? Nat. Rev. Drug Discovery. 5: 993-996.

Pabo, C. O., Lewis, M. 1982. The operator-binding domain of lambda repressor: structure and DNA recognition. Nature. 298 (5873): 443-447.

Palmer, M. S., Berta, P., Sinclair, A. H., Pym, B., Goodfellow, P. N. 1990. Comparison of human ZFY and ZFX transcripts. Proc. Natl. Acad. Sci. 87: 1681-1685.

Page, D. C., Mosher, R., Simpson, E. M., Fisher, E. M., Mardon, G., Pollack, J., McGillivray, B., Chapelle, A., Brown, L. G. 1987. The sex-determining region of the human Y chromosome encodes a finger protein. Cell. 51: 1091-1104.

Park,S. S,, Ko, B. J., Kim, B. G. 2005. Mass spectrometric screening of transcriptional regulators using DNA affinity capture assay. Analytical Biochemistry. 344: 152-154.

Patel, D. J., 1997. Structural analysis of nucleic acid aptamers. Curr. Opin. Chem. Biol. 1: 32-46.

Patel, D. J., Suri, A. K., Jiang, F., Jiang, L. C., Fan, P., Kumar, R. A., Nonin, S. 1997. Structure, recognition and adaptive binding in RNA aptamer complexes. J. Mol. Biol. 272: 645-664.

Pavletich, N. P., Pabo, C. O. 1991 Zinc finger-DNA recognition: crystal structure of a Zif268-DNA complex at 2.1 A. Science. 252: 809-817.

Pavletich, N. P., Pabo, C. O. 1993. Crystal structure of a five-ginger GLI-DNA complex: new perspectives on zinc fingers. Science. 261: 1701-1707.

Pearson, H. 2008. The fate of fingers. Nature. 455: 160-164.

Pedone, P. V., Ghirlando, R., Clore, G. M., Gronenborn, A. M., Felsenfeld, G., Omichinski, J. G. 1996. The single Cys2-His2 zinc finger domain of the GAGA protein flanked by basic residues is sufficient for high-affinity specific DNA binding. Proc. Natl. Acad. Sci. 93: 2822-2826.

Petersen, M., Wengel, J. 2003. LNA: a versatile tool for therapeutics and genomics. Trends Biotechnol. 21: 74-81.

Phillips Jr, G. N., Fox, B. G., Markley, J. L., Volkman, B. F., Bae, E., Bitto, E., Bingman, C. A., Frederick, R. O., McCoy, J. G., Lytle, B. L., Pierce, B. S., Song, J., Twigger, S. N. 2007. Structures of proteins of biomedical interest from the center for eurkaryotic structural genomics. J. Struct Funct Genomics. 8: 73-84.

Picard, B., Wegnez, M. 1979. Isolation of a 7S particle from *Xenopus laevis oocytes*: a 5S RNA-protein complex. Proc. Natl. Acad. Sci. USA. 76: 241-245.

Pieler, T., Guddat, U., Oei, S. L., Erdmann, V. A. 1986. Analysis of the RNA structural elements involved in the binding of the transcription factor III A from *Xenopus laevis*. Nucleic Acids Res. 14(15): 6313-6326.

Pieler, T., Erdmann, V. A., Appel, B. 1984. Structural requirements fort he interaction of 5S rRNA with the eukaryotic transcription factor IIIA. Nucleic Acids Res. 12(22): 8393-8406.

Pileur, F., Andreola, M. L., Dausse, E., Michel, J., Moreau, S., Yamada, H., Gaidamakov, S. A., Crouch, R. J., Toulme, J. J., Cazenave, C. 2003. Selective inhibitory DNA aptamers of the human RNase H1. Nucleic Acids Res. 31: 5776-5788.

Poschner, B. C., Reed, J., Langosch, D., Hofmann, M. W. 2007. An automated application for detconvolution of circular dichroism spectra of small peptides. Analytical Biochemistry. 363: 306-308.

Predki, P. F., Sarkar, B. 1994. Metal replacement in zinc finger and its effect on DNA binding. Environ Health Perspect. 102(3): 195-198.

Proske, D., Gilch, S., Wopfner, F., Schatzl, H. M., Winnacker, E. L., Famulok, M. 2002. Prion-protein-specific aptamer reduces PrPSc formation. Chem-Biochemstry. 3: 717-725.

Reed J., Reed, T. A. 1997. A set of constructed type spectra for the practical estimation of peptide secondary structure from circular dichroism. Analytical Biochemistry. 254: 36-40

Rhie, A., Kirby, L., Sayer, N., Wellesley, R., Disterer, P., Sylvester, I., Gill, A., Hope, J., James, W., Tahiri-Alaoui, A. 2003. Characterization of 2'-fluoro-RNA aptamers that bind preferentially to disease-associated conformations of prion protein and inhibit conversion. J. Biol. Chem. 278: 39697-39705.

Rhodes, A., Deakin, A., Spaull, J., Coomber, B., Aitken, A., Life, P., Rees, S. 2000. The generation and characterization of antagonist RNA aptamers to human oncostatin M. J. Biol. Chem. 275: 28555-28561.

Rhodes, A., Smithers, N., Chapman, T., Parsons, S., Rees, S. 2001. The generation and characterization of antagonist RNA aptamers to MCP-1. FEBS Lett. 506: 85-90.

Roberts, R. W. and Szostak, J. W. 1997. RNA-peptide fusions for the *in vitro* selection of peptides and proteins. Proc. Natl. Acad. Sci. USA. 94: 12297-12302.

Romig, T. S., Bell, C., Drolet D. W. 1999. Aptamer affinity chromatography: combinatorial chemistry applied to protein purification. J. Chromatography. B. 731: 275-284.

Rosenbauer, F., Tenen, D. G., 2007. Transcription factors in myeloid development: balancing differentiation with transformation. Nature. 7: 105-117.

Ruckman, J., Green, L. S., Beeson, J., Waugh, S., Gillette, W. L., Henniger, D. D., Claesson-Welsh, L., Janjic, N. 1998. 2'-fluropyrimidine RNA-based aptamers to the 165-amino acid form of vascular endothelial growth factor (VEGF(165))-inhibition of receptor binding and VEGF-induced vascular permeability through interactions requiring the exon 7-encoded domain. J. Biol. Chem. 273: 20556-20567.

Rusconi, C. P., Yeh, A., Lyerly, H. K., Lawson, J. H., Sullenger B. A. 2000. Blocking the initiation of coagulation by RNA aptamers to factor VIIa. Thromb Haemost. 84(5): 841-848.

Rusconi C. P., Scardino, E., Layzer, J., Pitoc, G. A., Ortel, T. L., Monroe, D., Sullenger, B. A. 2002. RNA aptamers as reversible antagonists of coagulation factor IXa. Nature. 419(6902): 23-24.

Saito, T., Tomida, M. 2005. Generation of inhibitory DNA aptamers against human hepatocyte growth factor. DNA Cell Biol. 24: 624-633.

Sakaguchi, K., Appella, E., Omichinski, J. G., Clore, G. M., Gronenborn, A. M. 1991. Specific DNA binding to a major histocompatibility complex enhancer sequence by a synthetic 57-residue double zinc finger peptide from a human enhancer binding protein. The Journal of Biological Chemistry. 266: 7306-7311.

Sambrook, J., Russell, D. W. 2001. Molecular Cloning. 3rd edn. Cold Spring Harbor Laboratory Press. New York.

SantaLucia, J. Jr. 1998. A unified view of polymer, dumbbell, and oligonucleotide DNA nearest-neighbor thermodynamics. Proc. Natl. Acad. Sci. USA. 95: 1460-1465.

Seiwert, S. D., Nahreini,, T. S., Aigner, S., Ahn, N. G., Uhlenbeck, O. C. 2000. RNA aptamers as pathway-specific MAP kinase inhibitors. Chem. Biol. 7: 833-843.

Sevilimedu, A., Shi, H., Lis, J. T. 2008. TFIIB aptamers inhibit transcription by perturbing PIC formation at distinct stages. Nucleic Acids Res. 36(9): 3118-3127.

Schmidt, K. S., Borkowski, S., Kurreck, J., Stephens, A. W., Bald, R., Hecht, M., Friebe, M., Dinkelborg, L., Erdmann, V. A. 2004. Application of locked nucleic acids to improve aptamer in vivo stability and targeting function. Nucleic Acids Res. 32: 5757-5765.

Schneider, D., Tuerk, C., Gold, L. 1992. Selection of high affinity RNA ligands to the bacteriophage R17 coat protein. J. Mol. Biol. 228: 862-869.

Schneider, D., Gold, L., Platt, T. 1993. Selective enrichment of RNA species for right binding to *Escherichia coli* rho factor. FASEB J. 7: 201-207.

Schuh. R., Aicher, W., Gaul, U. 1986. A conserved family of nuclear proteins containing structural elements of the finger protein encoded by Krüppel, a Drosophila segmentation gene. Cell. 47: 1025-1032.

Srisawat, G. A., Engelke, D. R. 2001. Streptavidin aptamers: affinity tags for the study of RNAs and ribonucleoproteins. RNA. 7: 632-641.

Stark, B., C., Kole, R., Bowman, E., J., Altman, S. 1978. Ribonuclease P. an enzyme with an essential RNA component. Proc. Natl. Acad. Sci. USA. 75(8): 3717-3721.

Stoltenburg, R., Reinemann, C., Strehlitz, B. 2005. FluMag-*SELEX* as an advantageous method for DNA aptamer selection. Anal. Bioanal. Chem. 383: 83-91.

Stoltenburg, R., Reinemann, C., Strehlitz, B. 2007. *SELEX*-a (r)evolutionary method to generate high-affinity nucleic acid ligands. Biomolecular Engineering. 24(4): 381-403.

Stockley, P. G. 2001. Filter-binding assays. Methods Mol Biol. 148: 1-11.

Stormo, G. D., Fields, D. S. 1998. Specificity, free energy and information content in protein-DNA interactions. TIBS. 23: 109-113.

Tahiri-Alaoui, A., Frigotto, L., Manville, N., Ibrahim, J., Romby, P., James, W. 2002. High affinity nucleic acid aptamers for streptavidin incorporated into bi-specific capture ligands. Nucleic Acids Res. 30(10): e45

Takemura, K., Wang, P., Vorberg, I., Surewicz, W., Priola, S. A., Kanthasamy, A., Pottathil, R., Chen, S. G., Sreevatsan, S. 2006. DNA aptamers that bind to PrPC and not PrPSc show sequence and structure specificity. Exp. Biol. Med. 231: 204-214.

Terunuma, A., Shiba, K., Noda, T. 1997. A novel genetic system to isolate a dominant negative effector on DNA-binding activity of Oct-2. Nucleic Acids Res. 25(10): 1984-1990.

Theunissen, O., Rudt, F., Guddat, U., Mentzel, H., Pieler, T. 1992. RNA and DNA binding zinc fingers in Xenopus TFIIIA. Cell. 71(4): 679-690.

Thompson, J. D., Higgins, D. G., Gibson, T. J. 1994. CLUSTAL W: improving the sensitivity of progressive multiple sequence alignment through sequence weighting, position-specific gap penalties and weight matrix choice. Nucleic Acids Res. 22(22): 4673-4680.

Tuerk, C., Gold, L. 1990. Systematic evolution of ligands by exponential enrichment: RNA ligands to bacteriophage T4 DNA polymerase. Science. 249: 505-510.

Tuerk, C., MacDougal, S., Gold, L. 1992. RNA pseudoknots that inhibit human immunodeficiency virus type 1 reverse transcriptase. Proc. Natl. Acad. Sci. USA. 89: 6988-6992.

Tucker, C. E., Chen, L. S., Judkins, M. B., Farmer, J. A., Gill, S. C., Drolet, D. W. 1999. Detection and plasma pharmacokinetics of an anti-vascular endothelial growth factor oligonucleotide-aptamer (NX1838) in rhesus monkeys. J. Chromatogr. B. 732: 203-212.

Tupler, R., Perini, G., Green, M. R. 2001. Expressing the human genome. Nature. 409: 832-833.

Vater, A., Jarosch, F., Buchner, K., Klussmann, S. 2003. Short bioactive Spiegelmers to migraine-associated calcitonin gene-related peptide rapidly identified by a novel approch: tailored-*SELEX*. Nucleic Acids Res. 31(21): e130.

Vogelstein, B., Kinzler, K. W., 2004. Cancer genes and the pathways they control. Nature Medicine. 10(8): 789-799.

Wadman, I. A., Osada, H., Grütz, G. G., Agulnick, A. D., Westphal, H., Forster, A., Rabbitts, T. H. 1997. The LIM-only protein Lmo2 is a bridging molecule assembling an erythroid, DNA-binding complex which includes the TAL1, E47, GATA-1 and Ldb1/NLI proteins. The EMBO Journal. 16 (11): 3145-3157.

Weiss, M. A., Mason, K. A., Dahl, C. E., Keutmann, H. T. 1990a. Alternating zinc-finger motifs in the human male-associated protein ZFY. Biochemistry. 29 (24): 5660-5664.

Weiss, M. A., Keutmann, H. T. 1990b. Alternating zinc finger motifs in the male-associated protein ZFY: defining architectural rules by mutagenesis and design of an "aromatic swap" second-site revertant. Biochemistry. 29: 9808-9813.

Weiss, S., Proske, D., Neumann, M., Groschup, M. H., Kretzschmar, H. A., Famulok, M., Winnacker, E. L. 1997. RNA aptamers specifically interact with the prion protein PrP. J. Virol. 71(11): 8790-8797.

Wernig, M., Zhao, J. P., Pruszak, J., Hedlund, E., Fu, D., Soldner, F., Broccoli, V., Constantine-Paton, M., Isacson, O., Jaenisch, R. 2008. Neurons derived from reprogrammed fibroblasts functionally integrate into the fetal brain and improve symptoms of rats with Parkinson's disease. PNAS. 105 (15): 5856-5861.

White, R., Rusconi, C., Scardino, E., Wolberg, A., Lawson, J., Hoffman, M., Sullenger, B. 2001. Generation of species cross-reactive aptamers using 'toggle' *SELEX*. Mol. Ther. 4: 567-574.

White, R. R., Shan, S., Rusconi, C. P., Shetty, G., Dewhirst, M. W., Kontos, C. D., Sullenger, B. A. 2003. Inhibition of rat corneal angiogenesis by a nuclease-resistant RNA aptamer specific for angiopoietin-2. Proc. Natl. Acad. Sci. USA. 100(9): 5028-5033.

Wiegend, T. W., Williams, P. B., Dreskin, S. C., Jouvin, M. H., Kinet, J. P., Tasset, D. 1996. High-affinity oligonucleotide ligands to human IgE inhibit binding to Fc epsilon receptor I. J. Immunol. 157: 221-230.

Williams, K. P., Bartel, D. P. 1995. PCR product with strands of unequal length. Nucleic Acids Res. 23(20): 4220-4221.

Williams, K. P., Liu, X. H., Schumacher, T. N., Lin, H. Y., Ausiello, D. A., Kim, P. S., Bartel, D. P. 1997. Bioactive and nuclease-resistant L-DNA ligand of vasopressin. Proc. Natl. Acad. USA. 94: 11285-11290.

Wilson, D. S., Szostak, J. W. 1999. *In vitro* selection of functional nucleic acids. Annu. Rev. Biochem. 68: 611-647.

Wlotzka, B., Leva, S., Eschgfäller, B., Burmeister, J., Kleinjung, F., Kaduk, C., Muhn, P., Hess-Stumpp, H., Klussmann, S. 2002. *In vivo* properties of an anti-GnRH Spiegelmer: an example of an oligonulceotide-based therapeutic substance class. Proc. Natl. Acad. Sci. USA. 99(13): 8898-8902.

Wolfe, S. A., Nekludova, L., Pabo, C. O. 1999. DNA recognition by $Cys_2His_2$ Zinc finger proteins. Annu. Rev. Biophys. Biomol. Struct. 3: 183-212.

Wurster S. E., Maher III, L. J. 2008. Selection and characterization of anti-NF-kappaB p65 RNA aptamers. RNA. 14(6): 1037-1047.

Xu W., Ellington, A. D. 1996. Anti-peptide aptamers recognize amino acid sequence and bind a protein epitope. Proc. Natl. Acad. Sci. USA. 93: 7475-7480.

Valencia, C., A., Ju, W., L, R. 2007. Matrin 3 is a $Ca^{2+}$/calmodulin-binding protein cleaved by caspases. Biochemical and Biophysical Research Communications. 361: 281-286.

Yamamoto, R., Katahira, M., Nishikawa, S., Baba, T., Taira, K., Kumar, P. K. 2000. A novel RNA motif that binds efficiently and specifically to thte Ttat protein of HIV and inhibits the trans-activation by Tat of transcription *in vitro* and *in vivo*. Genes Cells. 5(5): 371-388.

Yamanoto-Fujita, R., Kumar, P. K. 2005. Aptamer-derived nucleic acid oligos: applications to develop nucleic acid chips to analyze proteins and small ligands. Anal. Chem. 77(17): 5460-5466.

Yaneva, M., Tempst, P. 2003. Affinity capture of specific DNA-binding proteins for mass spectrometric identification. Anal. Chem. 2003. 75: 6437-6448.

Yates J. R. 3rd. 2000. Mass spectrometry. From genomics to proteomics. Trends Genet. 16(1):5-8.

Ylera, F, Lurz, R., Erdmann, V. A., Fürste, J. P. 2002. Selection of RNA Aptamers to the Alzheimer's disease amyloid peptide. Biochemical and Biophysical Research Communications. 290: 1583-1588.

Zhai, G., Iskandar, M., Barilla, K., Romaniuk, P. J. 2001. Characterization of RNA aptamer binding by the wilms' tumor suppressor protein WT1. Biochemistry. 40: 2032-2040.

Zhan, L. S., Zhuo, H. L., Wang, H. Z., Peng, J. C., Wang, Q. L. 2005. Screening and characterization of aptamers of hepatitis C virus NS3 helicase. Progr. Biochem. Biophys. 32: 245-250.

Zhao, X., Shi, H., Sevilimedu, A., Liachko, N., Nelson, H. C. M., Lis, J. T. 2006. An RNA aptamer that interferes with the DNA binding of the HSF transcription activator. Nucleic Acids Res. 34(13): 3755-3761.

Zucker, M. 2003. Mfold web server for nucleic acid folding and hybridization prediction. Nucleic Acids Res. 31(13): 3406-3415.

# 9 Appendix

## 9.1 Materials

### 9.1.1 Devices and Consumption Materials

| | |
|---|---|
| Acute Wagon | Mettler AC 88, DeltaRange® |
| Agarose Gel Chamber | BioRad, Italy |
| Analytical Balance | Mettler AC 88 |
| Autoclave | Sterico 500-D. 150 l |
| Biacore X | Biacore AB |
| Cabinet Dryer | Heraeus |
| CD Spectropolarimeter J-600 | Jasco |
| Cool Centrifuge | Model J2-21, Beckman |
| Centrifuge Biofuge 13 | Heraeus |
| Centrifuge J2-21 | Beckman |
| Developer G150 | Agfa-Gefaert N. V. |
| Dewar Vessel | Hampton Research/Roth |
| Disposable Cuvettes 1x0.4x4.5 cm | Müller Ratiolab |
| Filters 0.45 uM, 0.2 uM | Millipore |
| Filter Holder | Sartorius, Fisher |
| Fixer G350 | Agfa-Gefaert N. V. |
| Fluor-Coated (60 F254) TLC Plate | Merck |
| Freezer -20ºC | Bosch |
| Freezer -80ºC | Heraeus |
| Freezer 4ºC | Bosch |
| Gel Document | Gel Dol 2000, Bio-Rad |
| Gel Dryer | Biometra |
| Gel Electrophoresis System | Renner GmBH |
| Gel Filtration Columns (NAP-5, 10 Column) | Pharmacia Biotech |
| Gel Filtration Columns (Nick™ Column) | Pharmacia Biotech |
| Gloves | Neolab |
| Glass Plate | Glaserei Graw & Meibert |
| Heating Cabinet | Heraeus |
| HPLC Instrument | Thermo Separation Products |
| Incubator Shaker | G25, New Brunswick Scientific, USA |
| Image Eraser | Molecular Dynamics |
| Kimwipes® | Kimberly-Clark |
| Lyophilizer Speed Vac | SC110AR, Savant |
| Magnetic Particle Seperator | Roche |
| Magnetic Stirrer | IKA-Combimag RCT |
| MALDI-TOF/TOF-MS Ultraflex II | Bruker Daltonics |
| Membrane Vacuum Pump | Vacuubrand |
| Microcon YM-10, 30, 50 Spin Filters | Millipore |
| Microwave ER-7720W | Toschiba |
| Mini-Spin Column Kit | Pierce |
| Nap 5, 10, 25 Columns | GE Healthcare |
| Nick Columns | GE Healthcare |
| Nitrocellulose Membrane 0.45 uM, 0.2 uM | Millipore |

| | |
|---|---|
| Oil Pump | Alcatel 10004 A C |
| PAA Gel Chamber | IBI |
| PAA Gel Chamber | Renner GMBH, Dannstadt |
| Petri Dishes | Greiner |
| PCR Apparatus | Biometra |
| PCR Tubes | Roth |
| PerfectBlue Semi-Dry Electro-blotter | PeQLab |
| pH-Meter | CyberScan 500 |
| Phosphorimager Exposure Cassette | Molecular Dynamics |
| Phosphorimager Storm 840 | Molecular Dynamics |
| Phosphor Screen | Molecular Dynamics |
| Pipettes P2, P20, P200, P2000 | Eppendorf |
| Pipette Tips | Greiner bio-one |
| Pipette Tips with Filters | Sorenson |
| Plate Sealing Film | American National Can TM |
| Plexis Container | Nalgene |
| Plexis Shield | Jencons |
| Power Supply | ECPS 3000/150, Pharmacia |
| PVDF Western Blotting Membrane | Roche |
| Purest Water Installation | Milli-Q, Millipore |
| Quartz Cuvette for Photometer | Hellma |
| Reaction Tubes, 0.5, 1.5, 2ml, Siliconized | Roth |
| Reaction Tubes 1.5 ml, 2 ml | Eppendorf |
| Reaction Tubes, 2 ml | Eppendorf |
| Reaction Tubes, 12 ml | Greiner Bio-one |
| Reaction Tubes, 50 ml | Greiner Bio-one |
| Refrigerated Vapor Trap | RVT400, Savant |
| Rotor JA-17 | Beckmann |
| Sensor Chip SA | Biacore AB |
| Shaker (Isotope Laboratory) | Yellow line, FHG-VERW |
| Syringe Filter 0.22µm | Roth |
| Syringe 2-50 ml | BD, Henke-Sass |
| Syringe Hypodermic Needle | B. Braun |
| Scintillation Counter | LS 6000, Beckman |
| Scintillation Tubes 20 ml Polyvial | Zinsser Analytic |
| Sterilizer | Typ400EP-Z, Varioklav® |
| Table-top Centrifuge | Eppendorf |
| Thermomixer | Eppendorf |
| UV-Visible Spectrophotometer | UV-1202, Shimadzu |
| UV Monitor Reprostar II | CAMAG |
| Vortex | Scientific Industries, Vortex Genie 2 |
| Wagon | Mettler PC4400, DeltaRange® |
| Water Bath | B. Braun |
| X-ray Film Cassette | Kodak |

### 9.1.2 Chemical Materials

| | |
|---|---|
| Acetic Acid | J. T. Baker |
| Acetonitril (HPLC grade) | Merck |
| Acetonitril (DNA synthesis grade) | Applied Biosystems |

| | |
|---|---|
| Acrylamide | Roth |
| Agar | Gibco BRL |
| Agarose | Roth |
| Ammonium Bicarbonate | Fluka |
| APS | Roth |
| ATP (adenosine 5’-triphosphate) | Promega |
| [γ–$^{32}$P] ATP | Amersham |
| Biotin | Sigma |
| Biotinyl-Angiotensin I/II (1-7) | Bachem |
| Boric Acid | Merck |
| Bradford Reagent | Roth |
| Bromphenol Blue | Merck |
| BSA | Sigma |
| Cadmium Chloride | Aldrich |
| Calcium Chloride | Merck |
| Cobalt Chloride | AppliChem |
| Coomassie | Roth |
| CTP(cytidine 5’-triphosphate) | Promega |
| [α–$^{32}$P]-dCTP | Amersham |
| EDTA | Merck |
| DMEM | PAA |
| DNA Ladder (100 bp) | BioLabs |
| DNA Ladder (25 bp) | Promega |
| dNTPs | Rapidozym |
| DTT | BD |
| Ethanol | Merck |
| Ethidium Bromide | Fluka |
| FKS | PAA |
| HEPES | Sigma Roth |
| Hydrochloride acid | Aldrich |
| LB-Agar | LAB M |
| GenTherm$^{TM}$ DNA Polymerase | Rapidozym |
| L-Glutamine | PAA |
| Glycerol | Merck |
| Glycine | Fermentas |
| Glycogen | Fermentas |
| GTP (Guanosine 5’-triphosphate) | Promega |
| Guanidine HCl | Roth |
| Hydrochloric Acid | Merck |
| Iodacetamide | Sigma |
| Magnesium Chloride | Merck |
| Methanol | Merck |
| Milk Powder (Blotting grade) | Roth |
| NEAA | PAA |
| NP-40 | Merck |
| PBS | Invitrogen |
| Penicillin/Streptomycin | PAA |
| Phenol/Chloroform/Isoamylalcohol | Roth |
| Ponceau Red | Roth |
| Potassium Chloride | Merck |
| Potassium Hydroxide | Merck |

| | |
|---|---|
| Poly(dI-dC) | Amersham |
| Protein Marker | Roth, Invitrogen |
| Protease Inhibitors | Sigma |
| Recombinant RNasin Ribonuclease Inhibitor | Promega |
| Reverse Transcriptase Enhancer | PeQlab |
| Roti-Blue-P (Colloidal Coomassie Staining) | Roth |
| SDS | Pierce |
| Sodium Acetate | Riedel de Haen |
| Sodium Chloride | Merck |
| Sodium Hydroxide | Aldrich |
| Streptavidin | BioLabs |
| TBE Buffer | Roth |
| TCEP, tri(2-carboxyethyl)phosphine | Pierce |
| TEMED | Roth |
| Tween 20 | Roth |
| Trifluoroacetate | Roth |
| Tris-HCl | Roth |
| Tris(hydroxymethyl)-Aminomethane | Roth |
| Triton X-100 | Boehringer Mannheim |
| t-RNA | Roche |
| Urea | Roth |
| UTP (Uridine 5'-triphosphate) | Promega |
| Xylencyanol | Serva |
| Zinc Chloride | Merck |

### 9.1.3 Others

| | |
|---|---|
| Anti-ZFX Serum | Dr. Boris Reizis, CUMC, USA |
| Goat anti Rabbit-HRP-Conjugate | Pierce |
| JM109 Competent Cell | Promega |
| Neutravidin™ Agarose | Pierce |
| NucleoSpin® Extract II Columns | MACHEREY-NAGEL |
| pGEM®-T Easy Vector System | Promega |
| Roti®-Blue (Colloidal Coomassie Staining ) | Roth |
| StrataClean™ Resin | Stratagene |
| Streptavidin Magnetic Beads | Dynal |
| ZNF593 Recombinant Protein | Genway, USA |
| SuperSignal® West Dura Extended Duration Substrate | Pierce |

### 9.1.4 Enzymes

| | |
|---|---|
| Taq DNA Polymerase | BioLabs |
| Lambda Exonuclease | Fermentas |
| GenThermTM DNA Polymerase | Rapidozym |
| T4 DNA Ligase | BioLabs |
| T4 Polynucleotide Kinase | Fermentas |
| Trypsin (From bovine pancreas) | Roche |

### 9.1.5 Buffers

***Binding Buffer (5x)***

100 mM Hepes
10 mM $MgCl_2$
250 mM KCl
3 mM TCEP
25% Glycerol
250 µM $ZnCl_2$
0.25 mg/ml tRNA
pH 7.5

***Blotto (Blocking Buffer)***

1x TTBS
5% or 10% (w/v) Trockenmilch

***Buffer A for Cell Extraction (1x)***

10 mM Hepes, pH=7.9
1.5 mM $MgCl_2$
10 mM KCl
0.5 mM DTT
Including Protease Inhibitors:
-Aprotinin 100 µg/ml
-Leupeptin 5 µg/ml
-Pepstatin 1 µg/ml
-PMSF 0.5 mM

***Buffer C for Cell Extraction (1x)***

20 mM Hepes, pH=7.9
1.5 mM $MgCl_2$
420 mM NaCl
0.2 mM EDTA
25% (v/v) Glycerol
Including Protease Inhibitors:
-Aprotinin 100 µg/ml
-Leupeptin 5 µg/ml
-Pepstatin 1 µg/ml
-PMSF 0.5 mM

***Coomassie Staining Solution***

20 ml Methanol
60 ml $H_2O$
20 ml Roti®-Blue (5x)

***Loading Buffer for Agarose Gel (6x)***

0.4% Orange G
0.03% Bromphenolblau
0.03% Xylencyanol
15% Ficoll®400
10 mM Tris-HCl (pH 7.5)
50 mM EDTA (pH 8.0)

***Digestion Buffer for Lambda Exonuclease (10x)***

670 mM glycine-KOH (pH 9.4)
25 mM $MgCl_2$
0.1% Triton X-100

***Loading Buffer for Urea PAGE (2x)***

2x TBE
16 M Urea
0.04% Bromphenolblau
0.04% Xylencyanol

***Loading Buffer for Laemmli SDS Protein Gel (2x)***

125 mM Tris, pH 6.8
20% Glycerol
0.1% Bromphenolblau
4% (w/v) SDS
10% (v/v) ß-Mercaptoethanol
0.02% (w/v) Bromphenolblau

***PCR Reaction Buffer (10x)***

160 mM $(NH_4)_2SO_4$
670 mM Tris-HCl
0.1% Tween 20
pH 8.8

***Running Buffer (Biacore) (1x)***

20 mM Hepes
150 mM KCl
50 µM $ZnCl_2$
2 mM $MgCl_2$
50 mM NaCl
0.1 mM TCEP
pH 7.5

***SDS Lysis Buffer (2x)***

125 mM Tris pH 6.8
4% (w/v) SDS
20% (v/v) Glycerol
0.1% Bromphenolblau
100 mM DTT

***SDS Gel Electrophoresis Buffer (5x)***

125 mM Tris
1250 mM Glycine (pH 8.3)
0.5% (w/v) SDS

***SELEX Buffer A (5x)***

10 mM $MgCl_2$
350 mM KCl
100 mM Hepes (pH 7.5)
3 mM TCEP
25% Glycerol
250 µM $ZnCl_2$
0.25% Triton X-100

***SELEX Buffer B (5x)***

10 mM $MgCl_2$
750 mM KCl
100 mM Hepes (pH 7.5)
3 mM TCEP
25% Glycerol
250 µM $ZnCl_2$
0.025% Triton X-100

***Semidry Buffer (Blot Buffer)***

47.9 mM Tris-HCl
38.9 mM Glycine
0.038% (w/v) SDS
20% (v/v) Methanol

***TAE Buffer (10x)***
242 g Tris
57.1 ml Acetic Acid
100 ml 0.5 M EDTA, pH 8.0
Add 1 l with dd. $H_2O$

***TBE Buffer (10x)***

108 g Tris
37.2 g Boric Acid
40 ml 0.5 M EDTA, pH 8.0
Add 1 l with dd. $H_2O$

***TBS Buffer (10x)***

20 mM Tris-HCl
150 mM NaCl
pH 7.5

***T4 DNA Ligase Buffer (10x)***

500 mM Tris-HCl, pH 7.5
100 mM $MgCl_2$
100 mM DTT
10 mM ATP
250 µg/ml BSA

***ThermoPol PCR Buffer (10x)***

100 mM KCl
100 mM $(NH_4)_2SO_4$
200 mM Tris-HCl
20 mM $MgSO_4$
1% Triton X-100
pH 8.8

***TTBS Buffer (1x)***

1x TBS
0.1% Tween 20

***T4 Polynucleotide Kinase Buffer (10x)***

500 mM Tris-HCl, pH 7.6
100 mM $MgCl_2$
50 mM DTT
1 mM Spermidine
1 mM EDTA

### 9.1.6 Media

***LB-Agar Plate***

15 g/l Agar
10 g/l Tryptone
5 g/l Yeast Extract
10 g/l Sodium Chloride
pH 7.0 ± 0.2
Sterilization: 15 min, 121°C
Add ampicillin at ~47°C
(End Conc. 100 µg/ml)
Fill into Sterilized Petri Dishes

***SOC Medium***

0.5% (w/v) Yeast Extract
2.0% (w/v) Tryptone
10 mM NaCl
2.5 mM KCl
Sterilization: 15 min, 121°C
Add 20 mM $MgCl_2$
Add 20 mM Glucose (Sterile Filtrated)
Adjust pH to 7.0 with NaOH

***M1 Medium***

500 ml DMEM (Low Glucose)
50 ml FKS (-10%)
5 ml 200 mM L-Glutamin
5 ml (100x) NEAA
5 ml (100x) Penicillin/Streptomycin

### 9.1.7 Randomized Pool Sequences and Primers

*Randomized Pool (90 nt):*

5'-d[GCGAATTGGGTACCGCATCC-$N_{50}$-GAATTCTGCAGGATCCGCCC]-3'

*Forward Primer (20 nt):*

5´-d[GCGAATTGGGTACCGCATCC]-3´

*Forward Primer (5'-Modified with Biotin; 20 nt):*

5´-d[(Biotin)GCGAATTGGGTACCGCATCC]-3´

*Reverse Primer (20 nt):*

5´-d[GGGCGGATCCTGCAGAATTC]-3´

*Reverse Primer-terminator (41 nt):*

5´-d[AAAAAAAAAAAAAAAAAAAAXGGGCGGATCCTGCAGAATTC]-3´

X: Hexaethyleneglycol (HEGL); $HOC_2H_4OC_2H_4OC_2H_4OC_2H_4OC_2H_4OH$

*ReverseRP Primer (5'-Modified with Phosphate; 20 nt):*

3'-d[CTTAAGACGTCCTAGGCGGG(Phosphate)]-5'

*pUC/M13 Primer for Sequencing (24 nt):*

5’-d[CCGCAGGGTTTTCCCAGTCACGAC]-3’

### 9.1.8 Peptide and Protein Targets

*ZFY*: Btn-Ahx-KTYQCQYCEKRFADSSNLKTHIKTKHSKEK-Amide

*GLI*: Btn-Ahx-KPYVCKLPGCTKRYTDPSSLRKHVKTVHG

*ZNF593*:

MKAKRRRPDLDEIHRELRPQGSARPQPDPNAEFDPDLPGGGLHRCLACARYFIDST
NLKTHFRSKDHKKRLKQLSVEPYSQEEAERAAGMGSYVPPRRLAVPTEVSTEVPE
MDTST

The region of zinc finger is underlined.

*Control Peptide:* Biotin-Ahx-RPMMHFGNDWEDRYYRENMNRYP

## 9.2 Abbreviations

| | |
|---|---|
| 3D | three dimensional |
| A | adenosin |
| $A_{260}$ | absorption at λ = 260 nm |
| Ac | acetate |
| ACN | acetonitrile |
| AD | activation domain |
| Ahx | 6-aminohexanoic acid |
| Amp | ampicillin |
| APS | ammonium persulfate |
| ATP | adenosine 5’-triphosphate |
| a.a. | amino acids |
| bidist. | bidistilled water |
| bp | base pair |
| Btn | biotin |
| c | concentration |
| °C | temperature in degrees Celsius |
| Cal. | calculated |
| Conc. | concentration |
| CD | circular dichroisum |
| cDNA | complementary DNA |
| CE | cell extraction |
| CGRP | calcitonin gene-related peptide |
| Ci | curie, 1 Ci = 37 MBq |
| CP | cell pellet |

| | |
|---|---|
| cpm | counts per minute |
| CTL. | cell total lysate |
| CTP | cytosine 5’-triphosphate |
| Da | dalton |
| DAD | diode-array detector |
| DBPB | dna binding protein B |
| DMSO | dimethylsulfoxide |
| DNA | deoxyribonucleic acid |
| DNase | desoxyribonuclease |
| dNTP | deoxyribonucleotide triphosphate |
| ds | double-stranded |
| DTT | dithiothreitol |
| ε | extinction coefficient |
| *E. coli* | *Escherichia coli* |
| EDTA | ethylenediaminetetraacetic acid |
| EtBr | ethidium bromide (3, 8-diamino-5-ethyl-6-phenyl phenanthridinium bromide) |
| fig. | figure |
| FUS | fusion gene in myxoid liposarcoma |
| g | gram |
| G | guanosine |
| GAR-HRP | goat anti rabbit-horseradish peroxidase |
| GDP | guanosine 5’-diphosphate |
| GLI | Glioma-associated oncogene |
| GnRH | gonadotropin-releasing hormone |
| GTP | guanosine 5’-triphosphate |
| h | hour |
| HEPES | 4-(2-hydroxyethyl)piperazine-1-ethanesulfonic acid |
| HIV | human immunodeficiency virus |
| hnRNP K | heterogeneous nuclear ribonucleoprotein K |
| HPLC | high performance liquid chromatography |
| $K_d$ | dissociation constant |
| l | liter |
| m | meter |
| M | mol/l, molar |
| MALDI TOF | matrix-assisted laser desorption/ionization time of flight |
| min | minute(s) |
| mol | mole(s) |
| mRNA | messenger ribonucleic acid |
| MRW | mean residue weight |
| MS | mass spectrometry |
| NE | nuclear extraction |
| NMR | nuclear magnetic resonance |
| N/OFQ | nociceptin/orphanin FQ |
| nt | nucleotide |
| NTP | nucleotide triphosphate |
| OD | optical density |
| PAGE | polyacrylamide gel electrophoresis |
| PCR | polymerase chain reaction |
| PK | protein kinase |
| PMF | peptide mass fingerprinting |

| | |
|---|---|
| rcf | relative centrifugal force |
| RBP56 | rna binding protein 56 |
| RNA | ribonucleic acid |
| rRNA | ribosomal ribonucleic acid |
| rpm | rotations per minute |
| RT | reverse transcription |
| RT | room temperature |
| RT | retention time |
| SDS | sodium dodecyl sulfate |
| s | second |
| SND1 | staphylococcal nuclease domain-containing protein 1 |
| ss | single-stranded |
| T | temperature |
| T | thymine |
| t | time |
| Tab. | table |
| TAE | tris-acetic acid-EDTA |
| TBE | tris-borate-EDTA |
| TCEP | tris(2-carboxyethyl)phosphine |
| TEMED | N,N,N',N'-tetramethylethylenediamine |
| TF | transcription factor |
| TLS | translocated in liposarcoma-associated protein |
| Tris | tris-(hydroxymethyl-)aminomethane |
| TTF | transcription termination factor |
| tRNA | transfer ribonucleic acid |
| U | units of enzymatic activity |
| U | uridine |
| µM | micro-molar |
| UV | ultra violet |
| V | volt (s) |
| V | volume |
| v/v | volume per volume |
| W | watt (s) |
| WT1 | wilm's tumor suppressor gene |
| w/v | weight per volume |
| ZFP | zinc finger protein |
| ZFY | zinc finger Y-chromosomal protein |
| Zf | zinc finger |

***Prefixes of units:***

| | |
|---|---|
| p (pico) | $10^{-12}$ |
| n (nano) | $10^{-9}$ |
| µ (micro) | $10^{-6}$ |
| m (milli) | $10^{-3}$ |
| k (kilo) | $10^{3}$ |
| M (mega) | $10^{6}$ |

## 9.3 Main Peak Lists of Peptide Mass Fingerprintings for Isolated Proteins in Affinity Capture Assays

| Direct Capture Nr. III | Direct Capture Nr. V | Competitive Capture Nr. I | Competitive Capture Nr. II |
|---|---|---|---|
| 762.3898449 | 687.2956266 | 607.2728423 | 680.3692837 |
| 803.3951455 | 705.3821718 | 612.200419 | 720.386611 |
| 819.4121906 | 800.3732712 | 647.2112662 | 778.4421137 |
| 853.4132478 | 806.3769885 | 680.376955 | 840.3696929 |
| 877.4263055 | 807.3265994 | 687.3396876 | 842.3653471 |
| 910.4370437 | 810.3466842 | 738.3366665 | 897.4470346 |
| 918.3767469 | 822.3914977 | 753.3291943 | 927.5100129 |
| 934.4563959 | 825.333933 | 768.3485848 | 935.4565631 |
| 958.5227902 | 845.3833242 | 825.3696696 | 1022.527901 |
| 977.4324567 | 855.4000708 | 882.3871656 | 1046.61494 |
| 1005.538468 | 860.4496748 | 887.2964807 | 1089.567378 |
| 1013.53186 | 882.3679302 | 895.454067 | 1118.64089 |
| 1021.551046 | 886.405821 | 919.5624975 | 1148.591091 |
| 1039.488911 | 895.5131231 | 927.5333401 | 1193.62875 |
| 1074.490265 | 927.4701354 | 928.5153133 | 1249.639739 |
| 1078.552223 | 952.5337685 | 942.4362397 | 1308.672291 |
| 1091.577254 | 984.4954121 | 963.5628644 | 1354.719234 |
| 1111.529622 | 988.5295053 | 968.4647629 | 1363.747634 |
| 1120.55634 | 1007.732619 | 1080.564469 | 1408.70174 |
| 1122.534803 | 1029.545672 | 1136.597747 | 1464.676303 |
| 1144.569983 | 1046.610878 | 1178.617285 | 1479.810818 |
| 1168.56046 | 1071.601818 | 1193.650131 | 1492.718911 |
| 1183.514057 | 1080.519707 | 1215.550949 | 1532.756404 |
| 1197.603288 | 1089.623609 | 1285.639999 | 1571.859455 |
| 1201.58833 | 1093.578143 | 1308.710213 | 1605.761028 |
| 1209.549775 | 1103.629721 | 1389.591963 | 1639.942693 |
| 1211.556436 | 1122.587191 | 1401.637448 | 1661.843179 |
| 1264.632698 | 1136.577378 | 1420.719018 | 1718.771466 |
| 1324.640365 | 1146.650303 | 1428.693998 | 1748.867541 |
| 1345.64702 | 1150.595282 | 1438.728303 | 1762.83742 |
| 1353.632297 | 1168.702064 | 1454.713447 | 1812.716994 |
| 1360.644436 | 1180.653172 | 1544.692906 | 1823.883271 |
| 1365.650193 | 1193.619067 | 1557.716873 | 1880.90396 |
| 1381.657196 | 1210.608547 | 1605.794462 | 1963.649334 |
| 1393.654553 | 1220.54575 | 1684.831891 | 2002.898714 |
| 1401.718097 | 1232.592859 | 1843.863602 | 2252.950076 |
| 1428.732372 | 1237.592461 | 2021.985772 | 2268.942832 |
| 1430.69755 | 1246.672741 | 2068.838673 | |
| 1460.787955 | 1275.626476 | 2185.075392 | |
| 1509.685549 | 1285.613559 | 2207.06299 | |
| 1521.740391 | 1288.67077 | 2975.319852 | |
| 1537.703657 | 1297.628269 | 2991.449805 | |
| 1573.741422 | 1300.668204 | | |
| 1647.796083 | 1303.690675 | | |
| 1697.73032 | 1320.705663 | | |
| 1705.794979 | 1336.666312 | | |
| 1714.856892 | 1342.641452 | | |
| 1730.716861 | 1357.76831 | | |
| 1745.830421 | 1360.690732 | | |
| 1778.849482 | 1370.634635 | | |
| 1792.830874 | 1377.730545 | | |
| 1849.838238 | 1390.726948 | | |
| 1894.025745 | 1401.634356 | | |
| 1971.889473 | 1428.661003 | | |

| continue | continue |
|---|---|
| 2032.805095 | 1438.693987 |
| 2036.981481 | 1448.789276 |
| 2074.904109 | 1454.698541 |
| 2181.965839 | 1464.777911 |
| 2230.9906 | 1495.721753 |
| 2233.024323 | 1511.751255 |
| 2271.013046 | 1524.800559 |
| 2274.044078 | 1541.863927 |
| 2292.001399 | 1544.672639 |
| 2297.875429 | 1555.862004 |
| 2310.051363 | 1557.71457 |
| 2361.953485 | 1566.800738 |
| 2426.976821 | 1581.82457 |
| 2451.050605 | 1608.850563 |
| 2466.025956 | 1614.724835 |
| 2695.141888 | 1629.728139 |
| 2726.165807 | 1657.858496 |
| 2926.048661 | 1670.813046 |
| 2940.05521 | 1684.84262 |
| | 1748.732826 |
| | 1751.879404 |
| | 1804.749045 |
| | 1815.984508 |
| | 1828.002405 |
| | 1833.912944 |
| | 1843.851963 |
| | 1862.759539 |
| | 1887.979237 |
| | 1919.938126 |
| | 1944.994571 |
| | 1960.9911 |
| | 2020.938794 |
| | 2068.820594 |
| | 2091.906261 |
| | 2097.950587 |
| | 2318.045045 |
| | 2346.992317 |
| | 2465.133203 |
| | 2975.173797 |
| | 2991.169821 |

## 9.4 List of Publications

**Poster Presentations:**

1. Lin, Y., Fuerste, J. P., Erdmann, V. A. *In vitro* selection of aptamers for recognition of zinc finger proteins (poster presentation in the 13th annual meeting of the RNA society), 07/2008, P404
2. Lin, Y., Fuerste, J. P., Erdmann, V. A. *In vitro* selection of DNA aptamers to zinc finger peptides (poster presentation in the 22nd international symposium on microscale bioseperations and methods for systems biology, MSB), 03/2008, P038

**Patent:**

One patent ‘‘Pharmazeutische Zusammensetzung zur Diagnose oder Behandlung von Zinkfinger Protein assoziierten Erkrankungen’’ in registration process.

**Publication:**

One manuscript ‘‘isolation and characterization of DNA aptamers for zinc finger proteins’’ in preparation (will be submitted after the registration of the patent).

## 9.5 Curriculum Vitae

For reason of data protection,
the curriculum vitae is not included in the online version.

## 9.6 Acknowledgments

First and foremost, I would like to express my sincere gratitude to my supervisor, Prof. Dr. Volker A. Erdmann for giving me the opportunity to work on this topic after my master thesis in his group. I am very grateful for his expertise, immense support, invaluable advices and continuous encouragement during my graduate experience.

I would like to thank Prof. Dr. Hans Lehrach for his support as my second supervisor.

I want to particularly thank Dr. Jens P. Fürste for many scientific discussions, suggestions and help during my work.

Great thanks to Dr. Christoph Weise, Dr. Marcus Menger, Dr. Christian Jaeckel, Sonja Niedrig, and Dr. Boris Reizis for their experimental supports.

I also appreciate very much that Prof. Dr. Jens Kurreck offered me great help and advices. Special thanks go to Dr. Andereas Zeressen-Harte for giving me many discussions and suggestions.

Together with the period of time during my master work, I have lots of warm memories of our department. I am grateful to all the colleagues here for their help, kindness, enduring my temperament and changes in mood.

I would also like to thank my friends and all the other persons who helped me in many different ways during these years of stay in Berlin.

I want to thank Dr. Dieter Jänchen, Dr. Konstantinos Natsias and also their families for their care during my stay in Europe.

In particular I would like to thank Xiaojiang Chen for his understanding and patience, who gave me continuous courage and confidence to keep going.

Last, but above all, I owe everything that I have achieved to my parents in China. Over these years I could not visit them as often as I wished and should. But no matter where I am, I always know that my family is right there supporting me, proud of me and believing in me.